Aspects of stomatal physiology during salt-stress-related disturbances of ion homeostasis

Dissertation to obtain the doctoral degree of Agricultural Sciences

(Dr. sc. agr.)

Faculty of Agricultural Sciences

University of Hohenheim

Institute of Crop Science

University of Hohenheim

submitted by

Bastian Leander Franzisky

from *Meckesheim*

2020

Die vorliegende Arbeit wurde am 18.12.2020 von der Fakultät Agrarwissenschaften der Universität Hohenheim als "Dissertation zur Erlangung des Grades eines Doktors der Agrarwissenschaften" angenommen.

Tag der mündlichen Prüfung: 18.12.2020

Leiter der Prüfung: Herr Prof. Dr. Uwe Ludewig

Berichterstatter, 1. Prüfer: Herr Prof. Dr. Christian Zörb

Mitberichterstatter, 2. Prüfer: Herr Prof. Dr. Christoph-Martin Geilfus

weitere Berichterin bzw. Prüferin: Frau Jun.-Prof. Dr. Sandra Schmöckel

Contents

Chapter 1

General introduction

1. General introduction

Soil salinization constrains global crop production. At present, 6% of global arable and 20% of irrigated land area are thought to be affected by a level of salinization that compromises plant growth and yield (Munns & Tester, 2008; Rengasamy, 2010). Moreover, salinization is becoming more extensive as a result of global climate change, land clearing and inadequate irrigation practices (Munns & Gilliham, 2015; Roy et al., 2014; Zörb et al., 2019) further reducing the limited arable land area. Therefore, we need to breed plants showing greater salt tolerance in order to increase crop performance under saline conditions.

1.1 Soil salinization

Saline soil is defined as having high concentrations of soluble salts that significantly reduce the yield of most crops, in particular, when the electrical conductivity of the saturated soil extract (EC_e) exceeds 4 dS m^{-1} (Richards, 1954). This threshold equals approximately 40 mM NaCl, which represents the most soluble and prevalent salt in soil (Butcher et al., 2016; Munns & Tester, 2008). Because soils are rarely saturated in the field, the salt concentrations experienced by roots can be several times that of the saturated soil extract (Shabala & Munns, 2012) resulting in concentrations of about 80-100 mM NaCl for soils with an EC_e of 4 dS m^{-1} (Rengasamy, 2002). Such conditions are primarily found in arid and semiarid climate areas, where salt ions from various sources have accumulated in soils over long periods (Rengasamy, 2002). In addition to natural sources for salt ions such as mineral weathering and evaporation and to the drawing of soluble salts from deep layers into the root zone, anthropogenic salinization can occur by field irrigation with saline ground water and poor quality waste water, and insufficient drainage obstructing the washing-off of excess salts (Panta et al., 2014). As a consequence, 2% of global arable dry land and 20% of irrigated land area are saline because of

anthropogenic salinization (Munns & Tester, 2008); this is expected to contribute substantially to the degradation of further arable land in the future (Panta et al., 2014).

1.2 Salt stress and mechanisms of tolerance in plants

Plant growth and yield are compromised by abiotic stress conditions such as soil salinity. The most important crop plants providing 90% of plant-based human food are sensitive to salt (Zörb et al., 2019). As a consequence, even moderate salinity in the range of 4-8 dS m^{-1} results in average yield reductions of 50-80% (Panta et al., 2014). Salt-related reductions in crop productivity result from mechanisms directly impacting on plant physiology, *viz.* osmotic and ion-specific effects (Munns, 2002), and indirect effects that result from the deterioration of soil physical and chemical properties and that thereby interfere with nutrient acquisition (Bronick & Lal, 2005; Butcher et al., 2016; Tester & Davenport, 2003). The initial phase of salt stress is characterized by osmotic stress resulting from high solute concentrations lowering the soil water potential outside the roots (Munns & Tester, 2008). In addition to rapid stomatal closure mediated by the accumulation of the plant stress hormone abscisic acid (Geilfus et al., 2018; Geilfus et al., 2015a), plant metabolism responds within minutes to such conditions by disturbances in nitrogen assimilation and activation of metabolic pathways favouring the scavenging of reactive oxygen species (Geilfus et al., 2015b). To alleviate the consequences of the lowered soil water potential, plants osmotically adapt by ion intake (Amede et al., 2015) and the biosynthesis of organic osmolytes (Hasegawa et al., 2000; Kabbadj et al., 2017). Osmotic adjustment by using salt ions is energetically cheaper than the biosynthesis of organic osmolytes (Munns et al., 2020) but only as long as the cellular capability for sequestrating salt ions into vacuoles and for balancing the resulting osmotic pressure by organic osmolytes in the cytosol is not exceeded (Munns & Gilliham, 2015; Munns et al., 2016). This trade-off illustrates the interplay of two major strategies for coping with salt in soil solution: (1) the exclusion of salt ions at the root level and the restriction of acropetal transport towards photosynthetically

active tissue ('ion exclusion') and (2) the strict regulation of subcellular ion compartmentation into vacuoles or photosynthetically non-active cells to avoid the rise of toxic Na^+ and Cl^- concentrations (Munns & Gilliham, 2015; Munns & Tester, 2008; Roy et al., 2014). In most glycophytes, Na^+ and Cl^- concentrations in leaves increase with continuous exposure to salinity because of weak ion exclusion capabilities leading to the disruption of ion homeostasis and symptoms of ion toxicity (Munns & Tester, 2008). The toxicity of high Na^+ is largely a result of interference with K^+ homeostasis. The chemical similarity of the cations (Benitoet al., 2014) enables Na^+ to compete with K^+ for the binding sites essential for cellular functioning such as enzyme activation and protein biosynthesis (Flowers et al., 2015; Tester & Davenport, 2003) thus, adversely affecting the cellular metabolism. In contrast, the stress effects of high Cl^- are less well understood than those of Na^+ (Bazihizina et al., 2018; Li et al., 2017; Teakle & Tyerman, 2010), despite its being the predominant anion in most saline soils (Munns & Tester, 2008). Increasing leaf Cl^- concentrations are primarily associated with reductions in photosynthetic capacity (Tavakkoli et al., 2010) and chlorophyll degradation (Geilfus, 2018). In glycophytic crops, photosynthetic capacity is possibly affected by excessive Cl^- accumulation within the chloroplasts (Teakle & Tyerman, 2010) because their outer envelopes have a high permeability for Cl^- (Bose et al., 2017; Heber & Heldt, 1981). Enrichment of Cl^- in chloroplasts is expected to cause reductions in quantum yield and plant growth (Tavakkoli et al., 2010). This is considered as a consequence of Cl^--induced disturbance of the structural organization of photosystem II and the degradation of chlorophyll (Geilfus, 2018), finally leading to chlorotic discolorations and later to necrotic leaf edges (Hanson et al., 1999).

1.3 Physiology of stomata

Stomata usually consist of two opposingly arranged guard cells and enable controlled gas exchange between the atmosphere and the inside of a leaf. A fine-tuned balancing of CO_2 intake and concomitant water loss is important to provide CO_2 for photosynthesis while retaining the

hydration of the plant (Lawson & Blatt, 2014; Lawson et al., 2010). The adjustment of stomatal aperture in response to endogenous and exogenous cues, such as their immediate response to soil salinity, is of tremendous significance because stomatal transpiration accounts for approximately 95% of the water loss of a plant (Ache et al., 2010). Optimization of the performance of the stomata is a key factor for the acclimatization of a plant to soil salinity because this structure controls transpiration and, therefore, the hydration and the extent of salt delivered to the shoot by mass flow (Hedrich & Shabala, 2018; Robinson et al., 1997). The fast responses of the stomata are facilitated by transient solute accumulation within their guard cells enabling rapid changes in turgor (MacRobbie & Kurup, 2007). During light-induced stomatal opening, the import of K^+, Cl^-, NO_3^- and small organic acids from the apoplast together with the biosynthesis of organic solutes such as malate are essential for the build-up of the osmotic potential within the guard cells (Jezek & Blatt, 2017; Santelia & Lawson, 2016). In this process, the guard cell metabolism plays a pivotal role because it provides energy equivalents for active transport of inorganic ions and for the biosynthesis of organic solutes (Kollist et al., 2014; Kopka et al., 1997). In response to light, starch degradation (Daloso et al., 2017; Horrer et al., 2016) and fatty acid breakdown of guard cells become activated (Horrer et al., 2016; McLachlan et al., 2016), favouring energy production *via* mitochondrial oxidative phosphorylation and peroxisomal β-oxidation, respectively. The produced energy equivalents feed the high energy demand of solute intake and biosynthesis, which trigger water influx, *i.e.* the inflating of the guard cells leading to stomatal opening. *Vice versa*, closing stomata are characterized by a reversal of the opening process in regard to osmolyte magnitude and flux direction. A signal cascade initiated, for example, by the stress hormone abscisic acid, triggers an initial anion release from guard cells, which in turn leads to the release of K^+ together with inorganic anions (Hedrich & Shabala, 2018; Jezek & Blatt, 2017). Organic anions are either metabolically decomposed or released to the apoplast when stress responses require fast turgor loss (Santelia & Lawson, 2016).

1.4 Objectives & main findings

A better understanding of stomatal processes contributing to salt tolerance in crop plants is becoming increasingly important for agriculture because of the serious impacts of soil salinity on plant yield and quality. In this thesis, a broad analysis of tolerance mechanisms is provided in terms of ion exclusion, tissue tolerance, and their impact on stomatal regulation and photosynthesis within selected populations of *V. faba* and *Z. mays* exposed to various salt treatments.

- Is there plasticity in the ability of ion retention and tissue tolerance of Na^+ and Cl^- between salt sensitive and tolerant *V. faba* varieties?

  ⇒ Tolerant *V. faba* varieties sequester Na^+ and exclude Cl^- from shoots.

- Is there plasticity in the ability of ion retention and tissue tolerance of Cl^- in diverse *Z. mays* genotypes?

  ⇒ Most *Z. mays* genotypes exclude Cl^- from shoot avoiding a deleterious Cl^- accumulation in photosynthetically active tissues.

- Are stomatal function and guard cell metabolism in *V. faba* affected by increasing leaf Na^+ and Cl^+ concentrations resulting from long-term salinity?

  ⇒ Stomata can still be opened and closed, albeit at slower speed. In contrast to mesophyll, guard cells do not show a salt stress metabolic signature.

References

Ache, P., Bauer, H., Kollist, H., Al-Rasheid, K. A., Lautner, S., Hartung, W., & Hedrich, R. (2010). Stomatal action directly feeds back on leaf turgor: new insights into the regulation of the plant water status from non-invasive pressure probe measurements. *The Plant Journal, 62*(6), 1072-1082.

Amede, T., Schubert, S., & Stahr, K. (2003). Mechanisms of drought resistance in grain legumes I: Osmotic adjustment. *Ethiopian Journal of Science, 26*(1), 37-46.

Bazihizina, N., Colmer, T. D., Cuin, T. A., Mancuso, S., & Shabala, S. (2018). Friend or Foe? Chloride Patterning in Halophytes. *Trends in Plant Science*, *24*(2), 142-151.

Benito, B., Haro, R., Amtmann, A., Cuin, T. A., & Dreyer, I. (2014). The twins K^+ and Na^+ in plants. *Journal of Plant Physiology, 171*(9), 723-731.

Bose, J., Munns, R., Shabala, S., Gilliham, M., Pogson, B., & Tyerman, S. D. (2017). Chloroplast function and ion regulation in plants growing on saline soils: lessons from halophytes. *Journal of Experimental Botany, 68*(12), 3129-3143.

Bronick, C. J., & Lal, R. (2005). Soil structure and management: a review. *Geoderma, 124*(1-2), 3-22.

Butcher, K., Wick, A. F., DeSutter, T., Chatterjee, A., & Harmon, J. (2016). Soil Salinity: A Threat to Global Food Security. *Agronomy Journal, 108*(6), 2189-2200.

Daloso, D. M., Medeiros, D. B., Dos Anjos, L., Yoshida, T., Araújo, W. L., & Fernie, A. R. (2017). Metabolism within the specialized guard cells of plants. *New Phytologist, 216*(4), 1018-1033.

Farooq, M., Hussain, M., Wakeel, A., & Siddique, K. H. M. (2015). Salt stress in maize: effects, resistance mechanisms, and management. A review. *Agronomy for Sustainable Development, 35*(2), 461-481.

Flowers, T. J., Munns, R., & Colmer, T. D. (2015). Sodium chloride toxicity and the cellular basis of salt tolerance in halophytes. *Annals of Botany, 115*(3), 419-431.

Food Agriculture Organization of the United Nations. (2011). *The state of the world's land and water resources for food and agriculture: Managing systems at risk.* Abingdon, UK: Earthscan.

Geilfus, C.-M. (2018). Chloride: from nutrient to toxicant. *Plant and Cell Physiology, 59*(5), 877-886.

Geilfus, C.-M., Ludwig-Müller, J., Bárdos, G., & Zörb, C. (2018). Early response to salt ions in maize (*Zea mays* L.). *Journal of Plant Physiology, 220*, 173-180.

Geilfus, C.-M., Mithofer, A., Ludwig-Muller, J., Zörb, C., & Mühling, K.-H. (2015a). Chloride-inducible transient apoplastic alkalinizations induce stomata closure by controlling abscisic acid distribution between leaf apoplast and guard cells in salt-stressed *Vicia faba*. *New Phytologist, 208*(3), 803-816.

Geilfus, C.-M., Niehaus, K., Godde, V., Hasler, M., Zörb, C., Gorzolka, K., Jezek, M., Senbayram, M., Ludwig-Muller, J., & Mühling, K. H. (2015b). Fast responses of metabolites in *Vicia faba* L. to moderate NaCl stress. *Plant Physiology and Biochemistry, 92*, 19-29.

Hanson, B., Grattan, S. R., & Fulton, A. (1999). *Agricultural salinity and drainage*: University of California Irrigation Program, University of California, Davis.

Hasegawa, P. M., Bressan, R. A., Zhu, J. K., & Bohnert, H. J. (2000). Plant Cellular and Molecular Responses to High Salinity. *Annual Review of Plant Physiology and Plant Molecular Biology, 51*(1), 463-499.

Heber, U., & Heldt, H. W. (1981). The Chloroplast Envelope: Structure, Function, and Role in Leaf Metabolism. *Annual Review of Plant Physiology, 32*(1), 139-168.

Hedrich, R., & Shabala, S. (2018). Stomata in a saline world. *Current Opinion in Plant Biology, 46*, 87-95.

Horrer, D., Flütsch, S., Pazmino, D., Matthews, J. S. A., Thalmann, M., Nigro, A., Leonhardt, N., Lawson, T., & Santelia, D. (2016). Blue light induces a distinct starch degradation pathway in guard cells for stomatal opening. *Current Biology, 26*(3), 362-370.

Jezek, M., & Blatt, M. R. (2017). The Membrane Transport System of the Guard Cell and Its Integration for Stomatal Dynamics. *Plant Physiology, 174*(2), 487-519.

Kabbadj, A., Makoudi, B., Mouradi, M., Pauly, N., Frendo, P., & Ghoulam, C. (2017). Physiological and biochemical responses involved in water deficit tolerance of nitrogen-fixing *Vicia faba*. *PloS one, 12*(12), e0190284.

Kollist, H., Nuhkat, M., & Roelfsema, M. R. G. (2014). Closing gaps: linking elements that control stomatal movement. *New Phytologist, 203*(1), 44-62.

Kopka, J., Provart, N. J., & Müller-Röber, B. (1997). Potato guard cells respond to drying soil by a complex change in the expression of genes related to carbon metabolism and turgor regulation. *The Plant Journal, 11*(4), 871-882.

Kotula, L., Garcia, P., Zörb, C., Colmer, T. D., & Flowers, T. J. (2020). Improving crop salt tolerance using transgenic approaches: an update and physiological analysis. *Plant, Cell & Environment, 43*(12), 2932-2956.

Lawson, T., & Blatt, M. R. (2014). Stomatal Size, Speed, and Responsiveness Impact on Photosynthesis and Water Use Efficiency. *Plant Physiology, 164*(4), 1556-1570.

Lawson, T., von Caemmerer, S., & Baroli, I. (2010). Photosynthesis and stomatal behaviour. *Progress in botany* 71 (pp. 265-304): Springer, Berlin, Heidelberg.

Li, B., Tester, M., & Gilliham, M. (2017). Chloride on the Move. *Trends in Plant Science, 22*(3), 236-248.

MacRobbie, E. A. C., & Kurup, S. (2007). Signalling mechanisms in the regulation of vacuolar ion release in guard cells. *New Phytologist, 175*(4), 630-640.

McLachlan, D. H., Lan, J., Geilfus, C.-M., Dodd, A. N., Larson, T., Baker, A., Hõrak, H., Kollist, H., He, Z., & Graham, I. (2016). The breakdown of stored triacylglycerols is required during light-induced stomatal opening. *Current Biology, 26*(5), 707-712.

Munns, R. (2002). Comparative physiology of salt and water stress. *Plant, Cell & Environment, 25*(2), 239-250.

Munns, R., & Gilliham, M. (2015). Salinity tolerance of crops – what is the cost? *New Phytologist, 208*(3), 668-673.

Munns, R., James, R. A., Gilliham, M., Flowers, T. J., & Colmer, T. D. (2016). Tissue tolerance: an essential but elusive trait for salt-tolerant crops. *Functional Plant Biology, 43*(12), 1103-1113.

Munns, R., Passioura, J. B., Colmer, T. D., & Byrt, C. S. (2020). Osmotic adjustment and energy limitations to plant growth in saline soil. *New Phytologist, 225*(3), 1091-1096.

Munns, R., & Tester, M. (2008). Mechanisms of salinity tolerance. *Annual Review of Plant Biology, 59*(1), 651-681.

Panta, S., Flowers, T., Lane, P., Doyle, R., Haros, G., & Shabala, S. (2014). Halophyte agriculture: success stories. *Environmental and Experimental Botany, 107*, 71-83.

Rengasamy, P. (2002). Transient salinity and subsoil constraints to dryland farming in Australian sodic soils: an overview. *Australian Journal of Experimental Agriculture, 42*(3), 351-361.

Rengasamy, P. (2010). Soil processes affecting crop production in salt-affected soils. *Functional Plant Biology, 37*(7), 613-620.

Richards, L. (1954). Diagnosis and improvement of saline and alkali soils. *Hand book no. 60 United States Department of Agriculture*: Washington, DC.

Robinson, M. F., Véry, A.-A., Sanders, D., & Mansfield, T. A. (1997). How Can Stomata Contribute to Salt Tolerance? *Annals of Botany, 80*(4), 387-393.

Roy, S. J., Negrão, S., & Tester, M. (2014). Salt resistant crop plants. *Current Opinion in Biotechnology, 26*, 115-124.

Santelia, D., & Lawson, T. (2016). Rethinking guard cell metabolism. *Plant Physiology, 172*(3), 1371-1392.

Shabala, S., & Munns, R. (2012). Salinity stress: physiological constraints and adaptive mechanisms. *Plant stress physiology, 1*(1), 59-93.

Tavakkoli, E., Rengasamy, P., & McDonald, G. K. (2010). High concentrations of Na^+ and Cl^- ions in soil solution have simultaneous detrimental effects on growth of faba bean under salinity stress. *Journal of Experimental Botany, 61*(15), 4449-4459.

Teakle, N. L., & Tyerman, S. D. (2010). Mechanisms of Cl^- transport contributing to salt tolerance. *Plant, Cell & Environment, 33*(4), 566-589.

Tester, M., & Davenport, R. (2003). Na^+ tolerance and Na^+ transport in higher plants. *Annals of Botany, 91*(5), 503-527.

Zörb, C., Geilfus, C.-M., & Dietz, K.-J. (2019). Salinity and crop yield. *Plant Biology, 21*, 31-38.

Chapter 2

Shoot chloride translocation as a determinant for NaCl tolerance in *Vicia faba* L.

Bastian L. Franzisky, Christoph-Martin Geilfus,
Markus Kränzlein, Xudong Zhang, Christian Zörb

Journal of Plant Physiology 236 (2019) 23-33

Journal of Plant Physiology 236 (2019) 23–33

Contents lists available at ScienceDirect

Journal of Plant Physiology

journal homepage: www.elsevier.com/locate/jplph

Shoot chloride translocation as a determinant for NaCl tolerance in *Vicia faba* L.

Bastian L. Franzisky[a], Christoph-Martin Geilfus[b], Markus Kränzlein[a], Xudong Zhang[a], Christian Zörb[a,*]

[a] University of Hohenheim, Institute of Crop Science, 340e, Schloss Westflügel, 70593, Stuttgart, Germany
[b] Humboldt-University of Berlin, Faculty of Life Sciences, Albrecht Daniel Thaer-Institute of Agricultural and Horticultural Sciences, Controlled Environment Horticulture, Albrecht-Thaer-Weg 1, 14195, Berlin, Germany

ARTICLE INFO

Keywords:
Vicia faba
Salt tolerance
Sodium
Chlorine
Chlorine salinity

ABSTRACT

Faba bean (*Vicia faba* L.) is sensitive to salinity. While toxic effects of sodium (Na^+) are well studied, toxicity aspects of chloride (Cl^-) and the underlying tolerance mechanisms to Cl^- are not well understood. For this reason, shoot Cl^- translocation and its effect as potential determinant for tolerance was tested. Diverse *V. faba* varieties were grown hydroponically and stressed with 100 mM NaCl until necrotic leaf spots appeared. At this point, biomass formation, oxidative damage of membranes as well as Na^+, Cl^- and potassium concentrations were measured. The *V. faba* varieties contrasted in the length of the period they could withstand the NaCl stress treatment. More tolerant varieties survived longer without evolving necrosis and were less affected by inhibitory effects on photosynthesis. The concentration of Cl^- at the time point of developing leaf necrosis was in the same range irrespective of the variety, while that of Na^+ varied. This indicates that Cl^- concentrations, and not Na^+ concentrations are critical for the formation of salt necrosis in faba bean. Tolerant varieties profited from lower Cl^- translocation to leaves. Therefore, photosynthesis was less affected in those varieties with lower Cl^-. This mechanism is a new trait of interest for salt tolerance in *V. faba*.

1. Introduction

Faba bean (*Vicia faba* L.) contributes to nitrogen input to soil and is often used in organic agriculture (Köpke and Nemecek, 2010; Turpin et al., 2002). Faba bean is an important legume crop that is used as feed and food because of its high dietary protein content (Crépon et al., 2010). Legumes and particularly faba bean are sensitive to high salt loadings in soil resulting in limitations in yield and biomass (Li et al., 2017; Tavakkoli et al., 2010). Faba bean is grown in the Middle East, the Mediterranean region, China and Ethiopia. Some of these regions may face a problem with high salt loadings (Jensen et al., 2010), with sodium chloride representing the most soluble and prevalent salt (Butcher et al., 2016; Munns and Tester, 2008). The initial phase of salt stress is usually dominated by osmotic stress resulting from high solute concentrations and low soil water potential and is therefore categorized as 'osmotic-phase' (Munns and Tester, 2008). In response to the osmotic imbalance, faba bean undergoes fast physiological adaptations within the first hour (Geilfus et al., 2015a). In addition to rapid stomatal closure, metabolites associated with the formation and scavenging of reactive oxygen species accumulate, while a reduction in glutamine synthetase activity indicates disturbances in nitrogen assimilation, even in the early phase of salt stress. Additionally, a proline analogue (*trans*-4-hydroxy-L-proline) known to inhibit cell elongation is increasingly synthesized after NaCl-stress initiation (Geilfus et al., 2015b). In order to alleviate the effect of reduced cell expansion and lack of water, plants osmotically adapt by ion uptake (Amede et al., 2003; Farooq et al., 2015) and the synthesis of compatible solutes (Hasegawa et al., 2000; Kabbadj et al., 2017). With a continuous exposure to salinity, the accumulated salt ions lead to the disruption of ion homeostasis and cause symptoms of ion toxicity (Munns and Tester, 2008). Moreover, a clear separation into osmotic and ionic stress phases is problematic, because the transition between the phases is fluent and phases often overlap. In faba bean, high shoot Na^+ concentrations interfere with K^+ and calcium nutrition, while the accumulation of Cl^- is associated with a decline of photosynthetic capacity (Tavakkoli et al., 2010). The restriction of salt ion fluxes is mandatory both for preventing intra- and intercellular Na^+ and Cl^- concentrations from rising to toxic concentrations and for ensuring K^+ homeostasis. The latter is essential for the functioning of protein biosynthesis and the various cytosolic enzymes that might be impaired by competition of Na^+ and K^+ (Flowers

* Corresponding author.
E-mail address: christian.zoerb@uni-hohenheim.de (C. Zörb).

https://doi.org/10.1016/j.jplph.2019.02.012
Received 20 December 2018; Received in revised form 15 February 2019; Accepted 18 February 2019
Available online 26 February 2019
0176-1617/ © 2019 Elsevier GmbH. All rights reserved.

et al., 2015; Tester and Davenport, 2003). One physiological strategy contributing to NaCl tolerance is salt ion exclusion at the root level and a restriction of ion transfer into the xylem to prevent them from being translocated acropetally towards the photosynthetically active leaves ('ion exclusion'). Another strategy is characterized by subcellular ion compartmentation into vacuoles or photosynthetically non-active cells to avoid the accumulation of harmful ions within the cytoplasm ('tissue tolerance') (Munns and Tester, 2008; Roy et al., 2014).

In faba bean, evidence has been presented illustrating variety-specific differences in the mechanisms regulating NaCl-based ion fluxes. In this study, a more tolerant genotype has been found to be capable of maintaining lower shoot Na^+ and Cl^- concentrations (Tavakkoli et al., 2010). However, information about intra-crop variance in terms of tissue tolerance is limited. When the internal Na^+ and Cl^- concentrations exceed the capacity of tissue tolerance, faba bean develops necrotic spots, starting on mature leaves. This is associated with a loss of photosynthetically active tissue that further compromises plant growth. This can occur after two weeks of growth under saline conditions in hydroponics, highlighting the sensitivity of the crop to salt (Slabu et al., 2009). In order to maintain growth under conditions of soil salinity, salt sensitive crops need to be improved with regard to their ability to withstand the negative soil properties that we expect to increase in the near future (Butcher et al., 2016; Wang et al., 2003).

The motivation behind this study was to evaluate on the basis of Cl^- and Na^+ accumulation pattern how key processes such as (*i*) ion retention and (*ii*) tissue tolerance contribute to increased performance under salinity. Another aim was to investigate the plasticity of the tolerance mechanisms of *V. faba* and to evaluate to which extent sensitive and tolerant varieties differ in their physiological stress response.

2. Materials and methods

2.1. Cultivation of plant material

For to screen a broad physiological range to salt tolerance thirteen diverse varieties of *Vicia faba* L. were selected for the study: 'Diva', 'Honey', 'Nebraska', 'Organdi' (Agri-Obtentions, Guyancourt, France), 'Espresso', 'Fuego', 'Lynx', 'Mallory', 'RLS57222', 'RLS67101', 'Scoop', 'Tiffany' (Norddeutsche Pflanzenzucht Hans-Georg Lembke KG, Hohenlieth, Germany) and 'Major' (Limagrain, Edemissen, Germany). This selection represents a broad genetic range of varieties of available German faba bean varieties from different breeding companies (population varieties). None of them was bred for salt tolerance. With the use of broadest genetic origin of these varieties we tend to evaluate the plasticity of stress reaction of faba bean under saline conditions. Plants were grown under hydroponic culture conditions in a walk-in climate chamber (14/10 h day/night; 22/18 °C; approx. 80–90% humidity, 500 µmol photons $m^2 s^{-1}$ at shoot level). Seeds were imbibed in aerated $CaSO_4$ (0.5 mM) solution for 1 d at room temperature and were subsequently placed in moistened quartz sand. After 10 d of germination, seedlings were transferred into plastic containers containing 1/4-strength aerated nutrient solution. The nutrient concentration was increased stepwise to prevent osmotic shock. The nutrient concentration was increased to 1/2-strength after 2 d, 3/4-strength after 3 d and to full-strength after 4 d. Full-strength nutrient solution had the following composition: 0.1 mM KH_2PO_4, 1.0 mM K_2SO_4, 2.0 mM $Ca(NO_3)_2$, 0.5 mM $MgSO_4$, 0.00464% (w/v) Sequestren (Ciba Geigy, Basel, Switzerland), 100 µM NaCl, 10 µM H_3BO_3, 2.0 µM $MnSO_4$, 0.5 µM $ZnSO_4$, 0.2 µM $CuSO_4$, 0.1 µM $CoCl_2$, 0.05 µM $(NH_4)_6Mo_7O_{24}$. After 4 d of growth under the full-strength nutrient concentration, NaCl treatment was introduced to the 16-day-old plants. Starting from 1/3-strength, the NaCl concentration was incrementally increased to 2/3-strength after 2 d and to full-strength after 4 d (100 mM NaCl). Our previous experiments confirmed this application as moderate salt treatment for *V. faba* resulting in a moderate stress answer with moderate growth reduction and at the most the development of symptoms such as black spots only at sensitive varieties (Richter et al., 2015; Slabu et al., 2009). The solution was changed every third day to avoid nutrient depletion. For each variety, five biological replicate plants were cultivated under control and salt stress conditions.

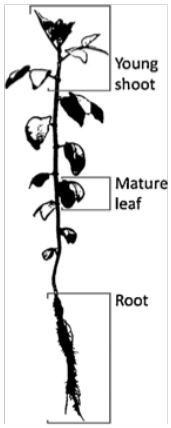

Fig. 1. Illustration of the sampled plant regions for the determination of biomass and ion analysis. Young shoot represents the plant region that started to develop under fullstrength NaCl treatment (100 mM). Mature leaf represents the 4th leaf at which leaf physiological measurements were conducted. The 4th leaf emerged under control conditions but developed during both the stress adaption phase and under conditions of 100 mM NaCl stress.

2.2. Transpiration, SPAD, biomass and electrolyte leakage

Assimilation (*A*) and transpiration (*E*) were measured by using a LC*i-SD* ultra compact photosynthesis system (ADC Bioscientific, U.K.) at the fully developed 4th leaf in the walk-in climate chamber (Fig. 1). The first measurement was conducted 3 d after the 100 mM NaCl stress was applied. Measurements were conducted in a randomized order and repeated every 2 to 3 d at the same time of a day (3 h after lights on). Chlorophyll content was estimated by SPAD values that were measured similarly to *A* and *E* by using a Minolta SPAD-502 Chlorophyll meter (Minolta Camera Co., Ltd., Osaka, Japan). Plants were harvested 1 d after necrotic salt lesions had occurred on the fully developed 4th leaves and when four out of five of the NaCl stressed biological replicates showed these symptoms. These symptoms were either (i) leaf necrotic spots (Fig. 2B) or (ii) visible loss of turgidity (Fig. 2C). The dry weights (DW) of total shoot, young shoot, 4th leaf and root were determined after drying to constant weight at 55 °C (Fig. 1). Electrolyte leakage (EL) was measured as described in Wedeking et al. (2017) by using four leaf discs (diameter of 0.8 mm) that had been cut from 5th leaf.

2.3. Potassium, sodium and chloride analysis

For ion extraction, a 50 mg sample of oven-dried plant material was solubilized in 8 mL 69% HNO_3 (v/v) and 4 mL H_2O_2 by microwave digestion at 190 °C for 25 min (MARS 5; CEM Cooperation, Matthews, NC, USA). To verify the extraction procedure, standard and blank samples were also digested. The digestates were filtered and analysed for K^+ and Na^+ concentrations by using an atomic absorbance spectrometer (3300 series; Thermo Fisher Scientific, Dreieich, Germany), whereas the Cl^- concentration was measured by using the ferricyanide method according to the protocol described by Munns et al. (2010).

2.4. Data analysis

Data were analysed by using *R* (R Development Core Team, 2017)

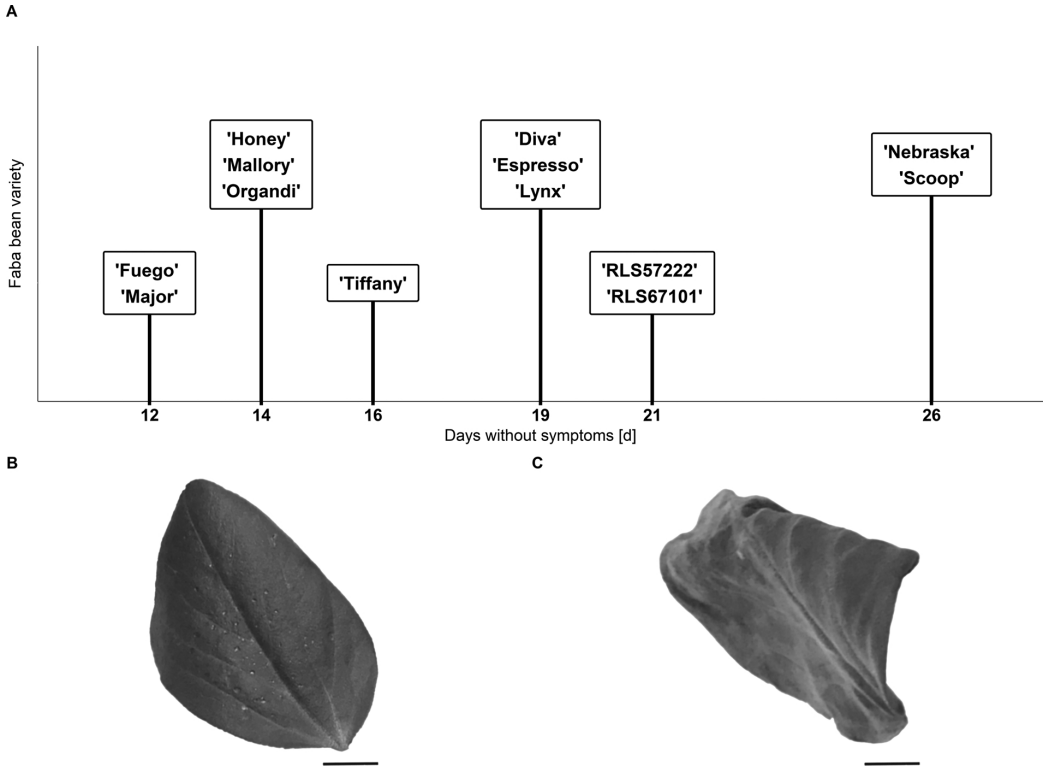

Fig. 2. Plasticity of faba bean varieties at 100 mM salt stress. A) Duration in days starting from full-strength salt application to development of leaf necrosis or loss of turgidity in at least four out of five salt-treated plants of a respective variety. Time point indicates harvest time; B) Faba bean leaf with necrotic spots. Image taken from a 4th leaf of 'Fuego' after 11 days of NaCl treatment; C) Faba bean leaf with loss of turgidity, from 3th leaf of 'Major' after 11 d of NaCl treatment. Scale bars represent 1 cm.

and the lme4-package to perform linear mixed effects analysis (Bates et al., 2015). As fixed effects, variety and treatment with an interaction term were entered into the model, whereas the positioning of the individual plants within the plastic containers of the hydroponics system was entered as a random effect. Residuals of statistical models were inspected visually and by using the DurbinWatson test from the car-package (Fox and Weisberg, 2011). Data were analysed on the basis of $p \leq 0.05$ by using the Tukey test algorithm and information of pairwise comparison and compact letter display was extracted by use of the multcompView package (Graves et al., 2015). Prior to clustering by using the stats package (R Development Core Team, 2017), optimal cluster number was estimated by using the fpc package (Hennig, 2015). Clustering was conducted according to the Hartigan and Wong algorithm with an estimated cluster number by optimum average silhouette width (R Development Core Team, 2017). Relative changes of dry weights were calculated relative to the non-stressed control group by subtracting log-transformed values. Changes of electrolyte leakage were calculated relative to the averaged non-stressed control group. Average ion accumulation was calculated as difference of salt stress concentrations and averaged non-stressed control group divided by the length of the exposure to NaCl stress. Data were visualized by using the ggplot2 package (Wickham, 2016), the ggbiplot package (Vu, 2011) and the corrplot package (Wei and Simko, 2017).

3. Results

3.1. Plasticity of faba bean varieties under salt stress

To identify the plasticity of stress physiological reactions and the range of diverse varieties in stress tolerance, faba bean varieties that contrast in their ability to withstand 100 mM NaCl stress were tested. Therefore, the experiment was conducted using a variable stress period, *i.e.* each variety grew as long as was needed to develop visible toxicity symptom. The plants of each variety were harvested when four out of five plants developed toxicity symptoms such as tiny leaf spot necrosis or severe loss of turgidity (Fig. 2B, C). By this, a comparison of the plasticity of the varieties at a similar physiological stress level was achieved. Salt-treated 'Major' plants suffered from severe loss of turgidity (Fig. 2C), whereas the other varieties developed tiny necrotic spots on leaves (Fig. 2B). The faba bean varieties differed in their stress response. Some of the varieties showed salt stress symptoms earlier, others later thus illustrating the contrast in their plasticity to withstand salt stress (Fig. 2A). In comparison of the 13 varieties 'Fuego' and 'Major' developed symptoms first (after 12 days of NaCl treatment). The other varieties developed leaf necrosis after 14, 16, 19, 21 and 26 days of NaCl treatment. The most tolerant varieties were 'Nebraska' and 'Scoop' which developed leaf necrosis after 26 days, this was 14 days later than the sensitive variety 'Fuego'.

3.2. Growth depression, membrane integrity, assimilation and transpiration

Of course, the absolute biomass formation increased with the

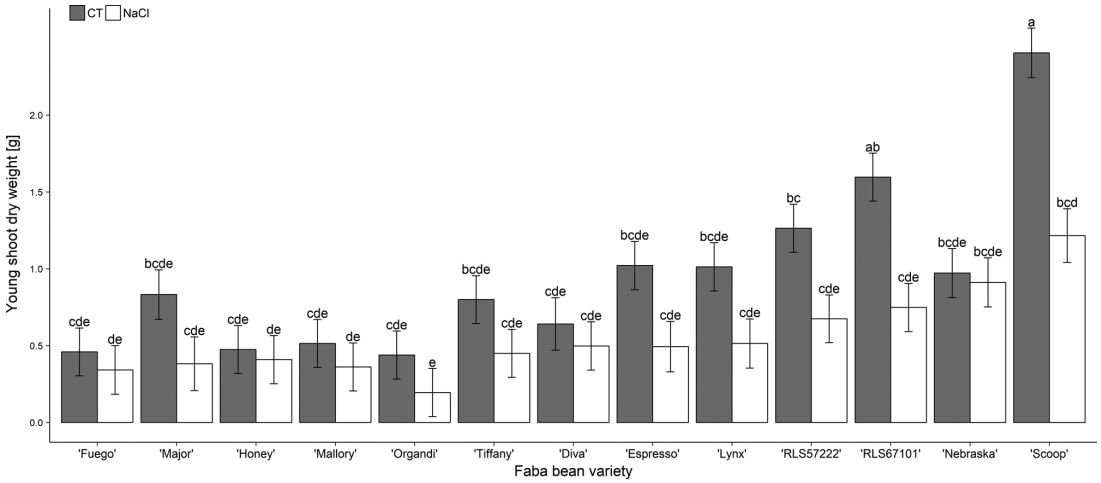

Fig. 3. Plasticity of faba bean varieties differing in young shoot biomass (at the individual day that the varieties displayed visible symptoms), dry weight of control (CT) and 100 mM NaCl. Plants were harvested when leaf necrosis or loss of turgidity occurred as indicated in Fig. 2. Adjusted means from linear mixed-effect model ± SE. Different letters indicate significant differences; $p \leq 0.05$; $n = 5$.

duration of the growth period under both control and NaCl conditions in all varieties showing that the treatment was moderate and not too harsh. The plasticity of the varieties was high because salt-induced growth depression ranged in average from 5 to 65% in young shoots that had developed under the influence of salt stress. However, growth depression was only significant for 'RLS67101' and 'Scoop' (Fig. 3). The most tolerant variety 'Nebraska' (Fig. 2A) did not show significant growth depression neither necrosis within 25 d of stress duration.

The status of the membrane integrity of mature leaf was assessed by measuring their electrolyte leakage. The electrolyte leakage was significantly increased by NaCl treatment in all varieties with the exception of the early salt-injury-developing varieties 'Fuego' and 'Honey', which had similar leakage rates under control and salt conditions (Fig. 4). With the exception of the two mentioned varieties, the relative increase of electrolyte leakage was at a similar level although the exposure time to NaCl varied (Fig. 2A).

Leaf transpiration rate (*E*) and CO_2 assimilation rate (*A*) were measured every 2nd or 3rd day, starting 3 d after full-strength NaCl application (Fig. 5). In comparison with control, salt treated plants had significantly reduced *E* and *A* with an average reduction of about 70% and 30%, respectively (Fig. 5). At the early stress phase (3 d since full-strength NaCl application), salt treated plants showed reduced *E* of about 1 mol H_2O m^{-2} s^{-1} that fluctuated only a little in the following days of the stress period. Conversely, *A* was about 5.5 µmol CO_2 m^{-2} s^{-1} and decreased significantly for most varieties in the subsequent period of 5 to 10 d of NaCl stress to rates of about 2 µmol CO_2 m^{-2} s^{-1} (Fig. 5). Two days after *A* decreased to this level, the varieties such as 'Fuego', 'Honey' and 'Mallory' already had developed necrotic spots. The *E* of 'RLS67101', 'Nebraska' and 'Scoop' was slightly higher in comparison with the other varieties. Furthermore, *A* decreased only to approx. 2.5 µmol CO_2 m^{-2} s^{-1} and did slightly recover to 3.5 µmol CO_2 m^{-2} s^{-1} in the period from 14 to 17 d of salt stress. The latter trend was also visible at 'Diva' and 'Espresso'.

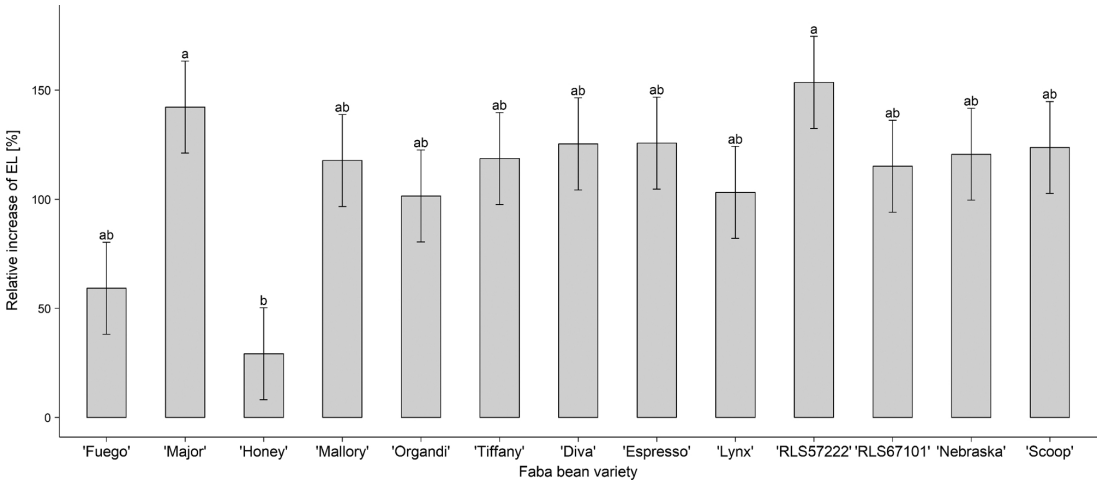

Fig. 4. Membrane integrity of faba bean varieties. EL, relative increase of electrolyte leakage after NaCl treatment in comparison to unstressed controls. Samples were taken when first symptoms occurred as indicated in Fig. 2. Means ± SE. Different letters indicate significant differences; $p \leq 0.05$; $n = 5$.

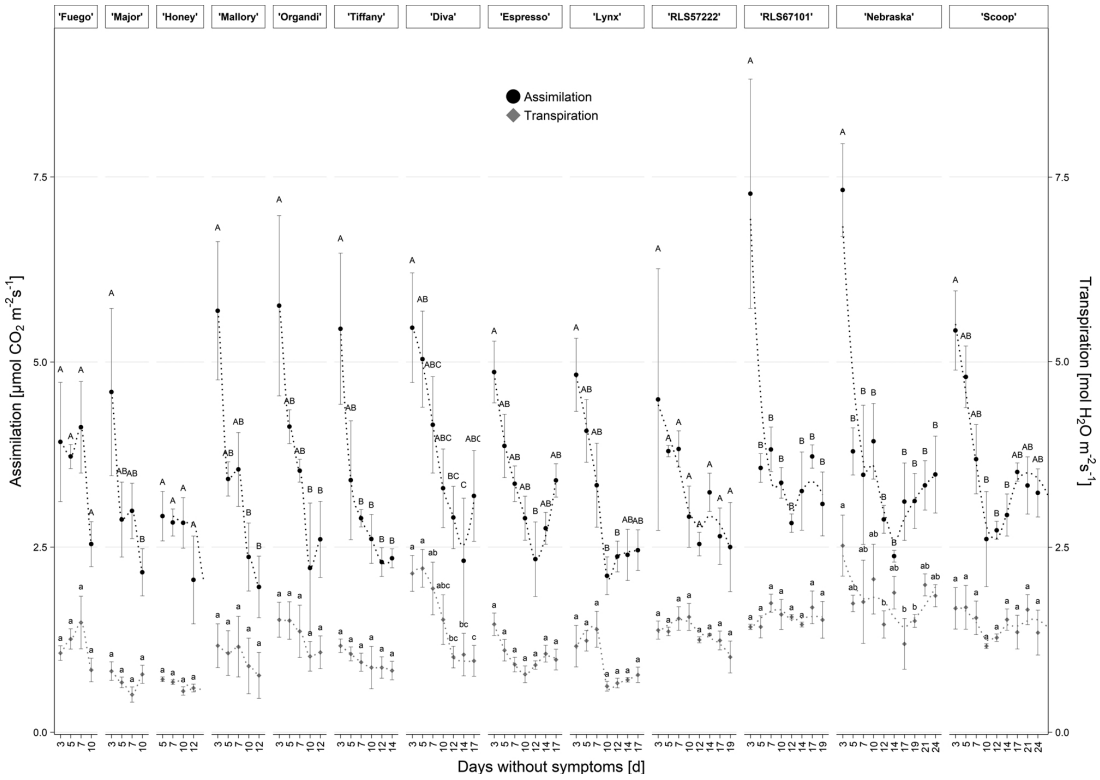

Fig. 5. Assimilation (A) and transpiration rate (E) of faba bean varieties grown at 100 mM NaCl. Measurements were conducted at mature leaves (4th) starting from 3 days after full-strength salt stress until the respective variety developed symptoms. Means ± SE with dotted trend line (local polynomial regression fit). Different letters indicate significant intra-variety differences of means; $p \leq 0.05$; $n = 3$.

3.3. Ion pattern

The concentrations of potassium [K^+], sodium [Na^+] and chloride [Cl^-] were analysed to determine plasticity of tissue specific ion patterns in these varieties. Sodium in control plants was hardly detectable, whereas the average [Cl^-] ranged from 150 to 200 µmol g DW^{-1} in young shoots and from 100 to 420 µmol g DW^{-1} in mature leaves (Figs. 6A, 7 A). The [K^+] was similar for most varieties, with concentrations ranging from 1050 µmol g DW^{-1} in young shoots to 1150 µmol g DW^{-1} in mature leaves of control plants (Figs. 6A; 7 A). The addition of 100 mM NaCl to the nutrient solution resulted in an accumulation of salt ions but the increase of Na^+ was about two-fold higher than that of Cl^- in both young shoots and mature leaves (Figs. 6A; 7 A). In mature leaves, [Na^+] and [Cl^-] were higher than in young shoots. In contrast, the reduction of [K^+] was more pronounced in mature leaves that had accumulated 84% more Na^+ than young shoots (Figs. 6A; 7 A). In comparison with the later symptom-developing varieties 'RLS67101', 'Nebraska' and 'Scoop', the early symptom-developing variety 'Fuego' accumulated less Na^+ in young shoot and mature leaf.

The pattern of Na^+ and K^+ concentrations in young shoots differed in relation to the duration that the plants grew under stress. The [Na^+] increased with the duration of NaCl stress ('days without symptoms') whereas that of [K^+] decreased (Suppl. Fig. 1). The varieties 'Nebraska' and 'Scoop', which developed symptoms later, showed higher [Na^+] in young shoots and mature leaves. These both varieties had also lower [K^+] compared with the more sensitive variety 'Fuego' which developed necrotic spots earlier (Fig. 6A). In contrast, the [Cl^-] differed much less at the time point when leaf necrotic spots appeared. This pattern was visualized by a density plot: in young shoots and mature leaves the densities of [Cl^-] were about double in comparison to [Na^+] (Figs. 6B; 7 B). However, in mature leaves the density of [Cl^-] was twice as high compared with young shoots (Fig. 7B). Moreover, the pattern for Cl^- shows narrow density peaks in comparison with Na^+ with broad peaks. In particular, [Cl^-] in young shoots was similar, irrespective of the variety and the various exposure time to NaCl (Fig. 6B). The common pattern was that plants, regardless of their variety, formed salt-stress symptoms at a specific Cl^- tissue concentration, whereas such a pattern was not observed for Na^+ (Figs. 6B; 7 B).

To find a tissue ion pattern for the diverse varieties a hierarchical clustering according to their Na^+ and Cl^- concentrations was done (Fig. 8A, B). In both leaf fractions (young and mature), varieties with lower ion concentrations clustered into one group (dark triangle) and other varieties with 1.5 to 2-fold higher tissue ion concentration clustered together (light triangle). Varieties such as 'RLS67101', 'Nebraska', and 'Scoop' developing symptoms later clustered into the group with higher tissue ion concentrations. However, [Cl^-] in young shoots was similar in all varieties except for 'Major' (Fig. 8A), which did not develop necrotic spots but showed loss of turgidity (Fig. 2C). Ion tissue concentrations in mature leaves were in general higher compared to young tissue and a diversification of the concentration pattern of all varieties was observable.

The average ion accumulation per day of NaCl stress exposure (stress dose) was calculated to relate the ion concentration at the time point of the appearance of symptoms to the length of the respective stress period. This value serves as an evaluation for the height of the daily ion-accumulation to show the potential differences between Na^+

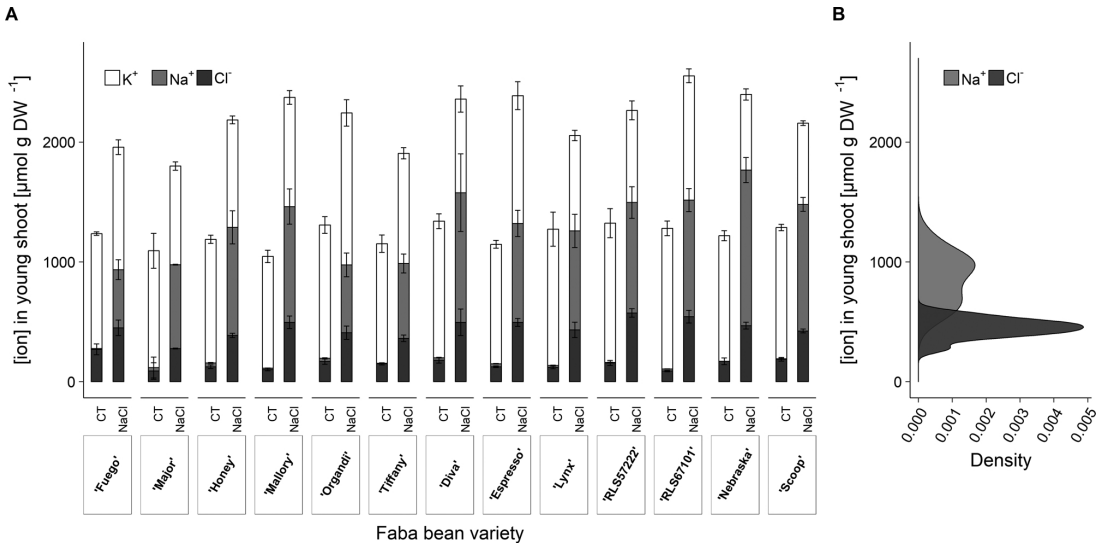

Fig. 6. Ion concentrations in young shoot of faba bean. A) Concentrations of sodium Na^+, chloride Cl^- and potassium K^+, non-stressed controls (CT), 100 mM NaCl (NaCl). B) density plot of Na^+ and Cl^- concentrations in young shoots of 13 averaged NaCl-treated faba bean varieties. Samples were taken when leaf necrosis or loss of turgidity occurred as indicated in Fig. 2. Adjusted means from linear mixed-effect model ± SE; n = 5.

and Cl^- intake of the diverse varieties. The average Na^+ accumulation in young shoot was similar in all varieties with values ranging from 40 to 60 µmol g DW^{-1} d^{-1} (Fig. 8C). Cl^- was accumulated up to 20 µmol g DW^{-1} d^{-1}. The variety 'Mallory' was significantly different to 'Scoop' that had lowest average accumulation of 10 µmol g DW^{-1} d^{-1}. In mature leaves, the average Na^+ accumulation was similar to that of young shoots for all varieties, ranging from 100 to 140 µmol g DW^{-1} d^{-1}, except of 'Honey' with 50 µmol g DW^{-1} d^{-1} (Fig. 8D). In most varieties, Cl^- accumulated up to 40 µmol g DW^{-1} d^{-1}, except for 'Mallory', 'Nebraska' and 'Scoop' which had lower values of about 25 µmol g DW^{-1} d^{-1}. The relative Na^+/K^+ ratios in young shoots and mature leaves increased with NaCl treatment (Fig. 8E, F). Highest increases in young shoot of 600-fold and 200-fold were found in those varieties ('Nebraska', 'Scoop', 'RLS57222') that developed symptoms later than others (Fig. 8E). In mature leaves, the relative Na^+/K^+ ratios of the earlier-symptom developing varieties ('Fuego', 'Major', 'Honey') increased by about 60 to 100-fold whereas the other varieties showed increases of 200-fold or higher (Fig. 8F).

Analysis of principle components (PCA) based on concentrations of Na^+, Cl^- and K^+ revealed that the more salt-sensitive 'Fuego', 'Honey' and 'Organdi' were separated due to higher [K^+] and lower [Na^+], whereas the contrary was found for the later symptom-developing

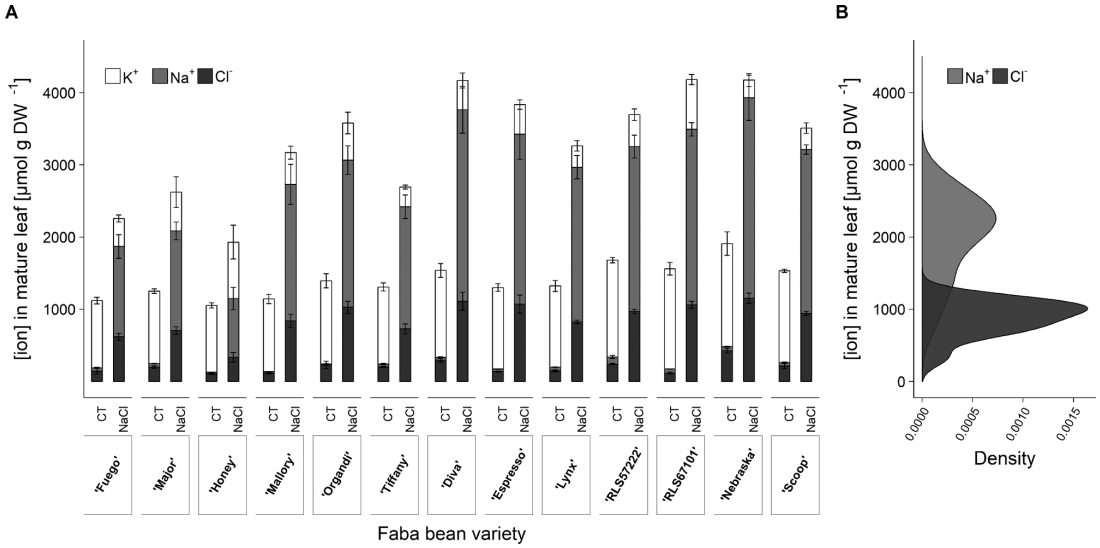

Fig. 7. Ion concentrations in mature leaf (4th) of faba bean. A) Concentrations of sodium Na^+, chloride Cl^- and potassium K^+, non-stressed controls (CT), 100 mM NaCl (NaCl). B) density plot of Na^+ and Cl^- concentrations in mature leaves of 13 averaged NaCl-treated faba bean varieties. Samples were taken when leaf necrosis or loss of turgidity occurred as indicated in Fig. 2. Adjusted means from linear mixed-effect model ± SE; n = 5.

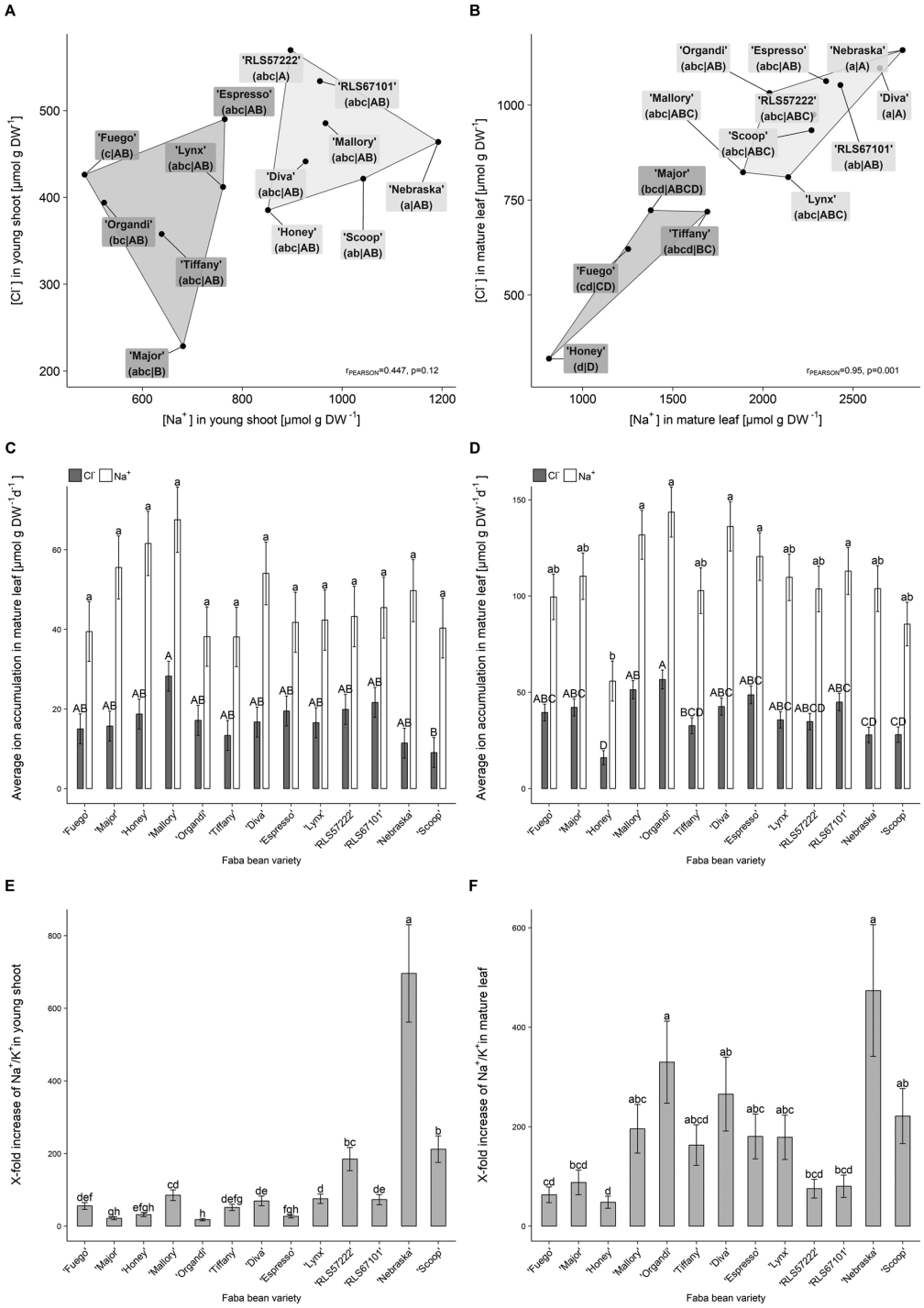

Fig. 8. Comparison of faba bean varieties by means of ion composition at one day after the development of symptoms (Fig. 2). A) Clustering of NaCl-treated faba bean varieties based on concentrations of sodium Na^+, chloride Cl^- and potassium K^+ in young shoot and B) mature leaf. C) Average Cl^- and Na^+ accumulation per day of NaCl application in young shoot and (D) mature leaf. E) Relative increase of Na^+/K^+ ratio in response to salt treatment in young shoot and (F) mature leaf. A–B) Adjusted means from linear mixed-effect model; C–F) Means ± SE. Different letters indicate significant differences: capital letters: Cl^-; lowercase letters: Na^+; $p \leq 0.05$; n = 5.

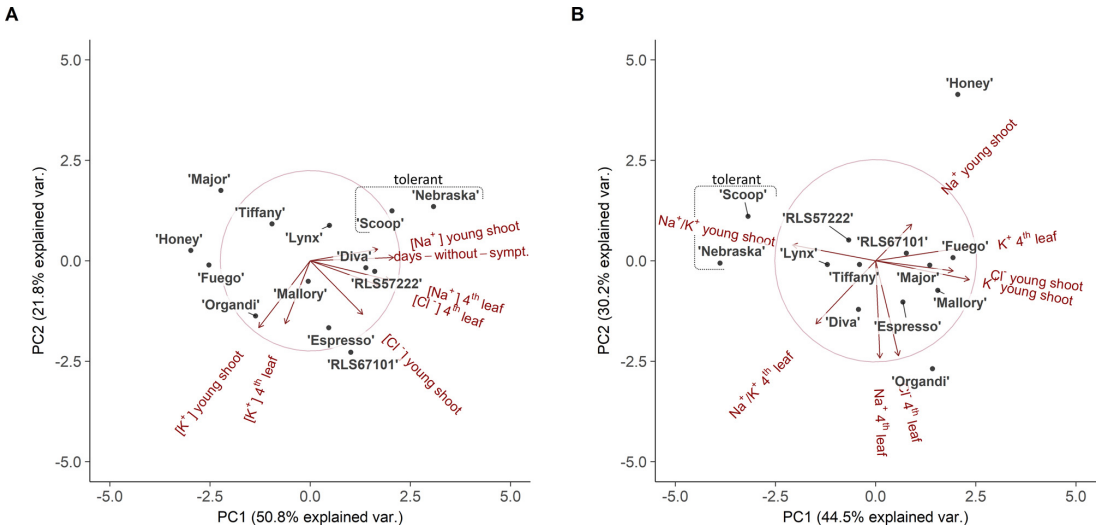

Fig. 9. Principal component analysis of NaCl-treated faba bean varieties A) based on concentrations of sodium Na^+, chloride Cl^- and potassium K^+ in young shoot and mature leaf and B) average Cl^- and Na^+ accumulation per day of NaCl application ('days without symptom') and relative increase of Na^+/K^+ ratio in response to salt treatment in young shoot and mature leaf.

varieties 'Nebraska' and 'Scoop' (Fig. 9A). The variety 'RLS67101', also belonging to the later symptom-developing varieties was characterized by higher $[K^+]$ combined with increased $[Cl^-]$ and $[Na^+]$ in mature leaves. Due to increased $[Na^+]$ and $[Cl^-]$ combined with low $[K^+]$, 'Nebraska' and 'Scoop' were at the right side (Fig. 9A). On the contrary, the variety 'Major' was separately arranged due to lowest $[Cl^-]$ in young shoot. PCA based on the calculated measures, average ion accumulation and increase in Na^+/K^+ ratio, illustrated that the later symptom developing varieties 'Nebraska' and 'Scoop' were separated due to low average shoot Cl^- and K^+ accumulation and highly increased shoot Na^+/K^+ ratio (Fig. 9B). Conversely, the early symptom developing 'Fuego' was at the right side due to higher average shoot Cl^- accumulation as well as higher K^+ accumulation in young shoot and mature leaf (Fig. 9B).

4. Discussion

4.1. Plasticity of NaCl tolerance in Vicia faba

In contrast to common experimental setups using fixed stress exposure time, our experiment was conducted with synchronized stress level to characterize the diverse faba bean varieties as salt sensitive or more tolerant and further evaluate on the basis of ion accumulation patterns how salt ion exclusion and retention mechanisms could have contributed to the observed differences in salt stress tolerance. With this approach it is possible to evaluate the plasticity of either sensitive or more tolerant genotypes differing in their physiological stress response.

Our experimental results show that faba bean varieties differ in their ability to withstand salinity. The plasticity of tolerance to salinity of *V. faba* seems to be broad and even without having the breeding goal of salt tolerance in these German varieties there is a high genetic and physiological variance within this trait. In response to prolonged salt treatment, all varieties except of 'Major' developed necrotic lesions on leaves. The necrotic spot symptom is attributed to the ionic part of salt stress which is an addition of an ionic imbalance together with an ion toxicity caused by high Na^+ concentrations and excess Cl^-. The plant either has to exclude excess ions or deal with these physiological inconveniences. This can be achieved by a so called 'tissue tolerance'. The differences in Na^+/K^+ ratio of the diverse varieties also showed the plasticity of *V. faba* in terms of dealing with ion homeostasis or excessive salt ion accumulation that may lead to cytotoxicity (necrosis) and consequently the loss of photosynthetically active tissue (Fig. 2B) (Geilfus, 2018; Slabu et al., 2009). In faba bean, this 'overcome of tissue tolerance' is a sudden process, as necrotic spots appeared mostly overnight and resulted in leaf senescence within about three days. The difference among sensitive and tolerant varieties was approximately double in NaCl dose that caused symptoms, therefore we consider the plasticity of *V. faba* also as relatively high in terms of salt tolerance mechanisms. In contrast, in the literature *V. faba* is considered as salt sensitive crop (Li et al., 2017; Maas and Hoffman, 1977; Slabu et al., 2009). We think it is of great matter which variety has been used to evaluate this. Of note, the variety 'Major' showed a loss of turgidity and wilting, which represent symptoms that are attributed to osmotic stress (Fig. 2C). In that physiological stage, ion accumulation had likely not yet exceeded the tissue tolerance capacity.

By choosing this experimental setup, salt tolerant plants were evaluated according to their variety-specific growing days without symptoms. On the basis of the temporal difference in development of symptoms referred to as days without symptoms, the variety 'Fuego' was identified as salt sensitive whereas 'Nebraska' and 'Scoop' were more tolerant (Fig. 2A). As biomass increased with growth time (Suppl. Fig. 1), the tolerant varieties tended towards formation of higher biomass of the young shoot fraction, that had developed under full-strength NaCl treatment (100 mM NaCl) (Fig. 3). Interestingly, the shoot growth of the tolerant variety 'Nebraska' appeared to be unaffected by salt treatment although the respective plants had faced the longest stress period before developing symptoms. However, this might be due to a comparatively low growth performance also under control conditions and should therefore not lead to the erroneously conclusion that the variety 'Nebraska' is preferable to that of 'Scoop' in terms of biomass production in saline environments (Fig. 3).

4.2. Oxidative stress, assimilation and transpiration

In order to evaluate physiological parameters such as membrane integrity under stress conditions, we compared variety-specific increases in electrolyte leakage. These are ascribed to stress conditions such as salinity, drought or pathogen attack (Demidchik et al., 2014;

Miller et al., 2010). This membrane damage results from oxidative processes or stress-related decrease of the lipid to protein ratio (Borochov-Neori and Borochov, 1991; Dionisio-Sese and Tobita, 1998). The maintenance of low electrolyte leakage under stress conditions has been associated with tissue tolerance (Arefian and Malekzadeh Shafaroudi, 2015; Bose et al., 2014; Lee and Zhu, 2010; Sudhakar et al., 2001). In our study, electrolyte leakage was measured at the time point when salt lesions appeared meaning that the variety-specific capacity of tissue tolerance was overcome. In this context, electrolyte leakage represents a measure for the intensity of oxidative stress that the plants had been exposed to. In response to salt treatment, all varieties except for 'Major' and 'Honey' had similar electrolyte leakage when salt injuries occurred (Fig. 4). This indicates that the level of oxidative stress was similar for most varieties at the time point when leaf necrosis appeared. However, the membrane integrity of 'Fuego' and 'Honey' was less hampered under conditions of salt stress, but the two varieties were able to endure this stress only for 12 and 14 days, respectively. Because those varieties that developed symptoms later under stress conditions had increased relative electrolyte leakage, we conclude that impaired membrane integrity is a consequence of increasing salt ion accumulation but does not necessarily lead to the formation of leaf necrosis.

Leaf transpiration (*E*) and assimilation rate (*A*) are non-destructive measurements representing a physiological indicator for salt tolerance that allows conclusions to be made with regard to the health and functional integrity of leaves (Munns et al., 2016). We performed these non-destructive physiological measurements at the 4th leaves, which later were analyzed for their K^+, Na^+, and Cl^- concentrations for better comparison (Fig. 7A). Faba bean growing under saline conditions responded by reducing *E* to avoid undesired water loss (Fig. 5) (Geilfus et al., 2015a; Keisham et al., 2018; Roy et al., 2014). Unlike to our expectations the more tolerant varieties maintained even higher *E* than sensitive ones, in contrast one would expect that a reduction in *E* is an essential attribute to save water (Fig. 5). Moreover, as stomata regulate access of CO_2 to photosynthetic active tissues, a decreased stomatal conductivity is assumed to compromise assimilation rate by restricting CO_2 diffusion into leaves (Lawson and Blatt, 2014). Although *E* and therefore CO_2 influx did not decrease or only slightly decrease since the continuing stress period, a significant decrease of *A* was seen from 3 to 5 days after full-strength salt stress application for some varieties. Especially the salt sensitive varieties 'Fuego', 'Major' and 'Honey' showed this trend of a continuously decreasing *A* until salt lesions had occurred. In contrast, the tolerant varieties maintained higher *E* and *A* during prolonged exposure to salt (Fig. 5). Besides the inhibitory effect of osmotic stress that results in photorespiration and decrease of *A*, an unbalanced chloroplastidial Cl^- homeostasis is expected to compromise photosynthesis. Under salinity, field bean accumulates Cl^- in chloroplasts that might reduce photosynthetic quantum yield by reduction in chlorophyll content (Slabu et al., 2009; Tavakkoli et al., 2010). In addition, the inhibition of CO_2 fixing enzymes, disturbed dark relaxation of chloroplasts, damage of PSII reaction centers due to photoinhibition as well as excessive production of ROS in chloroplasts were associated with excess chloroplastidial Cl^- (Geilfus, 2018). Hence, a decreasing *A*, which is not directly limited by reduced stomatal conductivity, might be explained by excess Cl^- that had been translocated into the shoot and ultimately accumulated in chloroplasts. This explanation is consistent with the differences in variety-specific Cl^- translocation to the young shoot and mature leaves (Fig. 7C, D), which potentially enabled the tolerant varieties to protect their sites of primary photosynthesis more efficiently from excess Cl^- intake and thus may help preventing chlorophyll degradation and the resulting decrease of *A* (Fig. 5; Suppl. Table 1).

4.3. Tolerant *V. faba* varieties sequester Na^+ ions

All varieties accumulated Na^+ and Cl^- ions but to a different extent (Figs. 6A, 7 A). The Na^+ concentration increased with the length of NaCl-stress exposure. Consequently, longer growing varieties had higher Na^+/K^+ ratios compared with NaCl-sensitive varieties such as 'Fuego' (Fig. 7E, F). In particular, the most tolerant varieties 'Nebraska' and 'Scoop' showed highest and second highest relative Na^+/K^+ ratios in both young shoots and mature leaves (Figs. 8E, F; 9 B). Sodium is often referred to as the most toxic ion in plants at saline conditions, because high cytosolic concentrations disturb K^+-homeostasis and therefore interfere with enzyme function and the regulation of stomatal aperture under saline conditions (Deinlein et al., 2014; Flowers et al., 2015; Hasegawa, 2013; Munns et al., 2016). However, the ion pattern at the time point of a similar stress level revealed that the maintenance of a low Na^+/K^+ ratio seems to be a less important attribute for salt tolerance in faba bean. This finding is in line with previous work in which legumes were associated with Cl^- sensitivity (Geilfus, 2018; Li et al., 2017; Teakle and Tyerman, 2010). We found highly increased relative Na^+/K^+ ratio in leaves of such varieties that showed earlier leaf necrotic spots such as 'Mallory' and 'Organdi' (Fig. 7E, F) and in varieties that developed symptoms the latest, such as 'Scoop' and 'Nebraska'. This implies that the shoot Na^+ translocation of those varieties was less controlled, meaning that tolerance in terms of Na^+ exclusion and retention was less pronounced. Therefore, mechanisms enabling tolerance to Na^+ in faba bean occurred most probably as tissue tolerance, since the Na^+ accumulation appeared to predominantly depend on the length (dose) of the salt exposure. As a consequence, excessive Na^+ in the shoot needed to be effectively sequestered because K^+ homeostasis is essential for cell function (Munns et al., 2016; Zörb et al., 2014). The ability to maintain K^+ homeostasis in root and leaf tissues and thereby protecting balanced cytosolic Na^+/K^+ ratio under saline conditions represents an important trait contributing to salt tolerance (Hauser and Horie, 2010; Wu et al., 2018). Hence, those varieties showing highly increased Na^+/K^+ ratios must have been effectively compartmentalizing Na^+ away from the cytosol, *e.g. via* compartmentalization into the vacuole (Munns et al., 2016; Percey et al., 2016). This makes ions to a certain extent available as 'cheap' osmolytes (Blumwald, 2000; Keisham et al., 2018; Niu et al., 1995). The cheap usage of salt ions for osmotic adjustment represents a physiological adaption of naturally salt tolerant halophytes and preserves energy for growth, as the synthesis of organic solutes is energetically more expensive. Further, sequestering Na^+ into the vacuole is preferential over the removal into the apoplast, as it contributes to membrane potential *via* removing positive charge from the cytosol. Thereby, the relocation of K^+ from the vacuole into the cytosol and the retention of cytosolic K^+ is favored (Percey et al., 2016). Thus, the later symptom-developing field bean varieties may have been able to effectively sequester Na^+ ions into the vacuole enabling an increased K^+ retention and a better control of their water status (Fig. 5) (Flowers and Colmer, 2008; Mancarella et al., 2016; Pan et al., 2016; Wu et al., 2018).

4.4. Leaf necrosis appears at distinct Cl^- concentrations in all *V. faba* varieties

Many previous salt-stress experiments were rather focused on Na^+ than Cl^-. However, in few papers legumes have been reported to be sensitive to Cl^- (Li et al., 2017; Teakle and Tyerman, 2010). In addition to the role of Cl^- in the initiation of stomatal closure during the early NaCl-stress response (Geilfus and Mühling, 2013), some evidence has been found for Cl^- being the predominant toxic ion in faba bean, affecting photosynthesis and plant growth to a greater extent than Na^+ (Slabu et al., 2009; Tavakkoli et al., 2010). Besides indications on the adverse effects on *A* (Fig. 5), we have found that irrespective of the duration until symptoms occurred, all varieties, *e.g.* those growing 12 or 26 days, had comparable [Cl^-] in young shoots and mature leaves that were harvested when the plants had developed leaf necrosis (Figs. 6B; 7 B). Based on this observation and in line with previous work we conclude that the [Cl^-] in developing leaves might be the critical factor contributing to ion toxicity for faba bean growing under NaCl salinity

(Geilfus, 2018; Tavakkoli et al., 2010). A critical role for Na^+ appears less relevant, as Na^+ concentrations fluctuated across the varieties at the time point when symptoms occurred (Figs. 6B, 7 B, 9 A). Thus, NaCl tolerance and the ability to withstand salinity (´days without symptoms´) may depend on the ability to restrict the transfer of excess Cl^- to photosynthetically active tissues (Figs. 8C; 9 B). Of note, as Cl^- interferes with NO_3^- uptake an increased NO_3^- selectivity over Cl^-, representing a feature of naturally salt tolerant halophytes, might also be beneficial for glycophytes alongside with avoidance of excess Cl^- uptake (Bazihizina et al., 2018). However, the more tolerant 'Scoop' and 'Nebraska' accumulated fewer Cl^- and therefore might suffered less from excessive ROS production and chlorophyll degradation during the early stress phase than sensitive varieties (Bose et al., 2017; Tavakkoli et al., 2010). Therefore, Cl^- accumulation in the cytosol and further uptake into chloroplasts is expected to be a key factor of ion toxicity in faba bean finally resulting in leaf necrotic spots.

5. Conclusion

In faba bean, ion homeostasis-associated tolerance mechanisms seem to be handled opposingly for Na^+ and Cl^-. Faba bean varieties are tolerant to Na^+ accumulation and consequently Na^+/K^+ ratio is of less importance for evaluating their salt tolerance level. Presumably, tolerance to Na^+ occurred predominantly at the level of tissue tolerance after Na^+ had entered the leaf. Conversely, Cl^- tissue tolerance is weak throughout all 13 *V. faba* varieties as Cl^- concentrations were distinct at the time point of occurring symptoms. Therefore, tolerance to Cl^- was rather facilitated by a restriction of Cl^- entering the plant's shoot. In accordance with the hypothesized Cl^- sensitivity of legumes, Cl^- shoot translocation might be a key process explaining the observed physiological plasticity in the ability to withstand salinity between the diverse *V. faba* varieties.

Conflict of interest

We declare that there are no conflicts of interest.

Authors contribution

BLF, CMG and CZ conceived the study. BLF, MK and XZ conducted the experiments and analysed the data. BLF, CMG and CZ interpreted the data with input from XZ and MK. CZ, CMG and BLF wrote the manuscript. All authors reviewed and approved the manuscript.

Funding

This work was supported by the Deutsche Forschungsgemeinschaft (ZO/08); project number 320167376.

Acknowledgments

We thank our colleagues Dr. Monika Wimmer, Dr. Nikolaus Merkt, Maria L. Romo-Perez and Jan H. Behr for discussions and remarks.

Appendix A. Supplementary data

Supplementary material related to this article can be found, in the online version, at doi:https://doi.org/10.1016/j.jplph.2019.02.012.

References

Amede, T., Schubert, S., Stahr, K., 2003. Mechanisms of drought resistance in grain legumes I: osmotic adjustment. Ethiop. J. Sci. 26 (1), 37–46.
Arefian, M., Malekzadeh Shafaroudi, S., 2015. Physiological and gene expression analysis of extreme chickpea (*Cicer arietinum* L.) genotypes in response to salinity stress. Acta Physiol. Plant. 37 (9), 193. https://doi.org/10.1007/s11738-015-1945-1.
Bates, D., Maechler, M., Bolker, B., Walker, S., 2015. Fitting linear mixed-effects models using lme4. J. Stat. Softw. 1–48.
Bazihizina, N., Colmer, T.D., Cuin, T.A., Mancuso, S., Shabala, S., 2018. Friend or foe? Chloride patterning in halophytes. Trends Plant Sci. https://doi.org/10.1016/j.tplants.2018.11.003.
Blumwald, E., 2000. Sodium transport and salt tolerance in plants. Curr. Opin. Cell Biol. 12 (4), 431–434. https://doi.org/10.1016/S0955-0674(00)00112-5.
Borochov-Neori, H., Borochov, A., 1991. Response of melon plants to salt: 1. Growth, morphology and root membrane properties. J. Plant Physiol. 139 (1), 100–105.
Bose, J., Rodrigo-Moreno, A., Shabala, S., 2014. ROS homeostasis in halophytes in the context of salinity stress tolerance. J. Exp. Bot. 65 (5), 1241–1257. https://doi.org/10.1093/jxb/ert430.
Bose, J., Munns, R., Shabala, S., Gilliham, M., Pogson, B., Tyerman, S.D., 2017. Chloroplast function and ion regulation in plants growing on saline soils: lessons from halophytes. J. Exp. Bot. 68 (12), 3129–3143. https://doi.org/10.1093/jxb/erx142.
Butcher, K., Wick, A.F., DeSutter, T., Chatterjee, A., Harmon, J., 2016. Soil salinity: a threat to global food security. Agron. J. 108 (6), 2189–2200. https://doi.org/10.2134/agronj2016.06.0368.
Crépon, K., Marget, P., Peyronnet, C., Carrouée, B., Arese, P., Duc, G., 2010. Nutritional value of faba bean *(Vicia faba* L.) seeds for feed and food. Field Crops Res. 115 (3), 329–339. https://doi.org/10.1016/j.fcr.2009.09.016.
Deinlein, U., Stephan, A.B., Horie, T., Luo, W., Xu, G., Schroeder, J.I., 2014. Plant salt-tolerance mechanisms. Trends Plant Sci. 19 (6), 371–379. https://doi.org/10.1016/j.tplants.2014.02.001.
Demidchik, V., Straltsova, D., Medvedev, S.S., Pozhvanov, G.A., Sokolik, A., Yurin, V., 2014. Stress-induced electrolyte leakage: the role of K^+-permeable channels and involvement in programmed cell death and metabolic adjustment. J. Exp. Bot. 65 (5), 1259–1270. https://doi.org/10.1093/jxb/eru004.
Dionisio-Sese, M.L., Tobita, S., 1998. Antioxidant responses of rice seedlings to salinity stress. Plant Sci. 135 (1), 1–9. https://doi.org/10.1016/S0168-9452(98)00025-9.
Farooq, M., Hussain, M., Wakeel, A., Siddique, K.H.M., 2015. Salt stress in maize: effects, resistance mechanisms, and management. A review. Agron. Sustain. Dev. 35 (2), 461–481. https://doi.org/10.1007/s13593-015-0287-0.
Flowers, T.J., Colmer, T.D., 2008. Salinity tolerance in halophytes. New Phytol. 179 (4), 945–963. https://doi.org/10.1111/j.1469-8137.2008.02531.x.
Flowers, T.J., Munns, R., Colmer, T.D., 2015. Sodium chloride toxicity and the cellular basis of salt tolerance in halophytes. Ann. Bot. 115 (3), 419–431. https://doi.org/10.1093/aob/mcu217.
Fox, J., Weisberg, S., 2011. An {R} Companion to Applied Regression. R Foundation for Statistical Computing. Sage, Thousand Oaks {CA}.
Geilfus, C.-M., 2018. Chloride: from nutrient to toxicant. Plant Cell Physiol. 59 (5), 877–886. https://doi.org/10.1093/pcp/pcy071.
Geilfus, C.M., Mühling, K.H., 2013. Ratiometric monitoring of transient apoplastic alkalinizations in the leaf apoplast of living *Vicia faba* plants: chloride primes and $PM–H^+$-ATPase shapes NaCl-induced systemic alkalinizations. New Phytol. 197 (4), 1117–1129. https://doi.org/10.1111/nph.12046.
Geilfus, C.M., Mithofer, A., Ludwig-Muller, J., Zorb, C., Muehling, K.H., 2015a. Chloride-inducible transient apoplastic alkalinizations induce stomata closure by controlling abscisic acid distribution between leaf apoplast and guard cells in salt-stressed *Vicia faba*. New Phytol. 208 (3), 803–816. https://doi.org/10.1111/nph.13507.
Geilfus, C.M., Niehaus, K., Godde, V., Hasler, M., Zorb, C., Gorzolka, K., Jezek, M., Senbayram, M., Ludwig-Muller, J., Muhling, K.H., 2015b. Fast responses of metabolites in *Vicia faba* L. to moderate NaCl stress. Plant Physiol. Biochem. 92, 19–29. https://doi.org/10.1016/j.plaphy.2015.04.008.
Graves, S., Piepho, H.-P., Selzer, L., Dorai-Raj, S., 2015. multcompView: Visualizations of Paired Comparisons. R Package Version 0.1-7.multcompView: Visualizations of Paired Comparisons. R Package Version 0.1-7.
Hasegawa, P.M., 2013. Sodium (Na^+) homeostasis and salt tolerance of plants. Environ. Exp. Bot. 92, 19–31. https://doi.org/10.1016/j.envexpbot.2013.03.001.
Hasegawa, P.M., Bressan, R.A., Zhu, J.K., Bohnert, H.J., 2000. Plant cellular and molecular responses to high salinity. Annu. Rev. Plant Physiol. Plant Mol. Biol. 51 (1), 463–499. https://doi.org/10.1146/annurev.arplant.51.1.463.
Hauser, F., Horie, T., 2010. A conserved primary salt tolerance mechanism mediated by HKT transporters: a mechanism for sodium exclusion and maintenance of high K^+/Na^+ ratio in leaves during salinity stress. Plant Cell Environ. 33 (4), 552–565. https://doi.org/10.1111/j.1365-3040.2009.02056.x.
Hennig, C., 2015. fpc: Flexible Procedures for Clustering. R Package Version 2.1-10.
Jensen, E.S., Peoples, M.B., Hauggaard-Nielsen, H., 2010. Faba bean in cropping systems. Field Crops Res. 115 (3), 203–216. https://doi.org/10.1016/j.fcr.2009.10.008.
Kabbadj, A., Makoudi, B., Mouradi, M., Pauly, N., Frendo, P., Ghoulam, C., 2017. Physiological and biochemical responses involved in water deficit tolerance of nitrogen-fixing Vicia faba. PLoS One 12 (12), e0190284. https://doi.org/10.1371/journal.pone.0190284.
Keisham, M., Mukherjee, S., Bhatla, S.C., 2018. Mechanisms of sodium transport in plants—progresses and challenges. Int. J. Mol. Sci. 19 (3), 647. https://doi.org/10.3390/ijms19030647.
Köpke, U., Nemecek, T., 2010. Ecological services of faba bean. Field Crops Res. 115 (3), 217–233. https://doi.org/10.1016/j.fcr.2009.10.012.
Lawson, T., Blatt, M.R., 2014. Stomatal size, speed, and responsiveness impact on photosynthesis and water use efficiency. Plant Physiol. 164 (4), 1556–1570. https://doi.org/10.1104/pp.114.237107.
Lee, B.-h., Zhu, J.-K., 2010. Phenotypic analysis of Arabidopsis mutants: electrolyte leakage after freezing stress. Cold Spring Harb. Protoc. 2010 (1). https://doi.org/10.1101/pdb.prot4970. pdb. prot4970.
Li, B., Tester, M., Gilliham, M., 2017. Chloride on the move. Trends Plant Sci. 22 (3), 236–248. https://doi.org/10.1016/j.tplants.2016.12.004.
Maas, E., Hoffman, G., 1977. Crop salt tolerance – current assessment. J. Irrig. Drain. Div.

Am. Soc. Civil Eng. 103 (IR2), 115–134.
Mancarella, S., Orsini, F., Van Oosten, M.J., Sanoubar, R., Stanghellini, C., Kondo, S., Gianquinto, G., Maggio, A., 2016. Leaf sodium accumulation facilitates salt stress adaptation and preserves photosystem functionality in salt stressed *Ocimum basilicum*. Environ. Exp. Bot. 130, 162–173. https://doi.org/10.1016/j.envexpbot.2016.06.004.
Miller, G., Suzuki, N., Ciftci-Yilmaz, S., Mittler, R., 2010. Reactive oxygen species homeostasis and signalling during drought and salinity stresses. Plant Cell Environ. 33 (4), 453–467. https://doi.org/10.1111/j.1365-3040.2009.02041.x.
Munns, R., Tester, M., 2008. Mechanisms of salinity tolerance. Annu. Rev. Plant Biol. 59 (1), 651–681. https://doi.org/10.1146/annurev.arplant.59.032607.092911.
Munns, R., Wallace, P.A., Teakle, N.L., Colmer, T.D., 2010. Measuring soluble ion concentrations (Na^+, K^+, Cl^-) in salt-treated plants. In: Sunkar, R. (Ed.), Plant Stress Tolerance: Methods and Protocols. Humana Press, Totowa, NJ, pp. 371–382.
Munns, R., James, R.A., Gilliham, M., Flowers, T.J., Colmer, T.D., 2016. Tissue tolerance: an essential but elusive trait for salt-tolerant crops. Funct. Plant Biol. 43 (12), 1103–1113. https://doi.org/10.1071/FP16187.
Niu, X., Bressan, R.A., Hasegawa, P.M., Pardo, J.M., 1995. Ion homeostasis in NaCl stress environments. Plant Physiol. 109 (3), 735.
Pan, Y.-Q., Guo, H., Wang, S.-M., Zhao, B., Zhang, J.-L., Ma, Q., Yin, H.-J., Bao, A.-K., 2016. The photosynthesis, Na^+/K^+ homeostasis and osmotic adjustment of *Atriplex canescens* in response to salinity. Front. Plant Sci. 7, 848. https://doi.org/10.3389/fpls.2016.00848.
Percey, W.J., Shabala, L., Wu, Q., Su, N., Breadmore, M.C., Guijt, R.M., Bose, J., Shabala, S., 2016. Potassium retention in leaf mesophyll as an element of salinity tissue tolerance in halophytes. Plant Physiol. Biochem. 109, 346–354. https://doi.org/10.1016/j.plaphy.2016.10.011.
R Development Core Team, 2017. R: A Language and Environment for Statistical Computing. R Foundation for Statistical Computing, Vienna, Austria.
Richter, J.A., Erban, A., Kopka, J., Zörb, C., 2015. Metabolic contribution to salt stress in two maize hybrids with contrasting resistance. Plant Sci. 233, 107–115. https://doi.org/10.1016/j.plantsci.2015.01.006.
Roy, S.J., Negrão, S., Tester, M., 2014. Salt resistant crop plants. Curr. Opin. Biotechnol. 26, 115–124. https://doi.org/10.1016/j.copbio.2013.12.004.
Slabu, C., Zörb, C., Steffens, D., Schubert, S., 2009. Is salt stress of faba bean (*Vicia faba*) caused by Na^+ or Cl– toxicity? J. Plant Nutr. Soil Sci. (1999) 172 (5), 644–651. https://doi.org/10.1002/jpln.200900052.
Sudhakar, C., Lakshmi, A., Giridarakumar, S., 2001. Changes in the antioxidant enzyme efficacy in two high yielding genotypes of mulberry (*Morus alba* L.) under NaCl salinity. Plant Sci. 161 (3), 613–619. https://doi.org/10.1016/S0168-9452(01)00450-2.
Tavakkoli, E., Rengasamy, P., McDonald, G.K., 2010. High concentrations of Na^+ and Cl^- ions in soil solution have simultaneous detrimental effects on growth of faba bean under salinity stress. J. Exp. Bot. 61 (15), 4449–4459. https://doi.org/10.1093/jxb/erq251.
Teakle, N.L., Tyerman, S.D., 2010. Mechanisms of Cl^- transport contributing to salt tolerance. Plant Cell Environ. 33 (4), 566–589. https://doi.org/10.1111/j.1365-3040.2009.02060.x.
Tester, M., Davenport, R., 2003. Na^+ tolerance and Na^+ transport in higher plants. Ann. Bot. 91 (5), 503–527. https://doi.org/10.1093/aob/mcg058.
Turpin, J., Herridge, D., Robertson, M., 2002. Nitrogen fixation and soil nitrate interactions in field-grown chickpea (*Cicer arietinum*) and fababean (*Vicia faba*). Aust. J. Agric. Res. 53 (5), 599–608. https://doi.org/10.1071/AR01136.
Vu, V.Q., 2011. ggbiplot: A ggplot2 Based Biplot. R Package Version 0.55.
Wang, W., Vinocur, B., Altman, A., 2003. Plant responses to drought, salinity and extreme temperatures: towards genetic engineering for stress tolerance. Planta 218 (1), 1–14. https://doi.org/10.1007/s00425-003-1105-5.
Wedeking, R., Mahlein, A.-K., Steiner, U., Oerke, E.-C., Goldbach, H.E., Wimmer, M.A., 2017. Osmotic adjustment of young sugar beets *(Beta vulgaris*) under progressive drought stress and subsequent rewatering assessed by metabolite analysis and infrared thermography. Funct. Plant Biol. 44 (1), 119–133. https://doi.org/10.1071/FP16112.
Wei, T., Simko, V., 2017. R Package "corrplot": Visualization of a Correlation Matrix (Version 0.84).
Wickham, H., 2016. ggplot2: Elegant Graphics for Data Analysis. Springer-Verlag, New York.
Wu, H., Zhang, X., Giraldo, J.P., Shabala, S., 2018. It is not all about sodium: revealing tissue specificity and signalling roles of potassium in plant responses to salt stress. Plant Soil 431 (1), 1–17. https://doi.org/10.1007/s11104-018-3770-y.
Zörb, C., Senbayram, M., Peiter, E., 2014. Potassium in agriculture–status and perspectives. J. Plant Physiol. 171 (9), 656–669. https://doi.org/10.1016/j.jplph.2013.08.008.

Supplementary material

Supplementary material 1.1: Correlation matrix of ion concentrations and physiological measurements of 13 salt-stressed V. faba varieties (100 mM NaCl). Correlations between concentrations of sodium (Na^+), chloride (Cl^-) and potassium (K^+) in young shoots and mature leaves and electrolyte leakage, days without symptoms and stomatal conductivity. Plant material for ion determination was collected when plants of a variety developed visible salt injuries (see Fig. 2). Stomatal conductivity was measured at mature leaves (4^{th}) 3, 5, 7 and 10 days after full-strength NaCl treatment was applied. Correlations with $P \leq 0.01$ are colour-coded; blue, positive; red, negative.

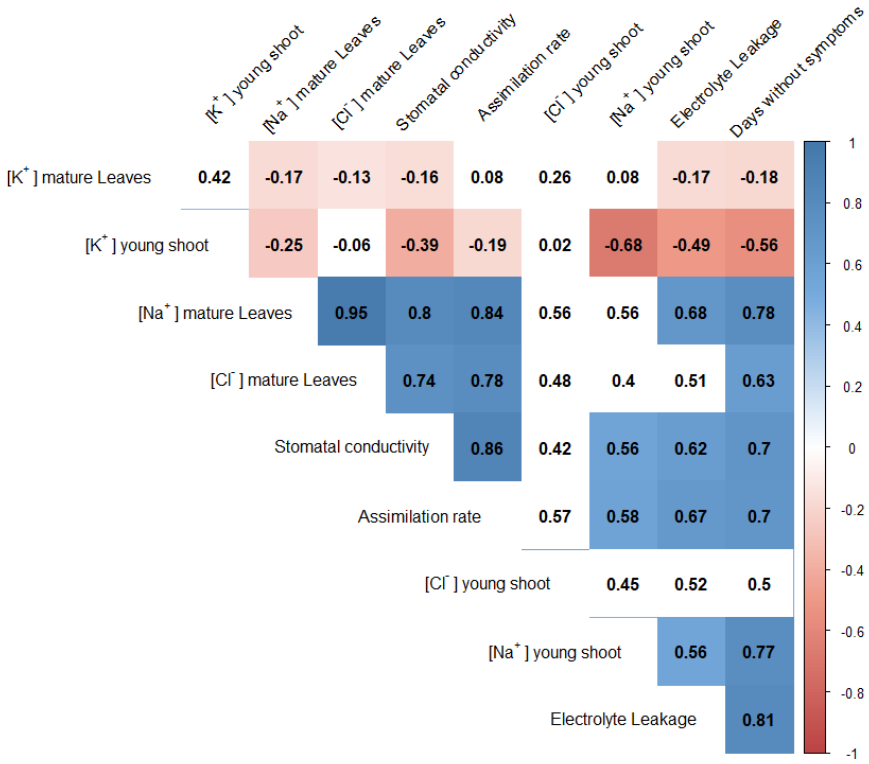

Supplementary material 1.2: Decrease of SPAD value of 13 salt-stressed (100 mM NaCl) *V. faba* varieties during various stress periods (according to days without symptoms). Initial SPAD was measured 3 days after full-strength NaCl stress was applied; Last SPAD measurement was conducted before symptoms occurred. Means from linear model ± SE. Different letters indicate significant inter-variety differences; $P \leq 0.05$; n = 3.

***V. faba* L. variety**	**SPAD decrase** [unitless]	**stress period** [d]
'Fuego'	-1.9±1.2 C	9
'Major'	-5.1±1.2 ABC	9
'Honey'	-3.0±1.2 BC	11
'Mallory'	-2.9±1.2 BC	11
'Organdi'	-2.1±1.2 BC	11
'Tiffany'	-1.9±1.2 C	13
'Diva'	-3.7±1.2 ABC	16
'Espresso'	-2.1±1.2 BC	16
'Lynx'	-3.9±1.2 ABC	16
'RLS5722'	-8.2±1.2 AB	18
'RLS67101'	-9.5±1.2 A	18
'Nebraska'	-4.0±1.2 ABC	23
'Scoop'	-4.0±1.2 ABC	23

Chapter 3

The early stress response of maize (*Zea mays* L.) to chloride salinity

Xudong Zhang, Christian Zörb, Markus Kränzlein,
Bastian L. Franzisky, Christoph-Martin Geilfus

Journal of Agronomy and Crop Science 205 (2019) 586-597

Received: 8 April 2019 | Revised: 18 June 2019 | Accepted: 21 June 2019

DOI: 10.1111/jac.12356

SALINITY STRESS

Journal of Agronomy and Crop Science | WILEY

The early stress response of maize (*Zea mays* L.) to chloride salinity

Xudong Zhang[1] | Christian Zörb[1] | Markus Kränzlein[1] | Bastian L. Franzisky[1] | Hartmut Kaiser[2] | Christoph-Martin Geilfus[3]

[1]Institute of Crop Science, Quality of Plant Products, University of Hohenheim, Stuttgart, Germany

[2]Botanisches Institut, Christian-Albrechts-Universität zu Kiel, Kiel, Germany

[3]Division of Controlled Environment Horticulture, Faculty of Life Sciences, Albrecht Daniel Thaer-Institute of Agricultural and Horticultural Sciences, Humboldt-University of Berlin, Berlin, Germany

Correspondence
Christoph-Martin Geilfus, Division of Controlled Environment Horticulture, Faculty of Life Sciences, Albrecht Daniel Thaer-Institute of Agricultural and Horticultural Sciences, Humboldt-University of Berlin, Albrecht-Thaer-Weg 1, 14195 Berlin, Germany.
Email: geilfusc@hu-berlin.de

Present address
Hartmut Kaiser, Instiut für Pflanzenernährung und Bodenkunde, Christian-Albrechts-Universität zu Kiel, Kiel, Germany

Funding information
Deutsche Forschungsgemeinschaft, Grant/Award Number: GE 3111/1-1; China Scholarship Council, Grant/Award Number: 201606300005

Abstract

Chloride is a micronutrient required for photosynthesis but when applied in the concentration of a macronutrient, it may also promote growth by regulating turgor. However, if chloride accumulates excessively, it can induce toxicity. The aim of this study was to identify physiological dysfunctions in maize (*Zea mays* L.) that arise in response to excessive chloride ion accumulation. For this, a novel water sensor was employed for the first time allowing the in vivo measurement of water content in the plant by using two near IR-wavelengths with different absorption of water. This enabled to analyse whether water imbalances occurred. Chloride was given together with calcium as companying counter cation. Results show that most of the tested maize genotypes were able to maintain growth, photosynthesis and normal water content when stressed with concentrations as high as 757.1 mg chloride/kg soil dry matter. Leaf blades accumulated only 8.5 mg chloride/g dry matter, with the most genotypes not even showing salt stress necrosis at the leaves. A comparison between more tolerant and more sensitive genotypes revealed that restriction of chloride root-to-shoot translocation is a trait of chloride tolerance.

KEYWORDS

chloride salinity, maize (*Zea mays* L.), photosynthetic rate, salt exclusion, tolerance, water content

1 | INTRODUCTION

Chloride (Cl^-) is an element, that is, required for photosynthesis (Arnon & Whatley, 1949). Moreover, it can stimulate the activity of the tonoplast-type H^+-ATPase (Churchill & Sze, 1984; Randall & Sze, 1986) and it can be effective in the regulation of turgor (Fromm & Eschrich, 1989; Geilfus, 2018a). Most glycophytic crop plants contain approximately 1–20 mg/g Cl^- dry matter (DM) (Marschner, 2011). Minimal Cl^- requirements vary in the shoots of crops such as rice (*Oryza sativa;* 3 mg/g DM), wheat (*Triticum aestivum;* 1.2–4 mg/g DM), barley (*Hordeum vulgare;* 0.14 mg/g DM) (Marschner, 2011). In cotton, Cl^- predominantly allocates in vegetative plant tissues such as leaf and stem, which is why the concentration is highest in leaves, being followed by stem, root, seed and fibre (Chen, He, He, Yang, Mishra, & Stoffella, 2010). Maize is regarded as a moderately sensitive crop with regard to NaCl (Farooq, Hussain, Hussain, Wakeel, & Siddique, 2015).

Chloride is the dominant form of chloride in soils. It is very mobile in soil solution because of its high water solubility (Reeder, 2006). For being taken up, Cl^- is transported from the soil solution to the

Correction added on 6 August 2019 after first online publication: One of the reference citations was removed from this version of the article.

root vascular stele, with symplastic transport as the dominant pathway for Cl^- (Teakle & Tyerman, 2010). Upon entering the root xylem, Cl^- is acropetally transported to the shoot (Gong et al., 2010), where it is released and may be compartmented by the phloem (Lessani & Marschner, 1978). Cl^- can also be stored in cell vacuoles (De Angeli, Zhang, Zhang, Meyer, & Martinoia, 2013).

Chloride was thought to improve yield in winter wheat by increasing turgor pressure of leaves, facilitating expanding growth (Christensen, Taylor, Taylor, Jackson, & Mitchell, 1981). Generally, Cl^- content is critical not only for yield but also for quality (Geilfus, 2018a). The osmotic properties of Cl^- can increase turgor enabling turgor-driven movements, drive water flow, promoting compound migration and influence source-sink partitioning (Romo & Haferkamp, 1987).

Excessive concentration of Cl^- in soil, as it occurs under NaCl based soil salinity, can lead to an increased Cl^- uptake. As a consequence, cellular Cl^- levels can rise up to toxic levels, hampering plant growth and development (Geilfus, 2018b). High Cl can also alter transcript abundance of abscisic acid (ABA) biosynthetic genes, as shown for maize (Geilfus, Ludwig-Müller, Ludwig-Müller, Bárdos, & Zörb, 2018) and alter compartmental distribution of ABA between the leaf apoplast and the guard cells (Geilfus, Mithöfer, Mithöfer, Ludwig-Müller, Zörb, & Muehling, 2015). The latter controls apoplastic pH (Geilfus, 2017) and stomata closure in salt-stressed field bean (*Vicia faba* L.). A Cl^--induced transient alkalinization of the leaf apoplast stiffens the cell wall during onset of Cl^- salinity in maize leaves, thus being related to the growth reduction under NaCl salinity (Geilfus, Tenhaken, Tenhaken, & Carpentier, 2017).

Excessive Cl^- may accumulate in the chloroplast, which is thought to negatively affect chlorophyll content due to degradation. (Slabu, Zörb, Zörb, Steffens, & Schubert, 2009). As a result, photosynthesis might be impeded giving rise for radical formation. Radicals can destroy photosystem II (PSII) reaction centres (Foyer, Lelandais, Lelandais, & Kunert, 1994). Since Cl^- also acts as an osmoticum, excessive NaCl concentrations in the leaf apoplast may cause cellular damage by disturbing cellular water relations (Oertli, 1968).

Salt exclusion is commonly implemented by preferably accumulating ions in the root or in some relatively insensitive tissues of the shoot of plants under NaCl stress (Boursier, Lynch et al. 1987). Moreover, ion partitioning status of various plant organs is highly related with their potential salt resistance mechanisms. Specifically speaking, a larger amount of Cl^- into the sheath relative to the blade tissue was found in the leaves of young barley (*Hordeurn vulgare L.*) exposed to moderate levels of NaCl salinity (Boursier, Lynch et al. 1987). Cl^- partitioning in the sheaths of plants was also observed in wheat (*Triticum aestivum L.*), maize (*Zea mays L.*) and sorghum (*Sorghum bicolor L.*) (Boursier, Lynch et al. 1984).

This work aimed to screen eight maize genotypes for differences in the ability to grow under conditions of excessive soil Cl^-. A comparison of the individual tissue distribution of Cl^- in those contrasting genotypes was conducted to give clues about the physiological basis of the ability to withstand high Cl^- concentration in the soil, being given as $CaCl_2{}^*2H_2O$. For this, maize were cultivated for nine weeks in Mitscherlich pots using sandy soil. To group the plants into Cl^- includer or excluder, the Cl^- root-to-shoot translocation was determined as the ratio of total shoot Cl^- content to the total root Cl^- content.

2 | MATERIALS AND METHODS

2.1 | Material

Eight maize genotypes (Table 1) were planted (one maize plant per pot) and grown under three Cl^- concentrations (8.75 [control], 63.2 and 757.1 mg Cl^-/kg soil DM, respectively). Chloride was given together with calcium as companying counter cation, using $CaCl_2{}^*2H_2O$. Control conditions equal normal non-saline soils. For the easy sake of reading, we abbreviated the three Cl^- concentrations with "control," "low" and "high" treatment, because Chen et al., (2010) previously reported that maize is a crop with high Cl^--endurance, which was able to tolerate more than 600 mg/kg dry soil without apparent disadvantageous effects. Plants were cultivated in a greenhouse for nine weeks using seven litre Mitscherlich pots filled with 7,840 g DM soil mixture. The soil mixture contained subfloor loam soil (C_{org}, 4.0%; Ostfilden, Stuttgart) homogenously mixed with sand of particle size 0–2 mm according to the ratio of 47.5%/47.5% (w/w). Sour turf soil (Baywa, Filderstadt) (pH = 3.7) was then added with 5% (w/w) based on the prepared soil-sand mixture (pH = 7.26) for adjusting the final pH to 7.06. The surface of the pots was covered with additional 600 g sand per pot. Seeds were sown on 9 June 2017, from then they were watered on a regular basis to maintain 70% (w/w) water holding capacity (WHC) of the potted soil. For fertilization, 2 g NH_4NO_3, 5 g KH_2PO_4, 2 g $MgSO_4{}^*7H_2O$ and 0.3 g Fetrilon-combi micronutrient solution (AgNova Technologies Pty Ltd) was given to each pot as liquid fertilizer. Fetrilon-combi contains micronutrients (1.5% boron, 0.6% copper, 4.0% iron, 3.0% manganese, 0.05% molybdenum and 4.0% zinc) and some macronutrients (0.8% magnesium and 1.3% sulphur). $CaCl_2{}^*2H_2O$ was used to treat the maize with Cl^-. The first Cl^- addition took place with either 21.1 or 252.4 mg Cl^-/kg dry soil DM (given as $CaCl_2{}^*2H_2O$), which were stepwise increased by 10.5 or 126.2 mg Cl^-/kg soil DM, respectively, every second day, finally reaching a maximum dose of either 63.2 for the "low"or 757.1 mg Cl^-/kg soil DM for the "high" (0.5 or 6.4 g/pot DM) after 8 days. The control was not enriched with Cl^-. Treated plants and corresponding controls grew 10 days after full stress treatment was set. At harvest, different plant

TABLE 1 The detailed information of eight maize genotypes

Genotypes	Suppliers
P8589	Pioneer Hi-Bred Northern Europe Sales Division GmbH
LG30222	LG c/o Limagrain GmbH
Tokala	Advanta c/o Limagrain GmbH
KWS-Stabil	KWS SAAT SE GmbH
Amamonte	KWS SAAT SE GmbH
P8400	Pioneer Hi-Bred Northern Europe Sales Division GmbH
LG30215	LG c/o Limagrain GmbH
ES-Metronom	Euralis Saaten GmbH

(A)

Plant fractions	Names given
a	9th leaf blade
b	Other leaf blades
c	Leaf sheaths
d	Shoot
e	Root

(B)

Parameters	Plant fractions used for analysis (shown on part C)
Fresh and dry weight	a, b, c, d, e
Water content	a
Chloride concentration	a, b, c, d, e
Osmolarity	a
Ion leakage	a
SPAD, transpiration rate, stomatal conductance and photosynthetic rate	a

(C)

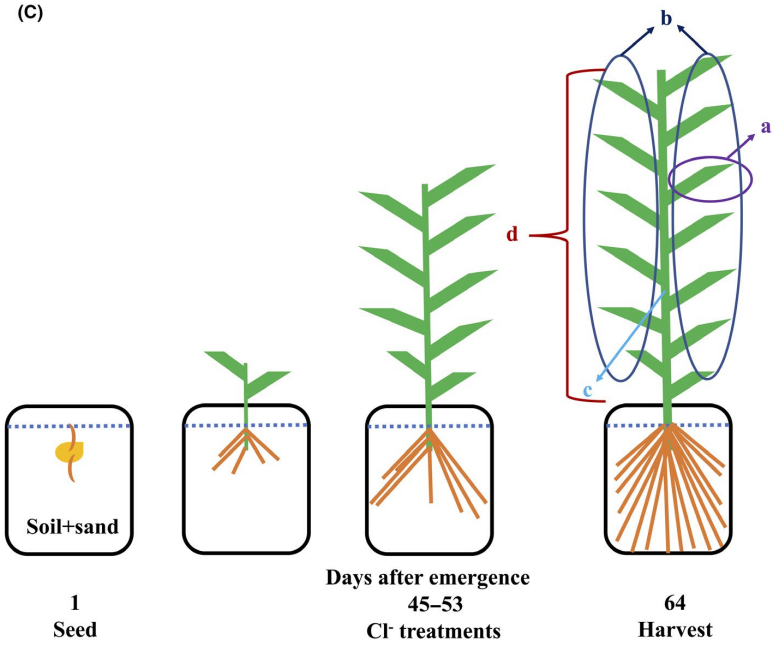

FIGURE 1 Overview of experiment set-up. The first Cl− additions took place with either 21.1 or 252.4 mg Cl−/kg dry soil, which were stepwise increased by 10.5 or 126.2 mg Cl−/kg soil, respectively, every second day, finally reaching a maximum dose of either 63.2 or 757.1 mg Cl−/kg soil (0.5 or 6.4 g/pot) after 8 days. (A) The table describing how plants were harvested into different fractions and how these fractions were named, (B) The table showing which fractions were used for the specific parameter measurements, (C) The schematic chart showing how plants were grown and treated by Cl− and finally harvested [Colour figure can be viewed at wileyonlinelibrary.com]

organs were put into fractions: (a) 9th leaf blade, (b) other leaf blades, (c) leaf sheaths, (d) shoot (all leaf blades and leaf sheaths) and (e) root (see Figure 1). It is important to note that fractions (a) and (b) did not contain any leaf sheaths. Each genotype was grown with one plant per pot in five biological replicates. All pots were randomly rearranged twice a week during the whole growth period.

2.2 | Methods

2.2.1 | Fresh weight and dry weight

Fresh weight (FW) of all plant fractions (Figure 1) was weighed immediately after harvest. Dry weight (DW) of plant material was determined after drying at 55°C for 72 hr in a ventilated oven.

2.2.2 | Water content

In order to quantify leaf water content *in planta*, a certain area (diameter = 1 cm) was marked on the 9th leaf blade. On this marked area, we repeated these non-invasive measurements over several days. A water content sensor based on infrared light emitting diodes (LED) and a photodiode linked to a custom device were calibrated against maize leaves and employed for non-invasive measurements of leaf water contents. The schematic diagram of this device was depicted in Figure S1. The underlying principle is the transmission recording of two near IR-wavelengths with different absorption of water penetrating the leaf at an angle of 45°. The ratio of transmission at these two wavelengths is linearly correlated with leaf water content. For calibration of water contents (Table S1), each leaf was completely saturated overnight by floating at 4°C in ddH_2O water, then the water content was determined at six time points (0, 10, 20, 30, 45, 60 min) after the removal from the water bath during the drying process. NIR-transmission ratio and gravimetrically measured leaf water content were determined simultaneously, yielding a linear calibration curve of leaf water content versus NIR-ratio specific for maize leaves.

2.2.3 | Cl^- measurement

Samples from all plant fractions and soils were homogeneously grounded to powder using a mill (Retsch ZM1) equipped with a 0.5 mm sieve. Plant tissues powder (200 mg on a dry basis) and soil powder (2 g on a dry basis) were subjected to Cl^- extraction by solving in 10 ml ddH_2O in glass tubes and heating in water bath at 80°C for 15 min. The suspension was cooled on ice for 7 min and finally filtered through a circular filter paper (90-mm diameter) into a 15 ml falcon tube. Cl^--concentration in the water extract was measured using a Cl^- metre 6610 (Eppendorf) (Ebert, Eberle, Eberle, Ali-Dinar, & Lüdders, 2002). For this, 600 µl of the water extract was mixed with 1 ml gelatin solution (Biorapid GmbH) and 15 ml acid buffer. The stock acid buffer (1 L) was prepared with 0.64% (v/v) nitric acid and 5.76% (v/v) acetic acid (100%). Four technical replicates were conducted.

2.2.4 | Osmolarity

The leaf sap was collected at 10 days after full stress treatment by squeezing the 9th leaf blade of each plant. Leaf sap was stored at −20°C. Osmolarity was measured with semi-micro osmometer (Knauer ML, Berlin, Germany) (Zimmermann et al., 2008) by diluting the original sap 1:4 using ddH_2O water. Aliquots of 200 µl were used for determination. A standard curve was made by 10, 20, 30 and 40 mM $CaCl_2{}^*2H_2O$ for calculating the osmolarity in leaf sap. Each measurement was conducted in replicates of four.

2.2.5 | Leaf electrolyte leakage

When harvesting the plant material, six 1 cm diameter discs were immediately collected from the 9th leaf blade and washed for four times with ddH_2O. Then, they were put into a 50 ml falcon tube containing 20 ml ddH_2O. The conductivity was firstly measured after 4 hr of shaking using a conductometer (WTW LF90 and a WTW KLE1 cell, Weilheim, Germany) (El Achouri et al., 2001). The leaf discs were stored overnight at −20°C, and then the total conductivity was recorded after thawing. Ion leakage was expressed as the ratio of the conductivity (4 hr) and the total conductivity.

2.2.6 | Electrical conductance and pH of soil solution

After harvest, electrical conductivity of potted soil solution was directly measured by a handheld readout device (Infield 7) equipped with Theta Probe (ML2x). For determination of soil pH, 2 g dry soil powder with a particle size of 0.5 mm was dissolved in 25 ml ddH_2O and incubated on a shaker for 45 min. After 15 min sedimentation, the pH in the supernatant was measured using a pH meter (WTW 538) (Ullrich, Menge, Menge, Schmid, Gübitz, & Krauss, 2001).

2.2.7 | Transpiration rate, stomatal conductance and photosynthetic rate

The area that was marked in the 9th leaf blade (Figure 1) for water content quantification (see section 2.2.22) was also used to monitor photosynthetic rate and transpiration rate using a LCi Portable Photosynthesis System (ADC BioScientific Ltd) (Ramani et al., 2006). A broad type chamber was used, the observed leaf area was 625 mm^2 and the light was natural sunlight lying between 0.4 and 3.0 microns. For maize leaves, CO_2 flowing into leaf chamber was around 400 vpm and H_2O flux was between 0.17 $\mu mol/m^2\ s^{-1}$.

2.2.8 | Chlorophyll concentration

The chlorophyll concentration in the 9th leaf blade was measured by a Chlorophyll meter (SPAD 502; Konica Minolta) (Netto, Campostrini, Campostrini, Oliveira, & Bressan-Smith, 2005). For each leaf, four measurements were conducted at different positions on opposite sides of the central vein.

2.3 | Statistical analysis

All data were expressed as mean ± standard error. To determine the significance difference between control and two levels of treatments, data were analysed by Duncan test (three and more variables) or *T* test (two variables) at the probability of 0.05 and 0.01 levels with SPSS software 19.0 (SPSS Inc), as indicated in the figures. Principal component analysis (PCA) was conducted by SPSS 19.0 on a basis of all parameters measured above. For each sample, every measurement had five biological replicates. Only Cl^- concentration and osmolarity measurements were technically repeated four times while other parameters had no technical replicates.

3 | RESULTS

3.1 | Fresh and dry biomass of different maize organs

Treating maize with either 0.5 (low) or 6.4 (high) g Cl^- per pot did not significantly change FW in the 9th leaf blade, other leaf blades, leaf sheaths and the shoot of almost all genotypes (Figure 2). This pattern was also reflected by DW (Figure 3B). The genotype P8589 was an exception because it developed leaf edge and leaf tip necrosis (Figure S2C) and FW and DW were significantly reduced in the fraction that we call "other leaf blades" (this fraction represents all leaf blades but not the ninth leaf blade) when high Cl^--treatment was applied (Figure 2). P8589 stood out for a second reason: this genotype increased FW and DW under low Cl^- treatment. However, this trend was only significant for FW in the leaf sheaths of P8589 (Figures 2 and 3). Root biomass was not affected by low or high Cl^- treatment in any genotype, except for KWS-Stabil, displaying significantly reduced root DW under high Cl^- (Figure 3E). Other leaf blades had significant lower calculated water content (58.5 g) under high Cl^- treatment in P8589 in comparison with control (72.3 g) (Figure 4B). However, this trend was not observed in leaf sheaths, in which low Cl^- supply increased calculated water content from 212.1 g to 243.8 g in P8589 (Figure 4C). Similarly, P8589 and P8400 exhibited a greater calculated water content (330.2 g and 296.8 g, respectively) in shoot under low Cl^- level than the corresponding controls (291.8 g and 266.9 g, respectively) (Figure 4D).

3.2 | Cl^- distribution in 9th leaf blade, other leaf blades, leaf sheaths, root and soil

In soil, Cl^- concentrations expressed as average over all pots of all genotypes were 8.8 mg Cl^-/kg soil DM in control, 26.4 mg Cl^-/kg soil DM in low treatment and 335.4 mg Cl^-/kg soil DM in high treatment (Figure 5E).

In the 9th leaf blade, other leaf blades, leaf sheaths, roots and soil, Cl^- concentration significantly increased with rising external Cl^- application. This was true for all genotypes except for the root

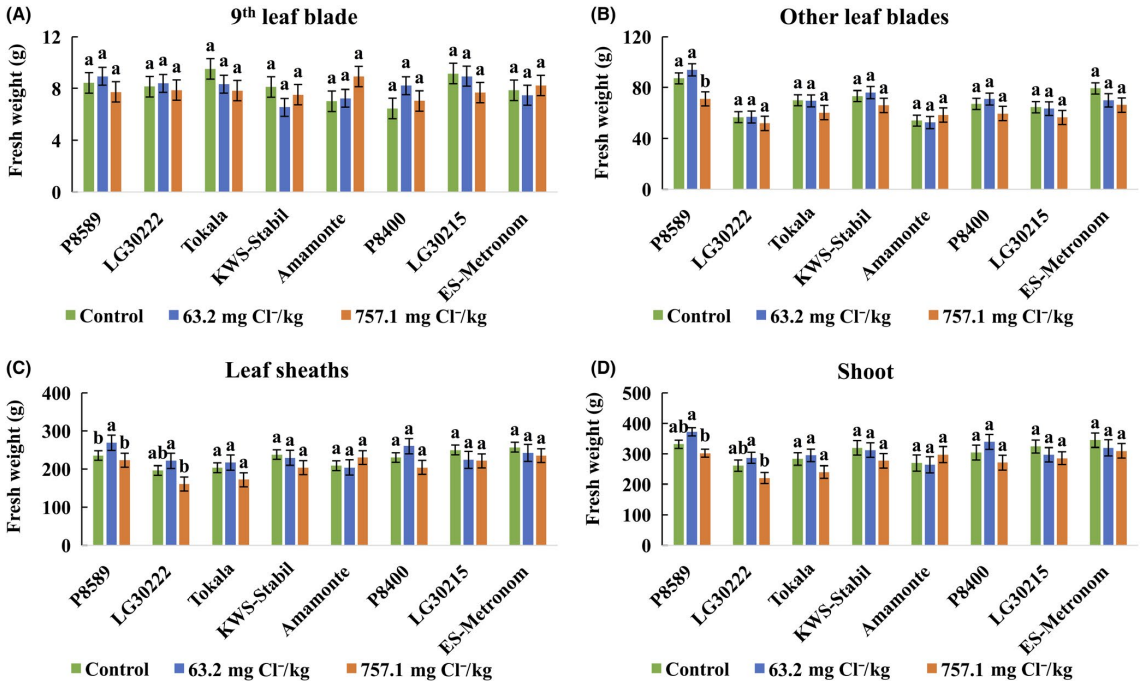

FIGURE 2 Fresh weight in different plant tissues. Small letters indicate significant FW mean difference ($p < 0.05$) under different treatments per genotype by Duncan Test. (A) Fresh weight of 9th leaf blade, (B) Fresh weight of other leaf blades, (C) Fresh weight of leaf sheaths, (D) Fresh weight of shoot [Colour figure can be viewed at wileyonlinelibrary.com]

of P8589, the 9th leaf blade of KWS-Stabil and the fraction "other leaf blades" (this fraction represents all leaf blades but not the ninth leaf blade) in ES-Metronom, where no significant increases in Cl^- concentration could be observed after low treatment compared with controls (Figure 5). When plants were stressed by a high Cl^--dose, as expected, all genotypes showed significant Cl^- increase in all plant fractions. Besides, LG30222 had the greatest shoot/root ratio and Amamonte, P8400 and ES-Metronom were the lowest under high Cl^- treatment (Figure 5F). The genotype Tokala showed the same low shoot/root ratio under either low or high treatment (Figure 5F).

3.3 | Water content

In comparison with control, low Cl^- treatment did not change the non-invasively quantified water content of all genotypes (Figure 6). However, as expected, non-invasively quantified water content was significantly reduced from 13.9 mg/cm^2 to 10.8 mg/cm^2 and from 12.7 mg/cm^2 to 10.6 mg/cm^2 in the genotypes Amamonte and P8589, respectively, by high Cl^- treatment. In contrast, genotypes KWS-Stabil and LG30215 had increased non-invasively quantified water content from 11.3 mg/cm^2 to 13.9 mg/cm^2 and from 9.8 mg/cm^2 to 11.6 mg/cm^2, respectively, when exposed to high Cl^- concentration. The non-invasively quantified water content in genotypes LG30222 and ES-Metronom remained unchanged irrespective of the treatment.

3.4 | Osmolarity and electrolyte leakage

Treating maize with either low or high Cl^- increased osmolarity from 258 mOsm/L to approximately 275 mOsm/L in Amamonte and from 277 mOsm/L to approximately 297 mOsm/L in LG30215, respectively, but did not affect osmolarity in Tokala, P8400, LG30222 and ES-Metronom (Figure 7A). Under high Cl^- treatment, the osmolarity of P8589 and KWS-Stabil increased from 245 mOsm/L to 292 mOsm/L and from 237 mOsm/L to 272 mOsm/L, respectively, whereas osmolarity was not affected by low Cl^- treatment in these two genotypes. None of the genotypes showed a significant difference in ion leakage between both Cl^- treatments (Figure 7B).

3.5 | Soil electrical conductance

Under both Cl^- treatments, electrical conductance in the soil kept the same value in comparison with controls among all genotypes (Figure 8). However, the genotypes KWS-Stabil and P8400 were the exceptions. Electrical conductance of soil in pots of KWS-Stabil increased under both Cl^- treatments. In contrast, soil

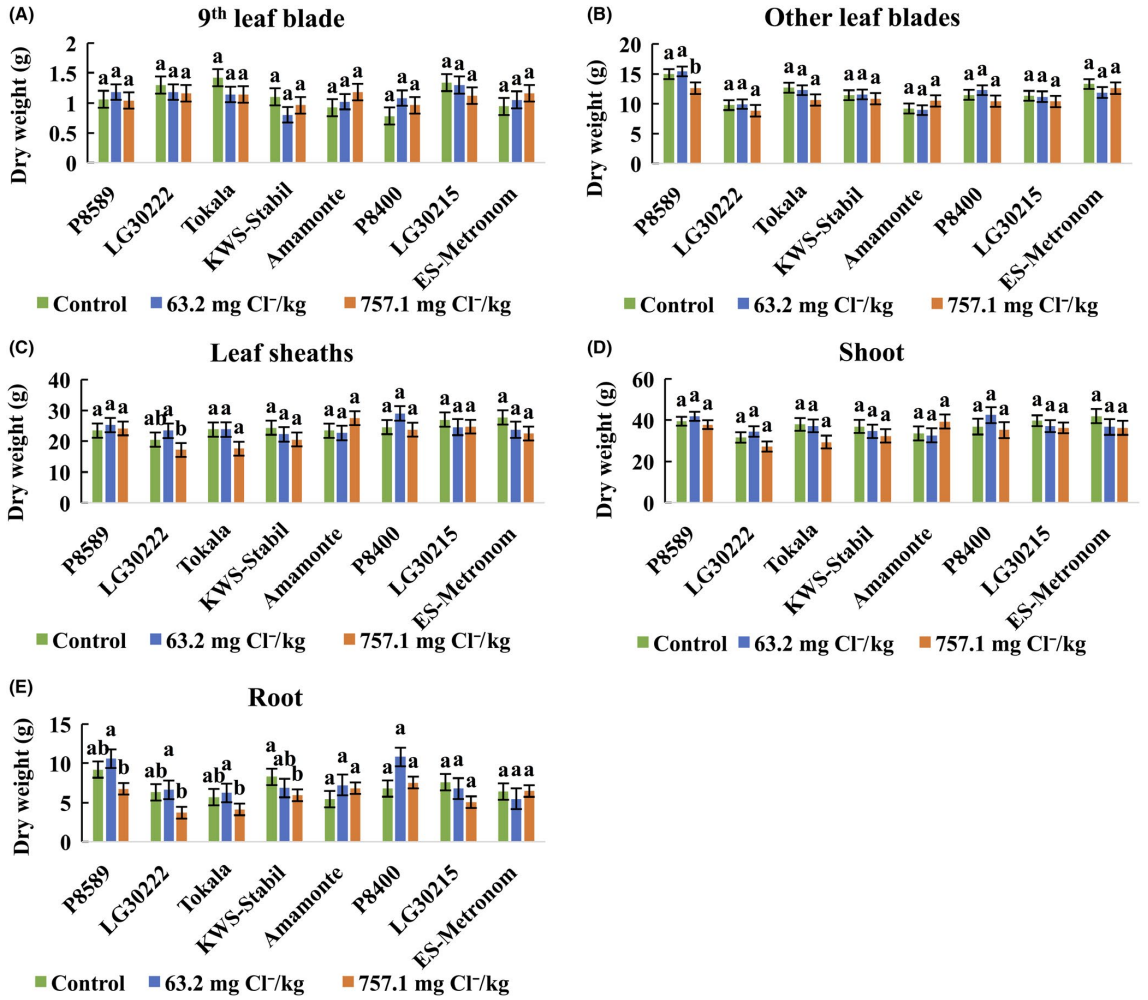

FIGURE 3 Dry weight in different plant tissues. Small letters indicate significant DW mean difference ($p < 0.05$) under different treatments per genotype by Duncan Test. (A) Dry weight of 9th leaf blade, (B) Dry weight of other leaf blades, (C) Dry weight of leaf sheaths, (D) Dry weight of shoot, (E) Dry weight of root [Colour figure can be viewed at wileyonlinelibrary.com]

electrical conductance of P8400 only increased with high Cl^- addition (Figure 8).

3.6 | Transpiration rate, stomatal conductance, photosynthetic rate and SPAD

Transpiration rate, stomatal conductance and photosynthetic rate of 9th leaf blades of all genotypes were unaltered by both Cl^- treatments during the whole growing period (Figure 9). However, an effect of Cl^- application on chlorophyll concentration estimated by SPAD measurements was found. In comparison with control, chlorophyll concentration of P8589, LG30222 and P8400 was significantly increased by low Cl^-. In contrast, high Cl^- treatment considerably decreased chlorophyll concentration from 50.7 to 49.3 and from 54.7 to 51.4 in genotypes LG30222 and LG30215, respectively.

3.7 | Principal component analysis

Principal component analysis (PCA) revealed that Cl^- concentration was the variable that explained most of the variance on principal component 1 (30.9%), whereas water content was the dominant factor for the variance on principal component 2 (16.3%) (Table S2 and Figure 10). Consequently, the genotypes clustered predominantly into groups being affected by the dose of the Cl^- treatment (Figure 10). However, two genotypes deviated from this trend. Low Cl^--treated P8589 was located in the group of high Cl^- concentration and low Cl^- treated ES-Metronom clustered into control group.

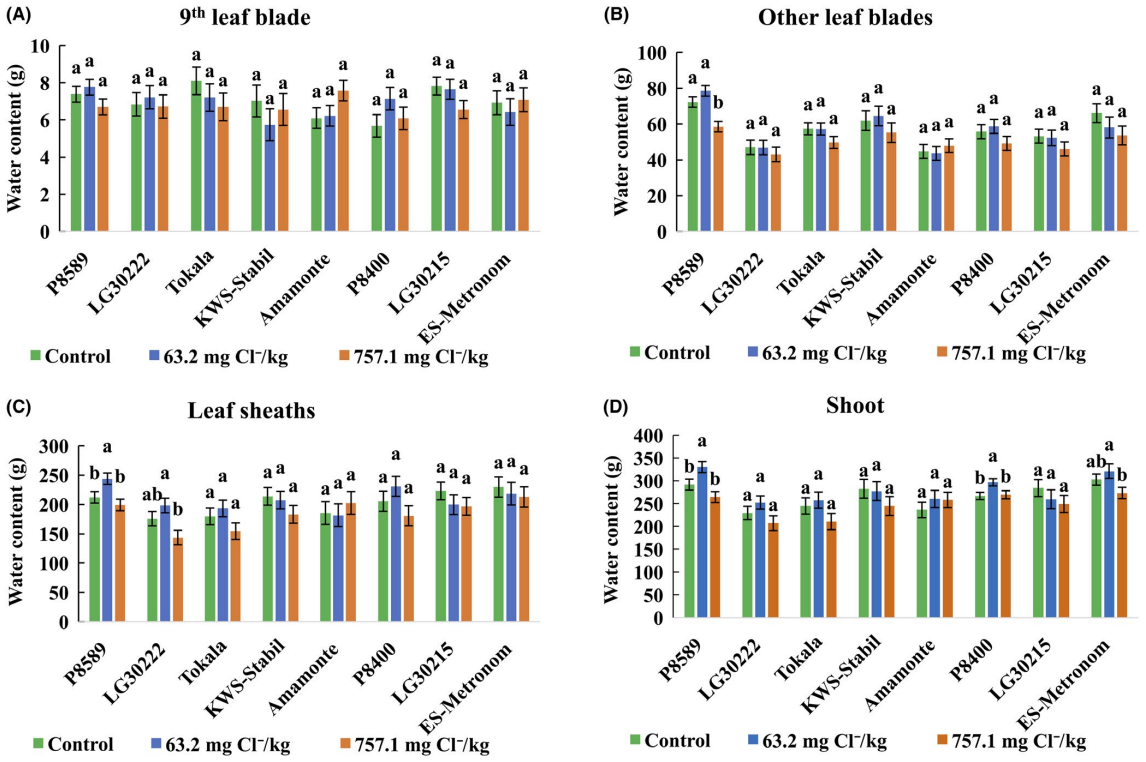

FIGURE 4 Calculated water content of plant fractions. Small letters indicate significant mean difference ($p < 0.05$) under different treatments per genotype by Duncan Test. (A) Water content of 9th leaf blade, (B) Water content of other leaf blades, (C) Water content of leaf sheaths, (D) Water content of shoot [Colour figure can be viewed at wileyonlinelibrary.com]

4 | DISCUSSION

4.1 | Treatment and soil condition

In this experiment, we applied calcium as Cl^- accompanying cation because the macronutrient calcium is not toxic at the applied concentration (Kirkby & Pilbeam, 1984; Marschner, 2011). Changing soil calcium concentration may influence soil pH, however, in our experiment soil pH was stable (Table S3). With these prerequisites, it is most likely that the series of physiological reactions and effects described in this work are attributable to different Cl^--treatments. The high amount of Cl^- applied (757.1 mg/kg soil) in the experiment was still mild stress for maize, because neither severe chlorotic nor necrotic lesions could be observed. Only genotype P8589 showed necrosis at the tip and margin of the 9th leaf under low and high treatment, respectively.

4.2 | Effects of chloride salinity in contrasting genotypes

Our data indicate that Cl^- root-to-shoot translocation was restricted in most maize genotypes, with the expectation of P8589, as the shoot-to-root ratio was less than 0.5 (Figure 5F). Thus, we conclude that maize is an Cl^- excluder. However, some Cl^- accumulates in the aerial part of the plant. Twice as much of Cl^- was present in the leaf sheaths as compared to the leaf blades under low and high treatment. This pattern could prevent harmful effects on photosynthesis, as leaf blades are more active in photosynthesis compared to the sheaths.

Although leaf sheaths DW of P8589 was similar under low and high Cl^- (Figure 3C), leaf sheaths FW of low Cl^- treated P8589 plants was higher than that of high Cl^- treatment (Figure 2C). This shows that only high Cl^- treatment induced stress in P8589. This was true for other leaf blades of P8589 as well (Figure 4B). This observation was also verified by sensor-measured water content and osmolarity data on the 9th leaf blade (Figures 6 and 7A) that underlined that high Cl^- treatment caused a reduction in water content, indicating osmotic stress. Furthermore, plant height of P8589 under low Cl^- concentration kept the same as control (Figure S2). However, this phenomenon was not seen under high Cl^- treatment, which indicates that the development of P8589 was reduced when Cl^- reached too high concentrations (Figure S2). Nevertheless, such reduction was probably attributed to the osmotic stress instead of ion toxicity, since the permeability and integrity of cellular membrane in leaf blades were not affected under such high Cl^- treatment (Figure 7B). Overall, the genotype P8589 was identified as being particularly sensitive to Cl^--stress, possibly due to problems in maintaining

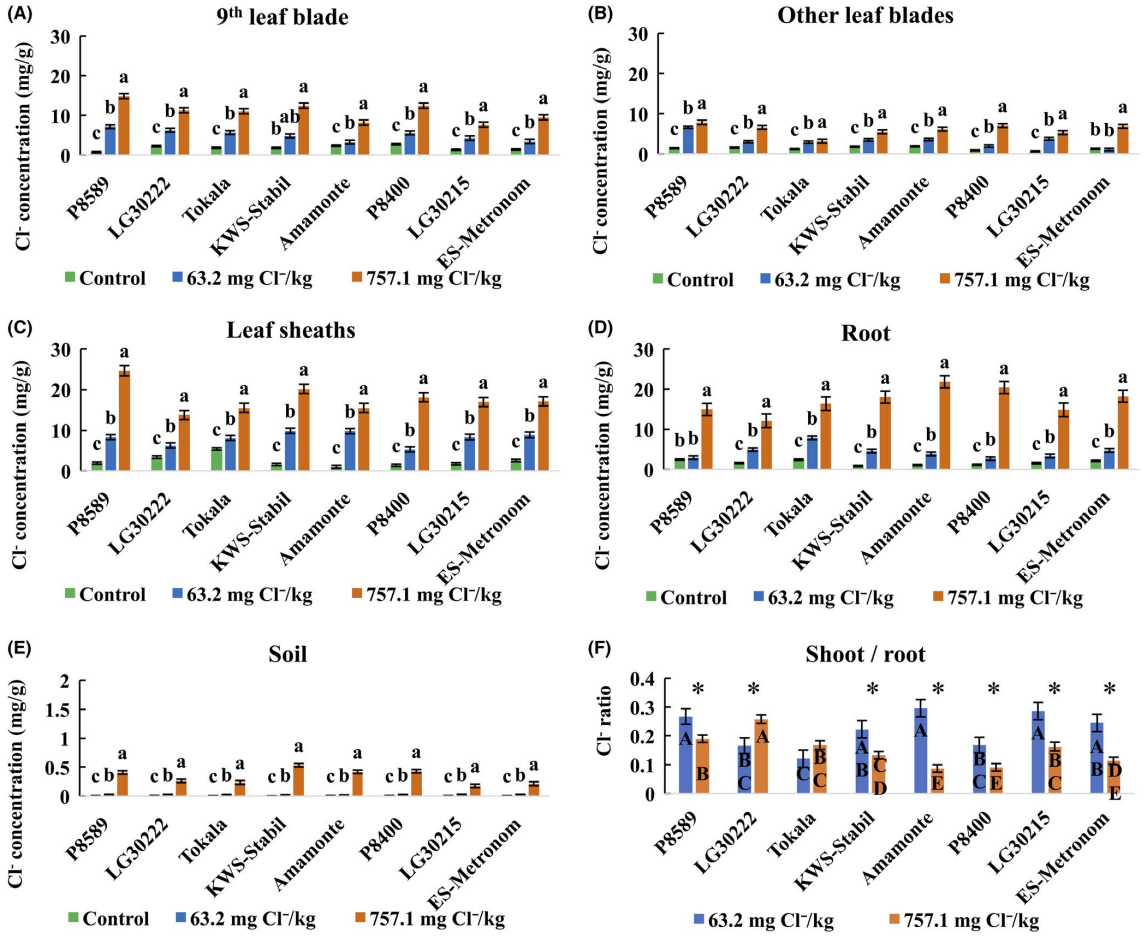

FIGURE 5 Chloride distribution in different plant tissues and soil. Small letters indicate significant mean difference ($p < 0.05$) under different treatments per genotype by Duncan Test; capital letters in shoot/root ratio indicate significant mean difference ($p < 0.05$) among all genotypes under one treatment; * and ** indicate significant mean differences ($p < 0.05$ and $p < 0.01$, respectively) *r* in shoot/root ratio between 63.15 mg Cl^-/kg and 757.11 mg Cl^-/kg for each genotype by Duncan Test. (A) Cl- concentration of 9th leaf blade, (B) Cl- concentration of other leaf blades, (C) Cl- concentration of leaf sheaths, (D) Cl- concentration of root, (E)Cl- concentration of soil, (F) The ratio of Cl- concentration between shoot and root [Colour figure can be viewed at wileyonlinelibrary.com]

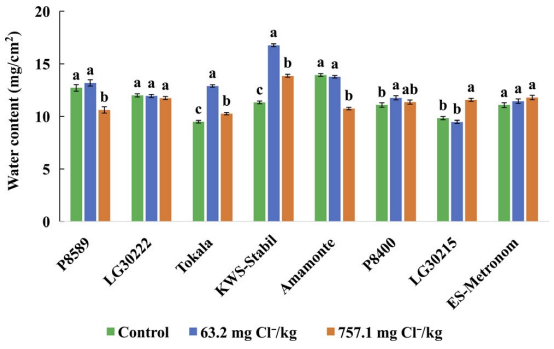

FIGURE 6 Water content in the 9th leaf blade. Small letters indicate mean significant difference in water content ($p < 0.05$) under different treatments per genotype by Duncan Test [Colour figure can be viewed at wileyonlinelibrary.com]

normal cellular water relations in plant tissues. Necrotic leaf edges witness chloride toxicity (Figure S2C).

A different tendency was detected in ES-Metronom. Neither low nor high Cl^- treatment influenced biomass formation (FW and DW), osmolarity or water content. Moreover, photosynthetic rate, stomatal conductance and transpiration rate of ES-Metronom were not affected by subjection to low or high Cl^- treatment (Figure 9). This implies that ES-Metronom was more tolerant to Cl^- stress than P8589 as even high Cl^- did not induce osmotic nor ion-toxic stress.

A potential explanation for the different performance under high Cl^- between P8589 and ES-Metronom could be attributed to a differing allocation of excess Cl^- within the plant organs according to shoot/root ratio (Figure 5F). In our findings, ES-Metronom

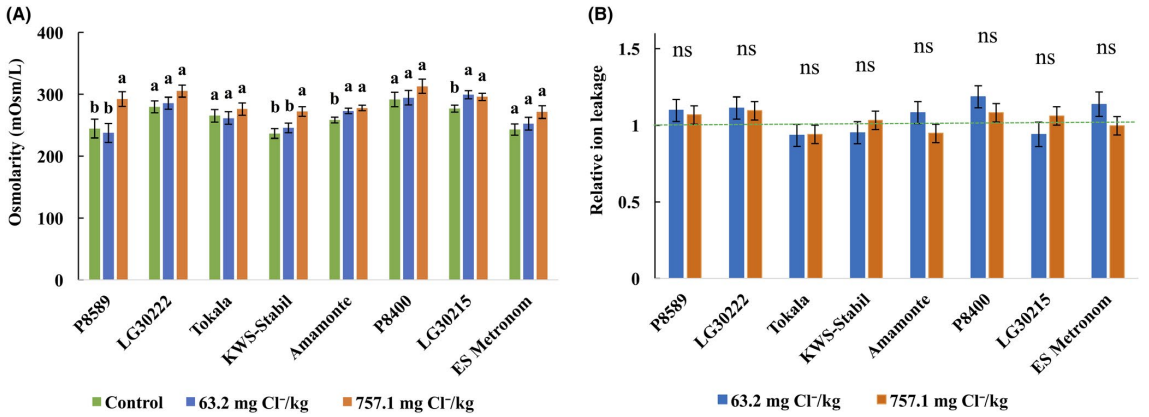

FIGURE 7 The osmolarity and electrolyte leakage in the 9th leaf blade sap. Small letters indicate significant mean difference ($p < 0.05$) in osmolarity under different treatments per genotype by Duncan Test; relative ion leakage was expressed as low treatment/control- and high treatment/ control-ratio; *T* test was used for analysing significant difference in electrolyte leakage. The sign "ns" means non-significant. (A) Osmolality of 9th leaf blade, (B) Relative ion leakage of 9th leaf blade [Colour figure can be viewed at wileyonlinelibrary.com]

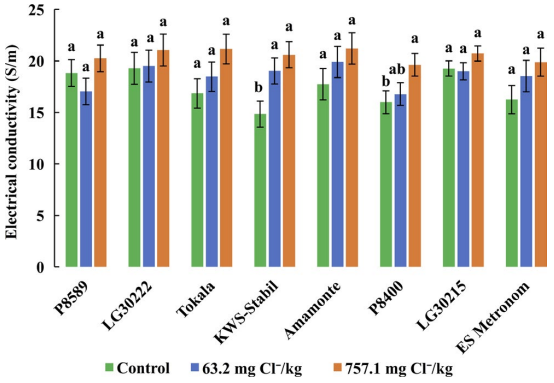

FIGURE 8 Electrical conductance of soil. Small letters indicate significant mean difference ($p < 0.05$) in electrical conductance under different treatments per genotype by Duncan Test [Colour figure can be viewed at wileyonlinelibrary.com]

had lower shoot/root ratio under both low and high treatment than P8589. This indicates that ES-Metronom was able to exclude Cl^- from being transported to the shoot. There is a strong correlation between sodium exclusion and salt tolerance in many cop species (Flowers & Yeo, 1986; Munns & James, 2003). Our data indicate this for Cl^-, as previously done by others (Brumos, Talon, Talon, Bouhlal, & J. M. COLMENERO-FLORES, 2010; Li et al., 2016; Teakle, Flowers, Flowers, Real, & Colmer, 2007).

This is useful as ongoing salt ion accumulation will cause osmotic imbalances and ion toxicities (Munns, James, James, & Läuchli, 2006). Therefore, restricting acropetal transport of Cl^- is likely to be an important factor contributing to low salt accumulation in leaves and might be the underlying mechanism of increased Cl^- tolerance of ES-Metronom (Munns, 2005; Pitman, 1984). We speculated that this reduced transport is based on restricted xylem loading, however, we have not tested this. However, Cl^- tolerance by Cl^- retention in root seems to be trade-off as the root growth of the respective genotypes was impaired to some extent, most likely due to the excessive Cl^- accumulation.

4.3 | No relation between osmolarity, Cl^- and growth

Osmolarity of P8589, KWS-Stabil, Amamonte and LG30215 (Figure 7A) was increased by high Cl^- treatment. Apparently, Cl^- accumulated in the cells, acted as osmoticum and facilitated water uptake. Growth, however, was not facilitated as it might have been possible in the light of the turgor-driven acid-growth. Shoot fresh and dry biomass of all maize genotypes were not affected by low or high chloride treatment in comparison with controls (Figures 2D and 3D). Similar results were reported by Hütsch, Keipp, Glaser, and Schubert (2018) who figured out that the potato cultivars Marabel and Désirée can be fertilized with KCl instead of K_2SO_4 without the risk of tuber yield depression.

4.4 | Chlorophyll concentration and photosynthetic rate

The chlorophyll concentration in genotypes LG30222 and LG30215, as estimated by SPAD readings (Figure 9D), was reduced by high Cl^- treatment in comparison with controls. Slabu et al. (2009) reported that a reduced chlorophyll concentration in leaves of *Vicia faba* after NaCl exposure (13 days after 100 mM treatment) is attributable to high chloroplastic Cl^- concentrations rather than the accumulation of sodium. Chloroplasts exhibit a high permeability for Cl^-, and a treatment with NaCl resulted in the accumulation of Cl^- and decline in SPAD values (Heber & Heldt, 1981). Furthermore, high

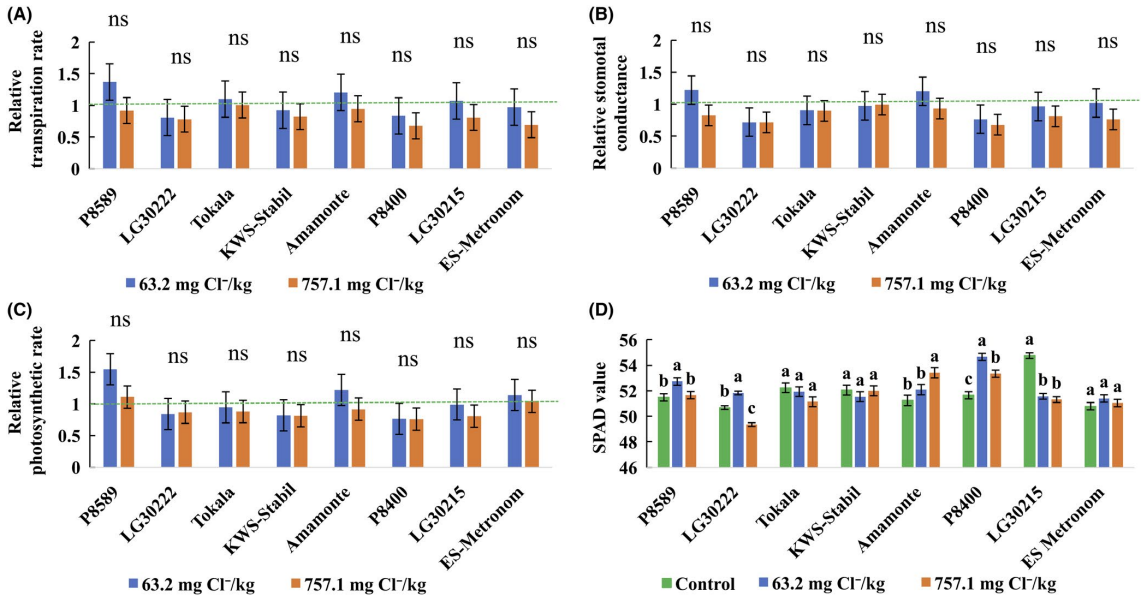

FIGURE 9 Transpiration rate, stomatal conductance, photosynthetic rate and SPAD value in the 9th leaf blade. Relative transpiration rate, relative stomatal conductance and relative photosynthetic rate were expressed as low treatment/control- and high treatment/ control-ratios; * and ** indicate significant mean differences ($p < 0.05$ and $p < 0.01$, respectively) between 63.2 mg Cl^-/kg and 757.1 mg Cl^-/kg for each genotype by *T* test. Small letters indicate significant mean difference ($p < 0.05$) in SPAD readings under different treatments per genotype by Duncan Test. The sign "ns" means non-significant. (A) Relative transpiration rate of 9th leaf blade, (B) Relative stomatal conductance of 9th leaf blade, (C) Relative photosynthetic rate of 9th leaf blade, (D) SPAD value of 9th leaf blade [Colour figure can be viewed at wileyonlinelibrary.com]

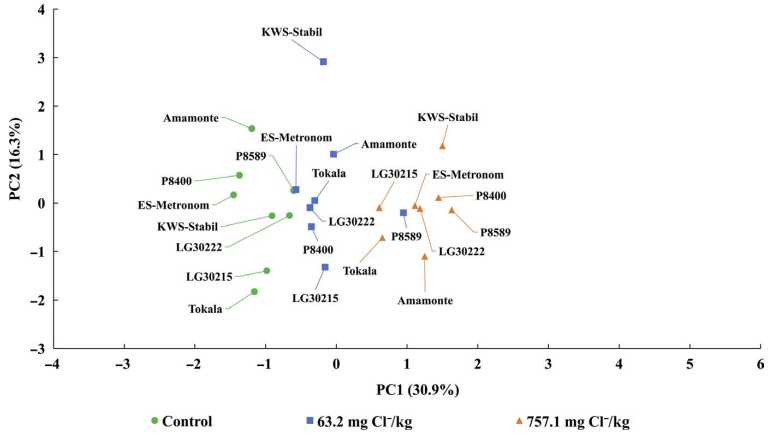

FIGURE 10 Principal component analysis (PCA) of eight maize genotypes under different treatments. In general, there are 24 parameters used for PCA analysis. They contain fresh weight in the 9th leaf blade, dry weight in the 9th leaf blade, fresh weight in other leaf blades, dry weight in other leaf blades, fresh weight in leaf sheaths, dry weight in leaf sheaths, dry weight in roots, stomatal conductance in stress induction phase (45th day to 53rd day), stomatal conductance in full stress phase (54th day to 64th day), photosynthetic rate in stress induction phase (45th day to 53rd day), photosynthetic rate in full stress phase (54th day to 64th day), transpiration rate in stress induction phase (45th day to 53rd day), transpiration rate in full stress phase (54th day to 64th day), water content in stress induction phase (45th day to 53rd day), water content (54th day to 64th day), soil electrical conductance, electrolyte leakage, osmolarity, soil pH, Cl^- concentration in the 9th leaf blade, Cl^- concentration in other leaf blades, Cl^- concentration in leaf sheaths, Cl^- concentration in roots and Cl^- concentration in the soil [Colour figure can be viewed at wileyonlinelibrary.com]

Cl^- concentration reduces the photosynthetic capacity and quantum yield in *Vicia faba* due to chlorophyll degradation which may result from a structural impact of high Cl^- concentration on PSII (Tavakkoli, Rengasamy, Rengasamy, & McDonald, 2010). In our study, the reduced chlorophyll concentration did not inhibit the photosynthesis rate in maize (Figure 9C,D). This might be attributable to the fact that the

given chlorophyll concentration, as indicated by the SPAD readings, is adequate for fulfilling the photosynthetic function in our control and stressed plants, spanning from 50.7 in LG30222 to 54.7 in LG30215 among total tested genotypes. A critical SPAD value of 48.6 ± 3.8 (mean value ± standard deviation) at vegetative stage (10th leaf) was suggested to be adequate to achieve high corn yield in a field condition (Sunderman, Pontius, Pontius, & Lawless, 1997). Besides, the maximum reduction of chlorophyll, as averaged over all maize genotypes (Figure 9D), was 6.3% under high Cl^- treatment in LG30215. For comparison: under water stress, a reduction of leaf chlorophyll concentration about 40% was still not severe enough to negatively affect photosynthetic rate at mid-day in maize (Sanchez, Hall, Hall, Trapani, & Hunau, 1983).

5 | CONCLUSIONS

Chloride is not harmful when reaching concentrations as high as 757.1 mg Cl^-/kg soil DM, except for the Cl-sensitive genotype P8589 that showed leaf edge necrosis. While an equimolar sodium concentration would affect biomass, photosynthesis rate or water content, the same parameters were not affected by Cl salinity. Data show that chloride root-to-shoot translocation is restricted in most maize genotypes, indicating that maize excludes Cl^- at the xylem, which might be useful for avoiding accumulation in the photosynthetic active leaf blades. The more Cl^- sensitive genotypes accumulated more Cl^- in the shoot compared to the more tolerant ones, viz. had a smaller shoot-to-root ratio.

ACKNOWLEDGEMENTS

We cordially thank Dr. Nikolaus Merkt for giving advicee with plant cultivation in the greenhouse. This work was financially supported by China Scholarship Council (CSC) with grant number 201606300005. This work was supported by a DFG research grant (GE 3111/1-1) which is gratefully acknowledged.

ORCID

Christoph-Martin Geilfus https://orcid.org/0000-0002-9820-8111

REFERENCES

Arnon, D. I., & Whatley, F. (1949). Is chloride a coenzyme of photosynthesis? *Science*, *110*, 554–556. https://doi.org/10.1126/science.110.2865.554

Boursier, P., Lynch, J., Lauchli, A. (1984). Chloride partitioning in leaves of four salt stressed grass species[C]. *PLANT PHYSIOLOGY*, *75*, 37.

Boursier, P., Lynch, J., Lauchli, A., & Epstein, E. (1987). Chloride partitioning in leaves of salt-stressed sorghum, maize, wheat and barley. *Functional Plant Biology*, *14*(4), 463–473.

Brumos, J., Talon, M., Bouhlal, R., & Colmenero-Flores, J. M. (2010). Cl-homeostasis in includer and excluder citrus rootstocks: Transport mechanisms and identification of candidate genes. *Plant, Cell & Environment*, *33*, 2012–2027. https://doi.org/10.1111/j.1365-3040.2010.02202.x

Chen, W., He, Z. L., Yang, X. E., Mishra, S., & Stoffella, P. J. (2010). Chlorine nutrition of higher plants: Progress and perspectives. *Journal of Plant Nutrition*, *33*, 943–952. https://doi.org/10.1080/01904160903242417

Christensen, N., Taylor, R., Jackson, T., & Mitchell, B. (1981). Chloride effects on water potentials and yield of Winter wheat infected with take-all root rot 1. *Agronomy Journal*, *73*, 1053–1058. https://doi.org/10.2134/agronj1981.00021962007300060035x

Churchill, K. A., & Sze, H. (1984). Anion-sensitive, H^+-pumping ATPase of oat roots: Direct effects of Cl^-, $NO3^-$, and a disulfonic stilbene. *Plant Physiology*, *76*, 490–497.

De Angeli, A., Zhang, J., Meyer, S., & Martinoia, E. (2013). AtALMT9 is a malate-activated vacuolar chloride channel required for stomatal opening in Arabidopsis. *Nature Communications*, *4*, 1804. https://doi.org/10.1038/ncomms2815

Ebert, G., Eberle, J., Ali-Dinar, H., & Lüdders, P. (2002). Ameliorating effects of Ca (NO3) 2 on growth, mineral uptake and photosynthesis of NaCl-stressed guava seedlings (Psidium guajava L.). *Scientia Horticulturae*, *93*, 125–135. https://doi.org/10.1016/S0304-4238(01)00325-9

El Achouri, M., Kertit, S., Gouttaya, H., Nciri, B., Bensouda, Y., Perez, L., … Elkacemi, K. (2001). Corrosion inhibition of iron in 1 M HCl by some gemini surfactants in the series of alkanediyl-α, ω-bis-(dimethyl tetradecyl ammonium bromide). *Progress in Organic Coatings*, *43*, 267–273. https://doi.org/10.1016/S0300-9440(01)00208-9

Farooq, M., Hussain, M., Wakeel, A., & Siddique, K. H. (2015). Salt stress in maize: Effects, resistance mechanisms, and management. A Review. *Agronomy for Sustainable Development*, *35*, 461–481. https://doi.org/10.1007/s13593-015-0287-0

Flowers, T., & Yeo, A. (1986). Ion relations of plants under drought and salinity. *Functional Plant Biology*, *13*, 75–91. https://doi.org/10.1071/PP9860075

Foyer, C. H., Lelandais, M., & Kunert, K. J. (1994). Photooxidative stress in plants. *Physiologia Plantarum*, *92*, 696–717. https://doi.org/10.1034/j.1399-3054.1994.920422.x

Fromm, J., & Eschrich, W. (1989). Correlation of ionic movements with phloem unloading and loading in barley leaves. *Plant Physiology and Biochemistry (France)*, *27*, 577–585.

Geilfus, C.-M. (2017). The pH of the apoplast: Dynamic factor with functional impact under stress. *Molecular Plant*, *10*, 1371–1386. https://doi.org/10.1016/j.molp.2017.09.018

Geilfus, C.-M. (2018a). Review on the significance of chlorine for crop yield and quality. *Plant Science*. https://doi.org/10.1016/j.plantsci.2018.02.014

Geilfus, C.-M. (2018b). Chloride: From nutrient to toxicant. *Plant and Cell Physiology*, *59*, 877–886. https://doi.org/10.1093/pcp/pcy071

Geilfus, C.-M., Ludwig-Müller, J., Bárdos, G., & Zörb, C. (2018). Early response to salt ions in maize (Zea mays L.). *Journal of Plant Physiology*, *220*, 173–180. https://doi.org/10.1016/j.jplph.2017.11.010

Geilfus, C. M., Mithöfer, A., Ludwig-Müller, J., Zörb, C., & Muehling, K. H. (2015). Chloride-inducible transient apoplastic alkalinizations induce stomata closure by controlling abscisic acid distribution between leaf apoplast and guard cells in salt-stressed Vicia faba. *New Phytologist*, *208*, 803–816.

Geilfus, C.-M., Tenhaken, R., & Carpentier, S. C. (2017). Transient alkalinization of the leaf apoplast stiffens the cell wall during onset of chloride salinity in corn leaves. *Journal of Biological Chemistry*, *292*, 18800–18813. https://doi.org/10.1074/jbc.M117.799866

Gong, H., Blackmore, D., Clingeleffer, P., Sykes, S., Jha, D., Tester, M., & Walker, R. (2010). Contrast in chloride exclusion between two grapevine genotypes and its variation in their hybrid progeny. *Journal of Experimental Botany*, *62*, 989–999. https://doi.org/10.1093/jxb/erq326

Heber, U., & Heldt, H. (1981). The chloroplast envelope: Structure, function, and role in leaf metabolism. *Annual Review of Plant Physiology*, *32*, 139–168. https://doi.org/10.1146/annurev.pp.32.060181.001035

Hütsch, B. W., Keipp, K., Glaser, A. K., & Schubert, S. (2018). Potato plants (Solanum tuberosum L.) are chloride-sensitive: Is this dogma valid? *Journal of the Science of Food and Agriculture*, *98*(8), 3161–3168.

Kirkby, E., & Pilbeam, D. (1984). Calcium as a plant nutrient. *Plant, Cell & Environment*, *7*, 397–405. https://doi.org/10.1111/j.1365-3040.1984.tb01429.x

Lessani, H., & Marschner, H. (1978). Relation between salt tolerance and long-distance transport of sodium and chloride in various crop species. *Functional Plant Biology*, *5*, 27–37. https://doi.org/10.1071/PP9780027

Li, B. O., Byrt, C., Qiu, J., Baumann, U., Hrmova, M., Evrard, A., … Roy, S. J. (2016). Identification of a stelar-localized transport protein that facilitates root-to-shoot transfer of chloride in Arabidopsis. *Plant Physiology*, *170*, 1014–1029. https://doi.org/10.1104/pp.15.01163

Marschner, H. (2011). *Marschner's mineral nutrition of higher plants*. Amsterdam, The Netherlands: Academic press.

Munns, R. (2005). Genes and salt tolerance: Bringing them together. *New Phytologist*, *167*, 645–663. https://doi.org/10.1111/j.1469-8137.2005.01487.x

Munns, R., & James, R. A. (2003). Screening methods for salinity tolerance: A case study with tetraploid wheat. *Plant and Soil*, *253*, 201–218. https://doi.org/10.1023/A:1024553303144

Munns, R., James, R. A., & Läuchli, A. (2006). Approaches to increasing the salt tolerance of wheat and other cereals. *Journal of Experimental Botany*, *57*, 1025–1043. https://doi.org/10.1093/jxb/erj100

Netto, A. T., Campostrini, E., de Oliveira, J. G., & Bressan-Smith, R. E. (2005). Photosynthetic pigments, nitrogen, chlorophyll a fluorescence and SPAD-502 readings in coffee leaves. *Scientia Horticulturae*, *104*, 199–209. https://doi.org/10.1016/j.scienta.2004.08.013

Oertli, J. (1968). Extracellular salt accumulation a possible mechanism of salt injury in plants. *Agrochimica*, *12*, 461–469.

Pitman, M. (1984). Transport across the root and shoot/root interactions. *Salinity Tolerance in Plants*, *Strategies for Crop Improvement*, 93–123.

Ramani, B., Reeck, T., Debez, A., Stelzer, R., Huchzermeyer, B., Schmidt, A., & Papenbrock, J. (2006). Aster tripolium L. and Sesuvium portulacastrum L.: Two halophytes, two strategies to survive in saline habitats. *Plant Physiology and Biochemistry*, *44*, 395–408.

Randall, S. K., & Sze, H. (1986). Properties of the partially purified tonoplast H+-pumping ATPase from oat roots. *Journal of Biological Chemistry*, *261*, 1364–1371.

Reeder, S. (2006). *Geochemical atlas of Europe. Part 2, Interpretation of geochemical maps, additional tables, figures, maps, and related publications*. Espoo, Finland: Geological Survey of Finland.

Romo, J. T., & Haferkamp, M. R. (1987). Effects of osmotic potential, potassium chloride, and sodium chloride on germination of greasewood (Sarcobatus vermiculatus). *The Great Basin Naturalist*, *47*(1), 110–116.

Sanchez, R., Hall, A., Trapani, N., & De Hunau, R. C. (1983). Effects of water stress on the chlorophyll content, nitrogen level and photosynthesis of leaves of two maize genotypes. *Photosynthesis Research*, *4*, 35–47. https://doi.org/10.1007/BF00041799

Slabu, C., Zörb, C., Steffens, D., & Schubert, S. (2009). Is salt stress of faba bean (Vicia faba) caused by Na^+ or Cl^- toxicity? *Journal of Plant Nutrition and Soil Science*, *172*, 644–651.

Sunderman, H., Pontius, J., & Lawless, J. (1997). Variability in leaf chlorophyll concentration among fully-fertilized corn hybrids. *Communications in Soil Science and Plant Analysis*, *28*, 1793–1803. https://doi.org/10.1080/00103629709369916

Tavakkoli, E., Rengasamy, P., & McDonald, G. K. (2010). High concentrations of Na^+ and Cl^- ions in soil solution have simultaneous detrimental effects on growth of faba bean under salinity stress. *Journal of Experimental Botany*, *61*, 4449–4459. https://doi.org/10.1093/jxb/erq251

Teakle, N., Flowers, T., Real, D., & Colmer, T. (2007). Lotus tenuis tolerates the interactive effects of salinity and waterlogging by 'excluding' Na^+ and Cl^- from the xylem. *Journal of Experimental Botany*, *58*, 2169–2180. https://doi.org/10.1093/jxb/erm102

Teakle, N. L., & Tyerman, S. D. (2010). Mechanisms of Cl-transport contributing to salt tolerance. *Plant, Cell & Environment*, *33*, 566–589.

Ullrich, T., Menge, S., Schmid, M., Gübitz, G., & Krauss, G. J. (2001). Enantioselective high-performance liquid chromatography of therapeutically relevant aminoalcohols as their fluorescent 1-naphthyl isocyanate derivatives. *Biomedical Chromatography*, *15*, 212–216.

Zimmermann, D., Zhou, A., Kiesel, M., Feldbauer, K., Terpitz, U., Haase, W., … Sukhorukov, V. (2008). Effects on capacitance by overexpression of membrane proteins. *Biochemical and Biophysical Research Communications*, *369*, 1022–1026. https://doi.org/10.1016/j.bbrc.2008.02.153

SUPPORTING INFORMATION

Additional supporting information may be found online in the Supporting Information section at the end of the article.

How to cite this article: Zhang X, Zörb C, Kränzlein M, Franzisky B, Kaiser H, Geilfus C-M. The early stress response of maize (*Zea mays* L.) to chloride salinity. *J Agro Crop Sci*. 2019;205:586–597. https://doi.org/10.1111/jac.12356

Supplementary material

Supplementary material 2.1: Soil pH of various *Zea mays* genotypes under control, low and high Cl^- treatment (low = 63.2 and high = 757.1 mg Cl^- kg^{-1} soil DM). Measurements were conducted after 10 days of treatment (64th day after sowing). Mean ± SE; different letters indicate significant differences between varieties and treatments (Duncan test; $P \leq 0.05$; n=5).

Genotypes	Control	63.2 mg Cl^- kg^{-1}	757.1 mg Cl^- kg^{-1}
P8589	7.29±0.01a	7.28±0.01a	7.30±0.01a
LG30222	7.20±0.01a	7.21±0.01a	7.21±0.01a
Tokala	7.09±0.03a	7.10±0.03a	7.14±0.03a
KWS-Stabil	7.25±0.01a	7.26±0.01a	7.23±0.01a
Amamonte	7.29±0.02a	7.24±0.02a	7.26±0.02a
P8400	7.27±0.01a	7.27±0.01a	7.29±0.01a
LG30215	7.28±0.02a	7.29±0.02a	7.26±0.02a
ES-Metronom	7.27±0.01a	7.25±0.02a	7.27±0.01a

Supplementary material 2.2: Examples of *Zea mays* phenotypes of contrasting genotypes and chlorotic symptoms in the genotype P8589 after 10 days under various Cl^- treatments (64th day after sowing). Plant phenotypes under control, low and high Cl^- treatment (low = 63.2 and high = 757.1 mg Cl^- kg^{-1} soil DM) of **(A)** the slightly Cl^--sensitive genotype P8589, **(B)** the slightly Cl^--tolerant genotype ES-Metronom, and (**C**) the 9th leaf blade of the slightly Cl^--sensitive genotype P8589 displaying chlorotic symptoms.

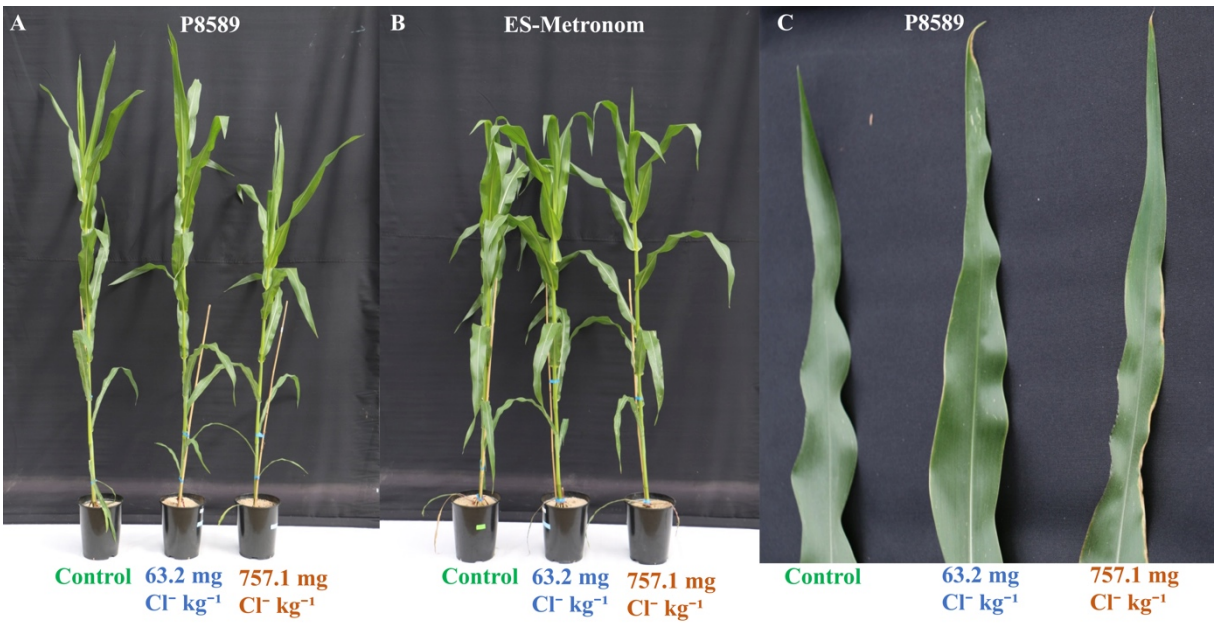

Supplementary material 2.3: Illustration of the water sensor operation principle. Leaf water content was measured by using a sensor consisting of infrared (IR) light-emitting diodes and a photodiode linked to a custom device. Transmissions of two near IR-wavelengths with various absorption characteristics for H_2O were recorded when IR light penetrated the leaves at an angle of 45°. The ratio of the transmission values at these two wavelengths is linearly correlated to the leaf water content. After calibration of the sensor to the respective leaf material, the leaf water content was calculated based on the transmission ratio.

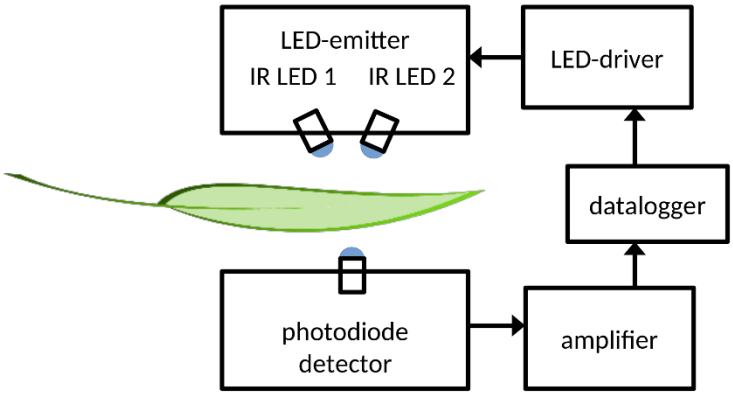

Supplementary material 2.4: Kinetics of the absolute water content of the 9th leaf blades of various *Zea mays* genotypes under control, low and high Cl^- treatment (low = 63.2 and high = 757.1 mg Cl^- kg^{-1} soil DM). The water contents were measured daily within the first 9 days of Cl^- treatment. Mean ± SE; n=5.

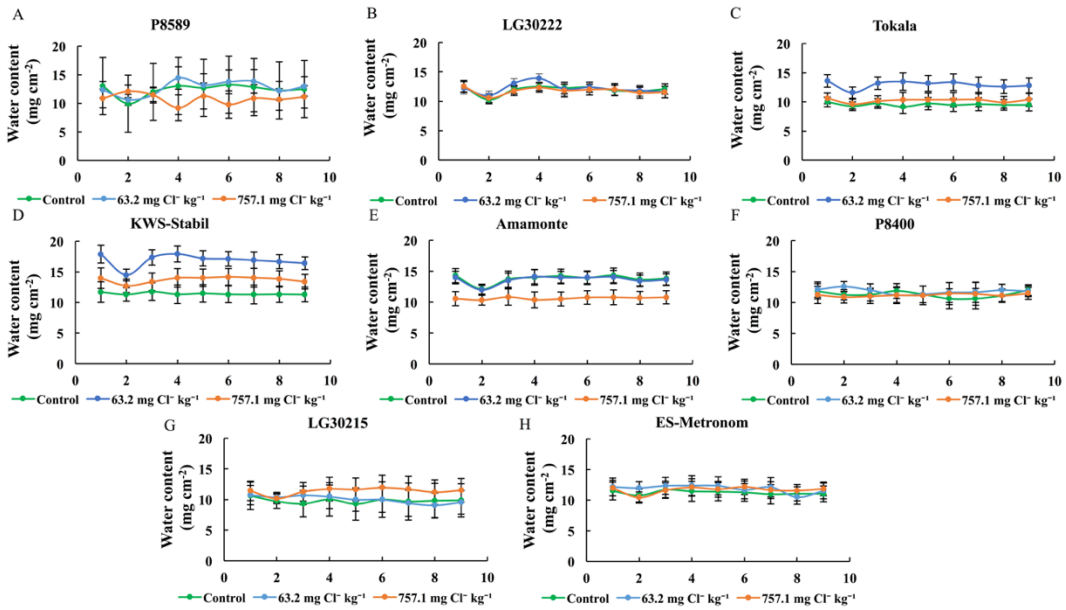

Supplementary material 2.5: Data of a water sensor calibration example for the *Zea mays* genotype Amamonte under control, low and high Cl^- treatment (low = 63.2 and high = 757.1 mg Cl^- kg^{-1} soil DM). (**A)** Measured weights of water per leaf disc and the corresponding near infrared (NIR) transmission ratios (water value) obtained from the water sensor based on the ratio of two recordings of the transmissions of two NIR-wavelengths with various absorption characteristics for H_2O and (**B)** the plotted values representing a water sensor calibration curve. Excised leaf discs were saturated by being floated at 4°C in double distilled H_2O overnight. After removal of the discs from the water bath, the water contents of the drying leaf discs were determined at six time points, namely 0, 10, 20, 30, 45 and 60 minutes, by being weighed and by using the water sensor.

A

Amamonte	weight of water / S (g cm^{-2})	water value
Control-1st time point	0.012346045	0.47192
Control-2nd time point	0.011279597	0.47298
Control-3rd time point	0.010925975	0.47518
Control-4th time point	0.010349014	0.48265
Control-5th time point	0.009833471	0.48257
Control-6th time point	0.009396097	0.4849
63.2 mg Cl^- kg^{-1} -1st time point	0.013661026	0.4469
63.2 mg Cl^- kg^{-1} -2nd time point	0.011870976	0.45265
63.2 mg Cl^- kg^{-1} -3rd time point	0.011421977	0.45583
63.2 mg Cl^- kg^{-1} -4th time point	0.010651839	0.46294
63.2 mg Cl^- kg^{-1} -5th time point	0.01003781	0.46678
63.2 mg Cl^- kg^{-1} -6th time point	0.009518933	0.4756
757.1 mg Cl^- kg^{-1} -1st time point	0.011850253	0.46328
757.1 mg Cl^- kg^{-1} -2nd time point	0.010493014	0.46512
757.1 mg Cl^- kg^{-1} -3rd time point	0.010038073	0.46854
757.1 mg Cl^- kg^{-1} -4th time point	0.009194538	0.47588
757.1 mg Cl^- kg^{-1} -5th time point	0.008527292	0.48327
757.1 mg Cl^- kg^{-1} -6th time point	0.007979468	0.4898

B

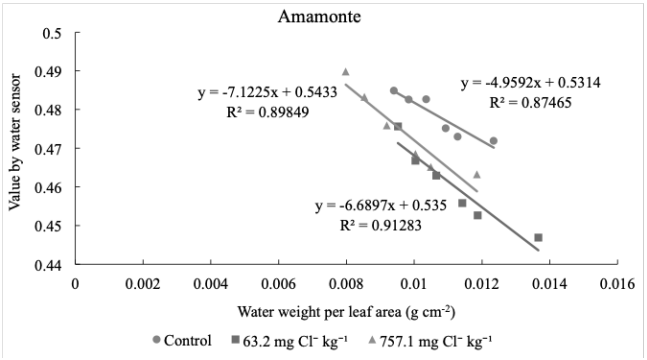

Supplementary material 2.6: Data of principle component analysis (PCA) based on the means of 24 measured variables of various *Zea mays* genotypes under control, low and high Cl^- treatment (low = 63.2 and high = 757.1 mg Cl^- kg^{-1} soil DM; n=5). (**A)** Listing and numbering of the individual variables, (**B)** matrix of the extracted components and (**C)** matrix of the rotated components (Method: Varimax with Kaiser normalization; 10 iterations).

A

VAR00001	Parameters
VAR00002	Fresh weight in the 9th leaf blade
VAR00003	Dry weight in the 9th leaf blade
VAR00004	Fresh weight in other leaf blades
VAR00005	Dry weight in other leaf blades
VAR00006	Fresh weight in leaf sheaths
VAR00007	Dry weight in leaf sheaths
VAR00008	Dry weight in the root
VAR00009	1st phase stomatal conductance
VAR00010	2nd* phase stomatal conductance
VAR00011	1st* phase photosynthetic rate
VAR00012	2nd* phase photosynthetic rate
VAR00013	1st* phase transpiration rate
VAR00014	2nd* phase transpiration rate
VAR00015	1st* phase water content
VAR00016	2nd* phase water content
VAR00017	Soil electrical conductance
VAR00018	Electrolyte leakage
VAR00019	Osmolarity
VAR00020	Soil pH
VAR00021	Cl^- concentration in the 9th leaf blade
VAR00022	Cl^- concentration in other leaf blades
VAR00023	Cl^- concentration leaf sheaths
VAR00024	Cl^- concentration in the root
VAR00025	Cl^- concentration in the soil

* 1st phase means stress induction phase (45th day to 53rd day); 2nd phase means full stress phase (54th day to 64th day)

B

Component Matrix[a]

	Component						
	1	2	3	4	5	6	7
VAR00024	-.888						
VAR00023	-.884						
VAR00021	-.860						
VAR00025	-.855						
VAR00017	-.828						
VAR00022	-.740						
VAR00019	-.654						
VAR00014							
VAR00005		.732					
VAR00006		.678					
VAR00004		.676					
VAR00010		-.671					
VAR00008		.655					
VAR00007							
VAR00016			.856				
VAR00015			.853				
VAR00003			-.848				
VAR00002			-.829				
VAR00012				.697			
VAR00009				-.615			
VAR00020							
VAR00011					.698		
VAR00013					.626		
VAR00018							-.623

Extraction Method: Principal Component Analysis.

C

Rotated Component Matrix[a]

	Component						
	1	2	3	4	5	6	7
VAR00022	.943						
VAR00021	.923						
VAR00023	.919						
VAR00024	.863						
VAR00025	.857						
VAR00017	.705						
VAR00015		.918					
VAR00016		.908					
VAR00003		-.840					
VAR00002		-.802					
VAR00004			.893				
VAR00005			.879				
VAR00019			-.719				
VAR00020				.817			
VAR00007				.777			
VAR00006				.746			
VAR00008				.704			
VAR00012					.917		
VAR00014					.835		
VAR00010					.730		
VAR00011						.934	
VAR00013						.902	
VAR00009						.662	
VAR00018							.734

Extraction Method: Principal Component Analysis.
Rotation Method: Varimax with Kaiser Normalization.
a. Rotation converged in 10 iterations.

Chapter 4

Acclimatisation of guard cell metabolism to long-term salinity

Bastian L. Franzisky, Christoph-Martin Geilfus, Maria Luisa Romo Pérez, Ines Fehrle, Alexander Erban, Joachim Kopka, Christian Zörb

Plant, Cell & Environment (2020)

Received: 30 April 2020 | Revised: 19 November 2020 | Accepted: 26 November 2020
DOI: 10.1111/pce.13964

Check for updates

ORIGINAL ARTICLE

Plant, Cell & Environment WILEY

Acclimatisation of guard cell metabolism to long-term salinity

Bastian Leander Franzisky[1] | Christoph-Martin Geilfus[2] | Maria Luisa Romo-Pérez[1] | Ines Fehrle[3] | Alexander Erban[3] | Joachim Kopka[3] | Christian Zörb[1]

[1]Institute of Crop Science, University of Hohenheim, Stuttgart, Germany

[2]Division of Controlled Environment Horticulture, Faculty of Life Sciences, Albrecht Daniel Thaer-Institute of Agricultural and Horticultural Sciences, Humboldt-University of Berlin, Berlin, Germany

[3]Max-Planck-Institute of Molecular Plant Physiology, Potsdam-Golm, Germany

Correspondence
Christian Zörb, University of Hohenheim, Institute of Crop Science, 340e, Schloss Westflügel, 70593, Stuttgart, Germany.
Email: Christian.zoerb@uni-hohenheim.de

Funding information
Deutsche Forschungsgemeinschaft, Grant/Award Number: 320167376

Abstract

Stomatal movements are enabled by changes in guard cell turgor facilitated via transient accumulation of inorganic and organic ions imported from the apoplast or biosynthesized within guard cells. Under salinity, excess salt ions accumulate within plant tissues resulting in osmotic and ionic stress. To elucidate whether (a) Na^+ and Cl^- concentrations increase in guard cells in response to long-term NaCl exposure and how (b) guard cell metabolism acclimates to the anticipated stress, we profiled the ions and primary metabolites of leaves, the apoplast and isolated guard cells at darkness and during light, that is, closed and fully opened stomata. In contrast to leaves, the primary metabolism of guard cell preparations remained predominantly unaffected by increased salt ion concentrations. Orchestrated reductions of stomatal aperture and guard cell osmolyte synthesis were found, but unlike in leaves, no increases of stress responsive metabolites or compatible solutes occurred. Diverging regulation of guard cell metabolism might be a prerequisite to facilitate the constant adjustment of turgor that affects aperture. Moreover, the photoperiod-dependent sucrose accumulation in the apoplast and guard cells changed to a permanently replete condition under NaCl, indicating that stress-related photosynthate accumulation in leaves contributes to the permanent closing response of stomata under stress.

KEYWORDS
apoplast, assimilation, chloride, field bean, guard cells, metabolite, salt stress, sodium, stomata, transpiration

1 | INTRODUCTION

Legumes and particularly *Vicia faba* L. are sensitive to salt and, therefore, undergo fast physiological changes attributable to osmotic stress, as early as the first hour after exposure to high salinity. In addition to the inhibition of nitrogen assimilation and the accumulation of metabolites associated with the formation and scavenging of reactive oxygen species (Geilfus et al., 2015; Geilfus, Mithofer, Ludwig-Muller, Zörb, & Mühling, 2015), abscisic acid signalling results in the rapid closure of stomatal pores, which are formed by pairs of highly specialized guard cells (GCs) (Jezek & Blatt, 2017). With continuous exposure to high salinity, salt ions accumulate within roots and leaves and, in turn, cause symptoms of ion toxicity as a result of disturbed ion homeostasis (Munns, James, Gilliham, Flowers, & Colmer, 2016). Such abiotic stress condition perturbs plant metabolism, for example, by hindering enzyme function and lowering the availability of substrates (Obata &

This is an open access article under the terms of the Creative Commons Attribution-NonCommercial License, which permits use, distribution and reproduction in any medium, provided the original work is properly cited and is not used for commercial purposes.
© 2020 The Authors. *Plant, Cell & Environment* published by John Wiley & Sons Ltd

Fernie, 2012). As part of an optimization of the biological system to the new environmental condition (Herrmann, Schwartz, & Johnson, 2019), metabolism acclimates by reconfiguring the metabolic network to adopt a new steady state (Obata & Fernie, 2012), which can help to avoid or mitigate harmful effects resulting from the prevailing stress condition (Schwachtje et al., 2019). The leaf metabolic acclimation of *V. faba* to salt stress is characterized by, for example, increased metabolite pools of *myo*-inositol, the presence of the general stress marker proline and decreased intermediates of the tricarboxylic acid (TCA) cycle and monosaccharides such as arabinose and xylose (Richter, Behr, Erban, Kopka, & Zörb, 2019), all of which reflect conserved patterns of metabolic acclimation to high salinity in legumes (Sanchez et al., 2011; Sanchez, Siahpoosh, Roessner, Udvardi, & Kopka, 2008). In contrast to the well-known metabolic acclimation of root and leaf tissues to high salinity, information about stress-related modifications of the specialized GC metabolome is limited.

Guard cells enable a controlled gas exchange between the atmosphere and the leaf internal space. This is important for balancing the trade-off between CO_2 intake and the concomitant water loss achieving CO_2 availability for Calvin cycle activity, the autotrophic production of organic compounds and the maintenance of the plant's hydration (Lawson & Blatt, 2014; McAusland et al., 2016), aspects essential for cell expansion and plant growth (Thompson, 2005). The adjustment of stomatal aperture in response to exogenous and endogenous cues is facilitated by the transient accumulation of osmotically active compounds within GCs thereby enabling rapid turgor changes (Jezek & Blatt, 2017). For this process, the import of K^+, Cl^- and NO_3^- from the apoplast is essential; however, organic solutes considerably contribute to the GC osmotic adjustment (Lawson & Matthews, 2020). Therefore, GC metabolism is not only important for feeding the high energy demand required for ion transport processes, but also for contributing to the built up of the osmotic gradient necessary for stomatal opening by the synthesis of organic solutes such as malate (Kollist, Nuhkat, & Roelfsema, 2014; Kopka, Provart, & Müller-Röber, 1997; Santelia & Lawson, 2016). In contrast to the increasing sucrose and starch content in mesophyll cells (Santelia & Lunn, 2017; Tcherkez, Boex-Fontvieille, Mahé, & Hodges, 2012), the degradation of starch (Daloso et al., 2017; Flütsch et al., 2020; Horrer et al., 2016) and the activation of glycolysis (Medeiros et al., 2018) occur in GCs in response to illumination indicating the demand for energy during stomatal opening. In agreement with this, the breakdown of lipid droplets and starch in GCs has been found to be essential for blue-light-stimulated stomatal opening (Horrer et al., 2016; McLachlan et al., 2016). The breakdown of fatty acids is proposed to favour adenosine triphosphate production via peroxisomal β-oxidation during the dark-to-day transition (McLachlan et al., 2016), whereas starch breakdown is suggested to replenish cytosolic sugar pools (Flütsch et al., 2020) and to stimulate the flux of carbon skeletons into mitochondria and the TCA cycle for energy production (Daloso et al., 2015; Daloso, Anjos, & Fernie, 2016; Lima et al., 2018; Medeiros et al., 2018). Guard cells in detached epidermal strips are able to respond to environmental cues such as light intensity and quality and changes in CO_2 solely (Mott, Sibbernsen, & Shope, 2008). Nevertheless, mesophyll derived sugars and organic acids have been shown to affect stomatal behaviour *in planta* (Antunes, de Menezes Daloso, Pinheiro, Williams, & Loureiro, 2017; Araújo et al., 2011; Kelly et al., 2013), providing evidence for metabolic feedback mechanisms correlating mesophyll photosynthetic demands with stomatal aperture. The accumulation of mesophyll-derived sucrose in the apoplast has been proposed as a mechanism for stimulating stomatal closure (Antunes et al., 2017; Granot & Kelly, 2019). This metabolic feedback of sucrose has been found to affect stomatal aperture via an abscisic acid pathway stimulating sugar-sensing hexokinase (Kelly et al., 2013; Lugassi et al., 2015), thereby coordinating mesophyll photosynthesis with transpirational water loss (Daloso et al., 2017; Lima et al., 2018).

The motivation behind the present study was to evaluate whether (a) long-term NaCl stress leads to Na^+ and Cl^- accumulation in GC preparations and whether (b) GCs reflect patterns of conserved metabolic response to high NaCl such as the accumulation of organic and amino acids. For this purpose, a non-targeted metabolomics workflow involving gas-chromatography mass-spectrometry was used to explore modulations of GC metabolism in comparison with that of leaves and the apoplast under long-term NaCl. To assess variation in the dark-to-light transition, we compared the physiological status of GCs under dark and light condition, that is, between closed and fully opened stomata.

2 | MATERIALS AND METHODS

2.1 | Cultivation of plant material

The *Vicia faba* L. varieties Fuego and Scoop (Norddeutsche Pflanzenzucht Hans-Georg Lembke KG, Hohenlieth, Germany) were grown under hydroponic culture conditions in a climate cabinet (WEISS HGC1014, Heuchelheim, Germany) (14/10 hr day/night; 22/18°C; approx. 80/60% humidity, 300 μmol photons m^2/s at shoot level). Seeds were immersed in aerated $CaSO_4$ (0.5 mM) solution for 1 day at room temperature and were subsequently placed in moistened quartz sand. After 12 days of germination, seedlings were transferred into plastic pots containing 1/4-strength aerated nutrient solution. The concentration of the nutrient solution was incrementally increased to 1/2-strength after 2 days, 3/4-strength after 3 days and to full-strength after 4 days. The full-strength nutrient solution had the following composition: 0.1 mM KH_2PO_4, 1.0 mM K_2SO_4, 2.0 mM $Ca(NO_3)_2$, 0.5 mM $MgSO_4$, 0.00464% (wt/vol) Sequestren (Ciba Geigy, Basel, Switzerland), 10 μM NaCl, 10 μM H_3BO_3, 2.0 μM $MnSO_4$, 0.5 μM $ZnSO_4$, 0.2 μM $CuSO_4$, 0.1 μM $CoCl_2$, 0.05 μM $(NH_4)_6Mo_7O_{24}$. After 4 days of growing under full-strength nutrient concentration, the NaCl treatment was introduced to the plants. During the following three consecutive days, the NaCl concentration was increased starting from 1/3-strength, over 2/3-strength to full-strength (100 mM NaCl), respectively. Concomitant to the replacement of the nutrient solution every third day, the plant roots were gently rinsed with deionized water. After 20 days of full-strength

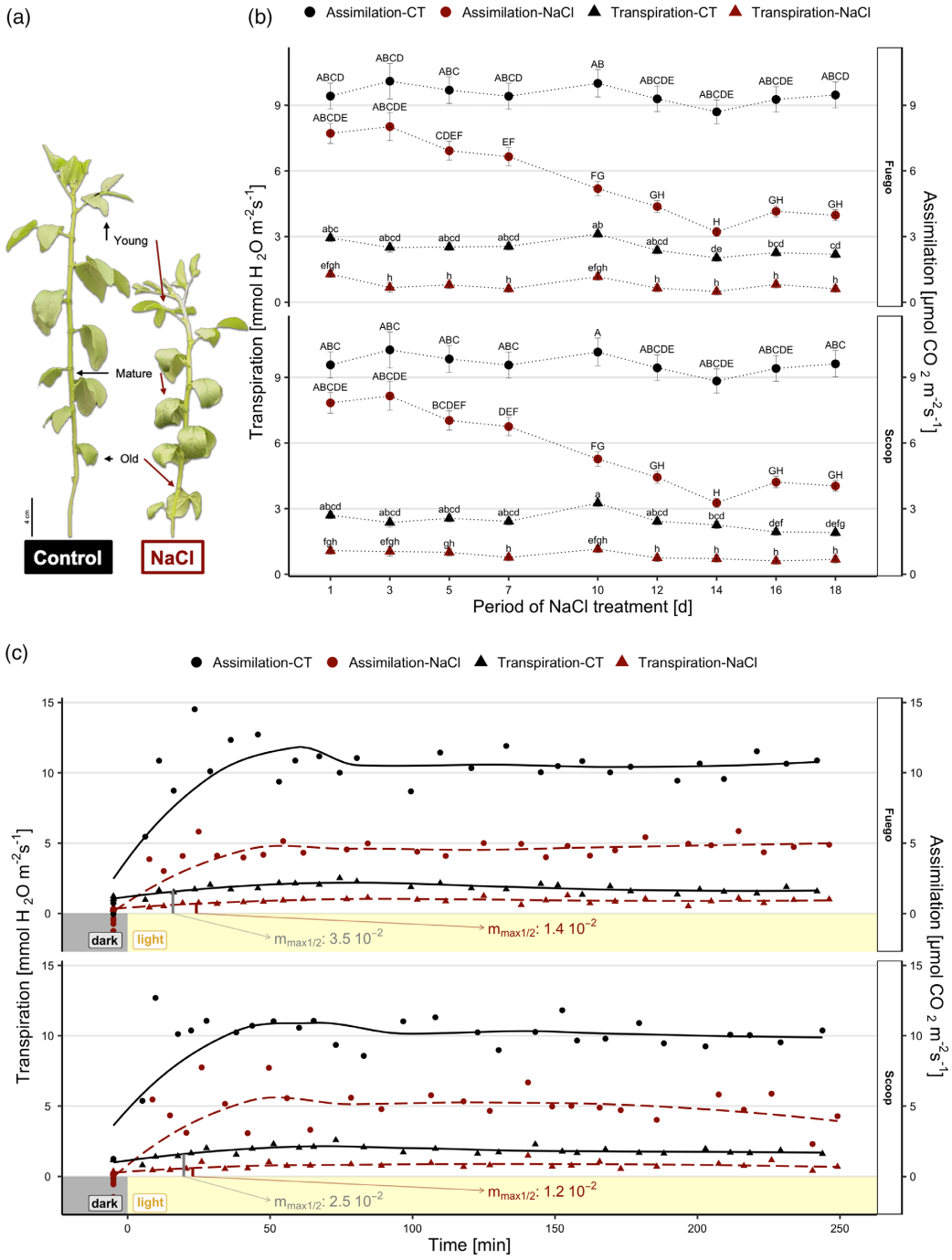

FIGURE 1 Gas exchange and the stomatal response to light in *Vicia faba* grown under NaCl. (a) Images of plant shoots from *V. faba* variety Fuego grown under control and 100 mM NaCl conditions (20 days). (b) Assimilation (A) and transpiration (E) rate of two *V. faba* varieties, Fuego and Scoop, grown under control and 100 mM NaCl. Measurements were conducted at fourth leaves from top after 100 mM NaCl treatment had been applied. Means ± SE; different letters indicate significant differences of means of comparison within variety (Tukey test; $p \leq .05$; $n = 5$). (c) The response of A and E rates of fourth leaves from top of Fuego and Scoop after 20 days NaCl stress and controls to light. Measurements of A and E rates with trend-line (local polynomial regression fit) during the transition from darkness to light indicated by labelled horizontal segments (grey: 0 µmol m^{-2} s^{-1}; yellow: 400 µmol m^{-2} s^{-1}). Vertical bars annotate the half of the maximum value ($max_{1/2}$) plus the slope (m) from the initial value to $max_{1/2}$ ($n = 3$) [Colour figure can be viewed at wileyonlinelibrary.com]

NaCl treatment, plant materials, all without salt-induced lesions, were harvested in a randomized order. Material referred to as light condition was collected starting from after 2.5 hr lights on. The material of the second, dark condition was collected identically, but the plants were kept in the darkness until harvest and the laboratory remained unlit (~1 μmol photons m^2/s) during the harvest (Figure S2).

2.2 | Isolation of guard cells

Guard cells for metabolomic analysis were isolated by the abaxial leaf epidermis being peeled off of at least 5 leaves as described earlier (Cornish & Zeevaart, 1986; Geilfus, Lan, & Carpentier, 2018). Peeled off strips were collected within 5 min in 10 ml 0.001% Tween20 on ice and then sonicated for 3 min by using 0.3 s pulses at approx. 35 W (SONOPULS HD 2070/UW 2070/M 73, Bandelin, Berlin, Germany). This procedure destroyed the epidermal cells, whereas the more robust GCs remained intact (Cornish & Zeevaart, 1986). After being rinsed with ice-cold deionized water in a sieve, isolated GCs (GC preparations) were shock-frozen in liquid nitrogen, lyophilized and stored at −80°C. To obtain sufficient material for ion analysis of GCs, a second GC isolation approach was used, namely, the ice blender method according to Bauer et al. (2013) with minor modifications. At least 6 leaves were blended (B-400, Büchi, Essen, Germany) in 200 ml deionized H_2O containing crushed ice for 30 s and, then, the tissue was collected and rinsed on a nylon mesh with a pore width of 210 μm. The collected tissue was subjected to a second blending step, as described above, and then, collected, shock-frozen in liquid nitrogen, lyophilized and stored at −80°C. The effectiveness of the two isolation methods was microscopically verified by means of viability stains (Geilfus et al., 2018; Geilfus, Mithofer, et al., 2015).

2.3 | Extraction of apoplastic washing fluids and sampling of leaf fractions

Cut leaves were infiltrated with deionized H_2O according to Lohaus, Pennewiss, Sattelmacher, Hussmann, and Mühling (2001). Apoplastic washing fluid (AWF) was collected within 3 min by carefully pulling the plunger of a syringe (without a needle) that was being gently pressed on the abaxial leaf side. Cytosolic AWF contamination (Floerl et al., 2008) was estimated by malate dehydrogenase (MDH) activity as described by Lohaus et al. (2001) (maximal relative activity of about 5%; Figure S1). The remaining leaf materials (symplastic leaf fractions) from which AWFs had been extracted, AWFs and non-treated leaf materials (non-sample controls) were shock-frozen in liquid nitrogen, lyophilized and stored at −80°C.

2.4 | Gas exchange and stomatal imprints

The transpiration and CO_2 assimilation rates of the fourth leaves (Figure 1a) were measured in the climate cabinet (see above) by using an LCi-*SD* ultra-compact photosynthesis system (ADC Bioscientific, U.K.) after 2.5 hr lights on. For the recording of the light-induced changes in gas exchange, sets of three plants of each condition were measured in rotation during dark-to-light (0–400 μmol photons m^2/s) transition until 4 hr after lights on. For recording of the stomatal closing response, leaf gas exchange was continuously measured of plants that had been transferred to dark. In addition to the transition to darkness, dry air (approx. 20% humidity) was supplied to the continuous flow leaf chamber. Epidermal imprints were taken under light (4 hr after lights on) and dark (4 hr after lights off at the end of the photoperiod) condition by applying a thin layer Formvar (2% in 1,2-dichlorethane). After being dried, the imprints were detached from the leaves by using adhesive strips and afterwards analysed microscopically.

2.5 | Ion extraction and measurement

Leaf ions were extracted and measured as described earlier (Franzisky, Geilfus, Kränzlein, Zhang, & Zörb, 2019). In brief, 50 mg ground plant material was solubilized by microwave digestion at 190°C for 25 min in 12 ml digestion solution (46% (vol/vol) HNO_3 and 10% (vol/vol) H_2O_2). Filtrated digestates were used for the analysis of cations by atomic absorbance spectroscopy whereas the Cl^- concentrations were measured by using the ferricyanide method (Munns, Wallace, Teakle, & Colmer, 2010). For the ion measurement of GC preparations and AWFs, approximately 15 mg DW or AWF aliquots of 100 μl were each added to 500 μl 0.5 M HNO_3, respectively, and then incubated at 85°C for 16 hr with repeated thorough mixing. Supernatants of centrifuged (20,800 g, 10 min 4°C) extracts were used for analysis. After the addition of internal Rh standard, concentrations were measured by using an inductively coupled plasma mass spectrometer (NexION 300 X, Perkin Elmer, Waltham, USA). AWFs were corrected by the subtraction of cytosolic ion contamination, which was calculated by the use of the respective fresh leaf ion concentrations and MDH activities (Figure S1). Although the ion concentrations of GC preparations do not refer to guard cell symplasts only (Raschke, 1979; Stevens & Martin, 1977), the approach allowed a qualitative analysis of the effect of the NaCl treatment on the ion contents.

2.6 | Metabolite extraction and metabolite profiling

Approximately 10 mg lyophilized leaf material or GC preparation was homogenized by using a Retsch MM300 TissueLyser (Haan, Germany). Soluble metabolites of leaves were extracted according to Richter et al. (2019) with modifications. In brief, metabolites were extracted in 360 μl methanol with added $U^{13}C_6$-sorbitol standard at 70°C for 1.5 hr. After the addition of 200 μl $CHCl_3$ the samples were agitated at 37°C for 0.5 hr. An aliquot of 400 μl bi-distilled H_2O was added to induce a liquid phase separation. After thorough mixing and centrifugation (20,800 g for 5 min), aliquots of 160 μl of the upper

polar phase were dried in a vacuum concentrator overnight at room temperature. AWFs were derivatized without further extraction. Primary metabolites of GC preparations were extracted with 600 µl premix containing MeOH/H_2O/$CHCl_3$: 2.5/1/1 (vol/vol/vol) without liquid partitioning into chloroform (Erban et al., 2020). Aliquots of 500 µl were dried in a vacuum concentrator overnight at room temperature. Chemical derivatization, that is, methoxyamination and trimethylsilylation, and subsequent gas chromatography-electron impact/time-of-flight mass-spectrometry (GasC-EI/TOF-MS)-based metabolite profiling was carried out as described earlier (Dethloff et al., 2014) in splitless mode for GC preparations and in splitless and split 1:30 mode for leaves and AWFs.

2.7 | Metabolite data processing

GasC-EI/TOF-MS chromatograms were acquired, visually controlled, baseline-corrected and exported in the NetCDF file format by using ChromaTOF software (Version 4.22; LECO, St. Joseph, USA). The processing of GasC-EI/TOF-MS data into a standardized numerical data matrix and compound identification were performed by using TagFinder software (Luedemann, Strassburg, Erban, & Kopka, 2008). Compounds were identified according to standardized guidelines (Dethloff et al., 2014) by mass spectral and retention time index matching to a reference collection of authenticated standard substances and of frequently observed but not yet identified mass spectral tags from the Golm Metabolome Database, GMD, (http://gmd.mpimp-golm.mpg.de/search.aspx) (Hummel et al., 2010; Kopka et al., 2005). In this study, individual hexoses could not be resolved because of co-elution. Because the extraction of the GC preparation metabolites had been performed without phase separation, an analysis of fatty acids and lipids was performed for GC preparations only. Data processing and numerical analysis were carried out according to Richter et al. (2019). Metabolite abundancies were normalized to weights, internal standards and the sum of the intensities of the respective sample to enable the analysis of compositional changes of metabolites separately within each of the three sample types, namely leaves, AWFs and GCs. Values are presented as the percent of maximum. Fold-changes for the comparison of metabolic changes in response to experimental conditions were calculated by numerical subtraction after $\log_2$-transformation.

2.8 | Statistical analysis

All fractions for metabolome profiling, but non-sample controls, were sampled from two independent experiments with each of 5 biological replicates yielding 10 biological replicates for AWFs, symplastic fractions and GC preparations (exceptions with n = 9 are given in Table S1). Symplastic fractions (leaf material from which AWFs had been extracted) were used to restrict analysis of AWF profiles to metabolite pools that remained unaffected by the extraction procedure ($p \leq .001$). Data processing, transformation, analyses of variance (ANOVA), models and the post-hoc test (Tukey's) were carried out by using R software for statistical computing (R Core Team, 2020). Data of repeated experiments were analysed by using the mixed model algorithm of "lmer" (Bates, Maechler, Bolker, & Walker, 2015) with the repeated experiments as a random factor by applying a significance threshold of $p < .05$. Other data were analysed by using linear models and applying the same threshold unless stated otherwise. Prior to computing the principal component analysis by using "stats", the data were restricted to metabolites with less than 10% missing values (NA); remaining NA were replaced by half of the minimum value. Data were plotted by using "ggplot2" (Wickham, 2016). Trend-lines were fitted with local polynomial regression by using "stats". Heatmaps and Euler diagrams were drawn by using "pheatmap" (Kolde, 2019) and "VennDiagram" (Chen & Boutros, 2011), respectively.

3 | RESULTS

3.1 | Leaf physiological measures

The two *Vicia faba* L. varieties Fuego and Scoop were selected to allow the evaluation of the broad stress response occurring in both varieties, which had shown plasticity in withstanding salt stress in a previous experiment (Franzisky et al., 2019). In addition, in this experiment, some plants of the variety Fuego showed salt-induced stress symptoms such as necrotic spots on leaves a few days earlier than Scoop. However, for the collection of plant material and physiological measurements only plants without symptoms were considered.

Under control conditions, mature leaves (Figure 1a) of both varieties exhibited similar assimilation and transpiration rates, with values of about 9 µmol CO_2 m^{-2}/s and 3 mmol H_2O m^{-2}/s, respectively (Figure 1b). In response to NaCl treatment, the transpiration rate significantly decreased by about 60% in comparison with controls. This reduction was constant over the measuring period for both varieties. Similar to the transpiration, the rate of CO_2 assimilation was slightly reduced at the beginning of the stress period but decreased continuously with prolonged exposure to NaCl stress to values of about 4 µmol CO_2 m^{-2}/s, although gas exchange in terms of transpiration remained at a similarly reduced level (Figure 1b). To assess the opening response of the stomata to light, we recorded the gas exchange characteristics during the dark-to-light transition after 20 days of NaCl stress. After lights on, the photosynthesis rate of both varieties increased within 25 mins to the respective maximum with no temporal differences between NaCl stressed and control plants (Figure 1c). However, the maximal assimilation rate of NaCl treated plants was half of that of controls (Figure 1b,c). In accordance with the course of assimilation rates, the transpiration rates increased with the duration of illumination, but in the salt stressed plants, the maximum rates were again half of that of the controls. The transpiration rates of NaCl stressed Fuego and Scoop reached maximal values after about 60 mins, which was about 30% later than controls (Figure 1c). The comparison of the slopes from initial values recorded at darkness to half of the maximum ($max_{1/2}$) illustrated that the speed of the light-

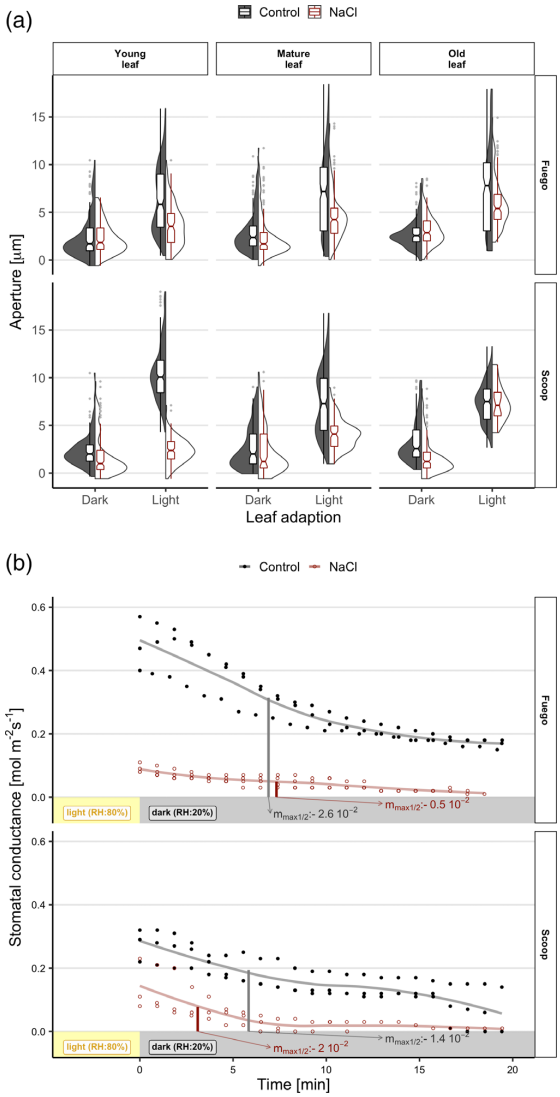

FIGURE 2 Analysis of stomatal apertures and the closing response in salt stressed *Vicia faba*. (a) Stomatal aperture of leaves of various developmental stages of two *V. faba* varieties, Fuego and Scoop, from control and 20 days 100 mM NaCl conditions. Epidermal imprints were taken from the abaxial side of young, mature and old leaves (Figure 1a) during dark and light. Data are presented as box plots featuring the maxima, 75 quartiles, medians, 25 quartiles and minima with density plots of individual apertures (n = 3). (b) The response of stomatal conductance of fourth leaves from top of Fuego and Scoop after 20 days NaCl stress and controls to combined darkness and dry air (approx. 20% humidity) as stomatal closing stimuli. Continuous measurement of stomatal conductance with trend-line (local polynomial regression fit) during the transition from light to dark and from 80 to 20% relative humidity (RH) indicated by labelled horizontal segments (yellow: 400 µmol m^{-2} s^{-1}, RH: ~80%; grey: 0 µmol m^{-2} s^{-1}, RH: ~20%). Vertical bars annotate the half of the maximum value ($max_{1/2}$) plus the slope (m) from the initial value to $max_{1/2}$ (n = 3) [Colour figure can be viewed at wileyonlinelibrary.com]

induced increase of transpiration, that is, the opening of the stomatal pores, was about 50% slower in long-term NaCl stressed plants than in the controls, irrespective of the variety.

In agreement with the reduced transpiration rates, the stomatal apertures of leaves of various developmental stages were reduced under light after 20 days of NaCl stress in comparison with controls (Figure 2a). However, the aperture of the stomatal pores of leaves of various developmental stages was differently regulated because the salt stress-induced reduction was weaker in old leaves than in mature and young leaves in both varieties. Moreover, young leaves of Scoop had more opened stomata under control conditions in comparison with Fuego whereas the apertures of both varieties were similar under NaCl condition. In contrast to the differential aperture regulation in light, the stomata of NaCl-treated plants were closed 4 hr after the end of the photoperiod (dark), the same as in the controls (Figure 2a). To assess the closing response of stomata, we recorded gas-exchange of plants that had been transferred to dark and were treated with dry air (approx. 20% humidity). In response to the combined closing stimuli, the rates of stomatal conductance of all plants declined markedly within 20 min (Figure 2b). Starting from about 0.4 to 0.6 mol m^{-2} s^{-1}, the stomatal conductance of controls decreased by at least 50% within 20 mins reaching a constant, basal plateau. In agreement with the reduced gas-exchange under NaCl stress, the initial rates of stomatal conductance of NaCl stressed plants were lower than that of the controls with values of 0.1 mol m^{-2} s^{-1}, which decreased in response to the closing stimuli to zero within 20 and 10 mins in Fuego and Scoop, respectively (Figure 2b). The comparison of the slopes from initial values to $max_{1/2}$ illustrated that the stomatal conductance declined about 50% faster in Fuego than in Scoop under control conditions. Under long-term salt stress however, the response to the closing stimuli was faster in Scoop than in the respective control, and four-fold faster in comparison with salt stressed Fuego.

3.2 | Ion concentrations of leaves, apoplast and guard cell preparations

In response to NaCl treatment, Na^+ and Cl^- concentrations increased in young and mature leaves of both varieties (Figure 3). Compared with younger leaves, the accumulation of Na^+ and Cl^- and the reductions in K^+ were higher in mature leaves. Mature leaves also showed a significant reduction in Mg^{2+} concentration, whereas stress-responsive increases in Ca^{2+} were higher in young leaves of both cultivars. An enrichment of salt ions was also found in the apoplastic space, that is, cell walls, with Na^+ and Cl^- concentrations being increased >100-fold and up to 26-fold in comparison with controls, respectively (Figure 3b). A similar trend was found for GC preparations because the Na^+ concentrations were increased three-fold and 7.6-fold in the NaCl-treated Fuego and Scoop varieties, respectively, whereas the Cl^- concentrations remained similar to those of the control (Figure 3c). The concentrations of K^+, being the major inorganic osmolyte for GC osmotic adjustment, were significantly reduced (0.1 to 0.2-fold) in comparison with controls (Figure 3c). Divalent cations such as Ca^{2+} and Mg^{2+} remained unchanged, the slight reductions being non-significant.

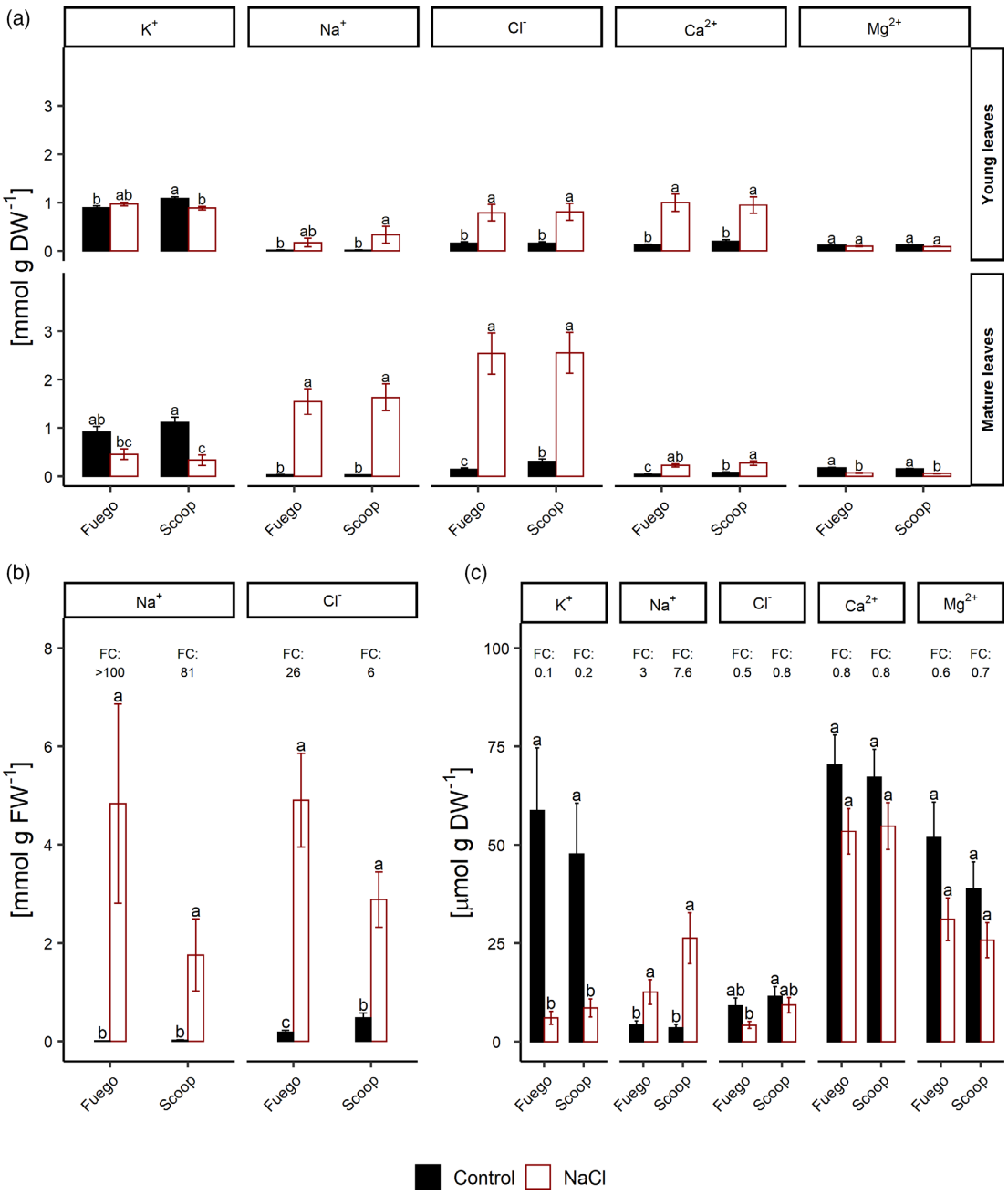

FIGURE 3 Ion compositions of various leaf fractions of *Vicia faba* grown under NaCl and control conditions. Ion concentrations of (a) young and mature leaves, (b) apoplastic washing fluids and (c) guard cell preparations of *V. faba* varieties, Fuego and Scoop, under control and 100 mM NaCl conditions. Concentrations of potassium (K^+), sodium (Na^+), chloride (Cl^-), calcium (Ca^{2+}) and magnesium (Mg^{2+}). Means ± SE; FC, fold change; different letters indicate significant differences of comparisons between varieties and treatments within ions; ($p \leq .05$; $n = 5$) [Colour figure can be viewed at wileyonlinelibrary.com]

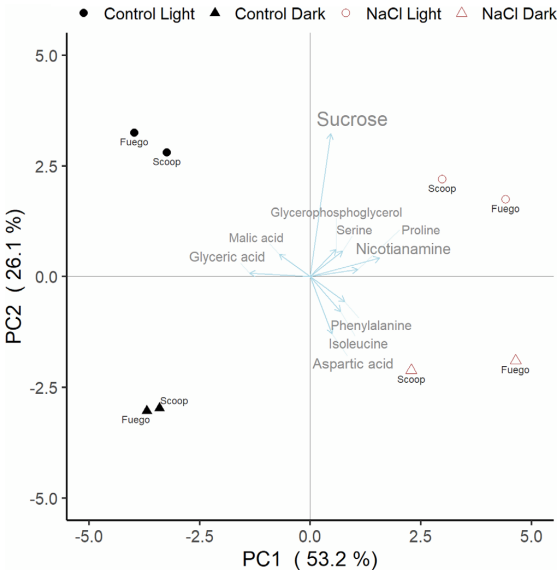

FIGURE 4 Unsupervised analysis of leaf primary metabolite content of *Vicia faba* in dark and light under NaCl and control conditions. Principal component analysis (PCA) of the relative leaf metabolite content of two *V. faba* varieties, Fuego and Scoop, under control and 100 mM NaCl, and dark and light conditions. Principal components (PCs) represent 79.3% of the total variance of the data with PC1 reflecting the differences between control and NaCl, and PC2 the differences between dark and light conditions. Top 10 influential metabolites of PC loadings are indicated by labels and blue arrows. The segment length and the size of the metabolite labels correspond to the influence on the separation (means of $n = 5$) [Colour figure can be viewed at wileyonlinelibrary.com]

3.3 | Leaf metabolic acclimation to long-term NaCl

For a comparison of the metabolic signatures of GCs, the apoplast and the leaves in response to long-term NaCl during dark and light, we applied non-targeted gas chromatography mass-spectrometry. The evaluation of the metabolites in each fraction was restricted to manually identified mass spectral tags consisting of known metabolites and to non-identified compounds with known mass spectrum and retention index properties.

To overview the general effects of the experimental conditions on the metabolome of the mesophyll dominated whole leaf fractions, from which the GC preparations and the AWFs had been isolated, we analysed the principal components of the leaf metabolomic data (Figure 4). The latter analysis illustrated a separation according to the long-term NaCl treatment (horizontally) and the light conditions (vertically). Correspondingly, the first principal component gave high loadings to NaCl-responsive metabolites such as the compatible solute proline and other amino acids such as aspartic acid, phenylalanine, isoleucine and serine whereas the separation along the second principal component was largely influenced by the light-dependent changes in sucrose content. More specifically, the leaf metabolic response to long-term NaCl was mainly characterized by lower levels of organic acids related to the TCA cycle (aconitic-, maleic- and malic acid), minor carbon hydrate metabolism (threonic acid) and photorespiratory pathway associated glyceric acid whereas the compatible solute proline and other amino acids, the stress-responsive *myo*-inositol, TCA cycle intermediate succinic acid and anti-oxidative and membrane-related compounds (nicotiamide, glycerophosphoglycerol) were increased (Figure 5a). Although the changes in metabolite pools in response to NaCl exposure showed variety-specific differences in their extent, these general trends were the same for Fuego and Scoop (Figure 5).

3.4 | Guard cell metabolic response to long-term NaCl diverges from that of leaves

Qualitative analysis revealed decreasing leaf and GC preparation metabolite pools having partly overlapping patterns in response to NaCl treatment (Figure 5). Decreases of 6 metabolite pools were found in GC preparations, with 5 (butanoic acid, 4-amino- [GABA], citric-, malic-, glutamic- and glyceric acid) being common between the two *V. faba* varieties (Figure 5a,b). Although the reduction of citric acid was the same for both varieties, the reductions of GABA, malic and glutamic acid pools in Fuego were about two-fold in comparison with Scoop (Figure 5a). Common decreases between leaves and GC preparations were found for glyceric and malic acid, and for A170001, with the last-mentioned for Fuego only (Figure 5b). In comparison with leaves, the reductions of malic acid pools of GC preparations were higher for each variety, whereas glyceric acid was similarly reduced (Figure 5a). In GC preparations 7 metabolites increased in response to NaCl treatment of which the fatty acid tetradecanoic acid was similar for both varieties (Figure 5a,c). However, there was no common increase between metabolite pools of leaves and GC preparations (Figure 5c).

3.5 | Deviations in guard cell metabolic response to light under long-term NaCl

For a detailed analysis of the metabolic response to light (Stitt, Lunn, & Usadel, 2010; Stitt & Zeeman, 2012; Szecowka et al., 2013) throughout the three leaf fractions, we looked at the changes resulting from the transition from dark to light (Figure 6). Similar patterns of light-induced increases were found for sucrose and malic acid representing the major photosynthate and a TCA cycle intermediate with a central role in primary metabolism and in GC turgor adjustments, respectively. However, malic acid pools in the leaf and AWF fractions showed only minor light-related increases under control conditions, because the levels were similar in darkness and light (Figure 7e,f). In contrast, the light-induced increases in the malic acid

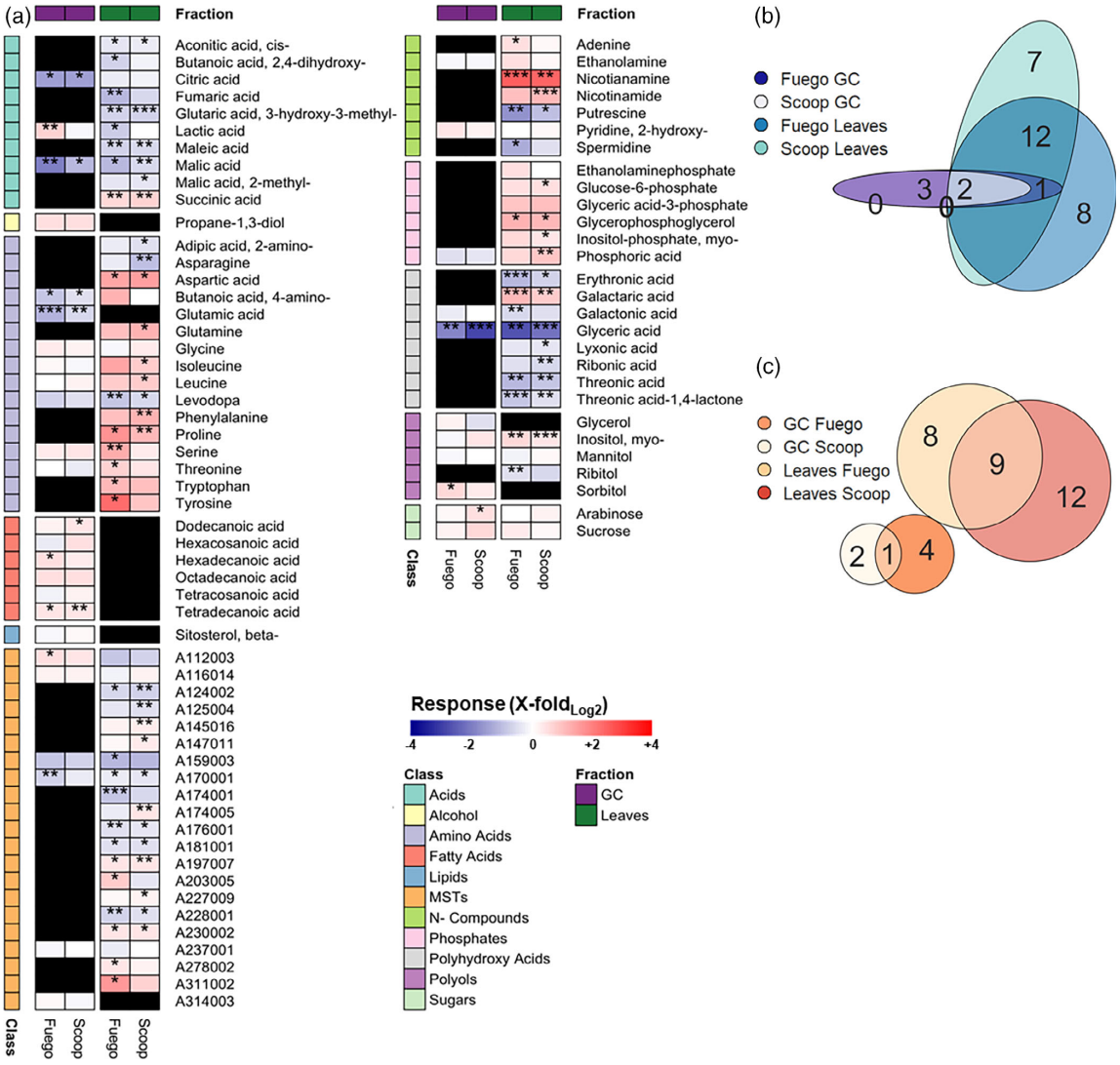

FIGURE 5 Analysis of common and specific metabolic changes in guard cell preparations and leaves of *Vicia faba* in response to NaCl. (a) Metabolic response to NaCl (100 mM, 20 days) in guard cell (GC) preparations and leaves of the *V. faba* varieties, Fuego and Scoop, under light condition. Means of the fold-change$_{log2}$ of the relative metabolite contents are indicated by a colour code. Asterisks indicate the level of significance (*$p \leq .05$; **$p \leq .01$; ***$p \leq .001$; GC: $n = 9–10$; leaves: $n = 5$; MST, mass spectral tag; the shown metabolites are restricted to detections in GCs plus affected leave metabolites; full data set provided in supplementary Table S1). (b, c) Comparison of common, significantly affected metabolites in leaves and GC preparations under light condition. Results of the qualitative assessment of decreased (b) and increased (c) metabolite pools are plotted as Euler diagrams with numbers indicating common and unique metabolites [Colour figure can be viewed at wileyonlinelibrary.com]

pools of GC preparations were more prominent, because the levels were low at darkness and high after acclimation to light (Figure 7d). Under NaCl, malic acid pools of leaf and AWF fractions only slightly increased in response to light, whereas light-related increases in GC preparations were diminished (Figure 7d–f). The sucrose pools increased under all conditions and in all fractions in response to illumination; however, increases in AWFs and GC preparations were slightly lower under NaCl conditions (Figure 6; Figure 7a–c). In comparison with the control, the sucrose levels of GC preparations and AWFs of NaCl-treated plants were higher at dark (Figure 7a,b). Pools of amino acids tended to decrease in AWFs and leaves in response to light, except for the increasing pools of photorespiratory-pathway-

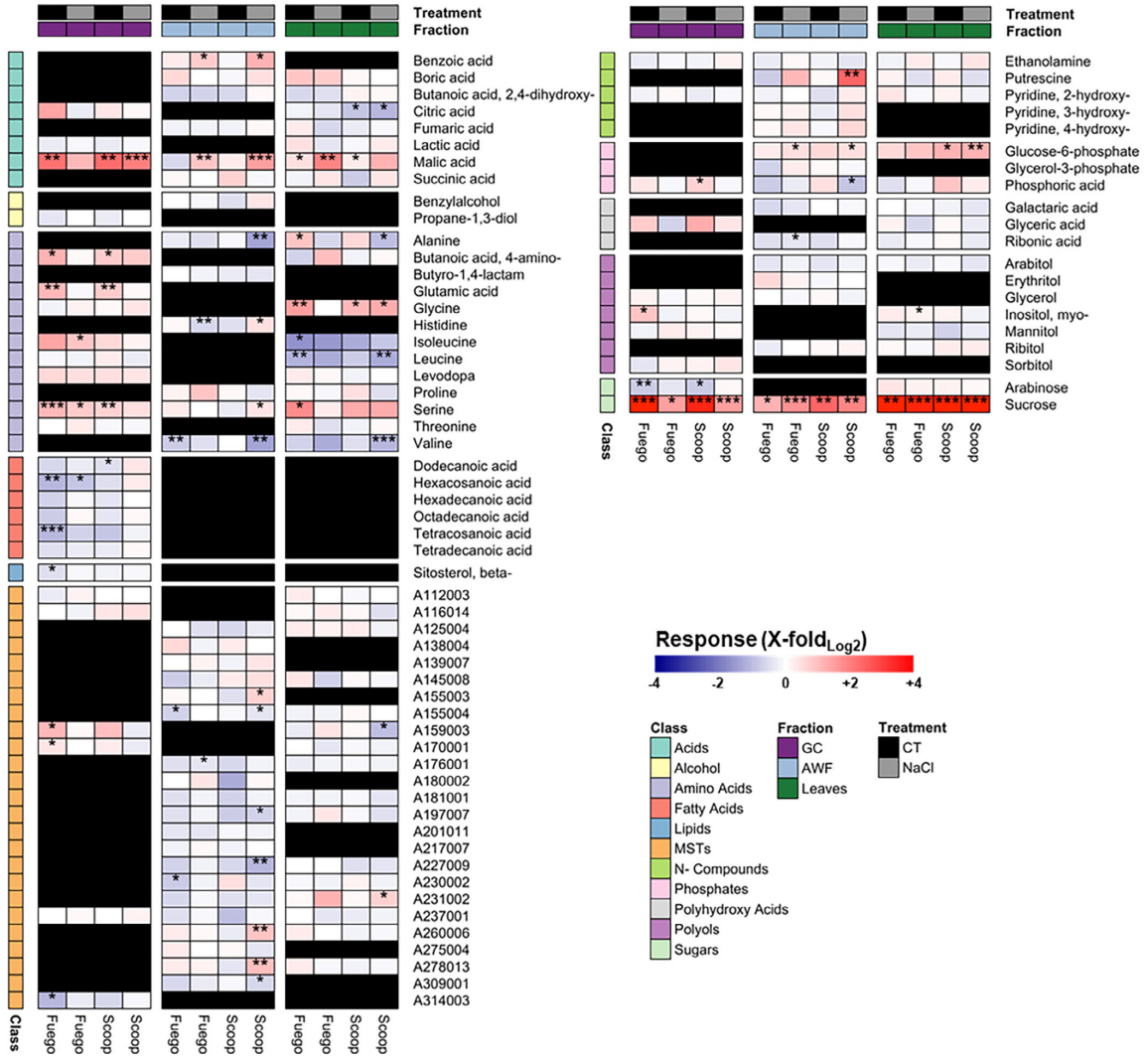

FIGURE 6 Metabolic response to light in guard cell preparations, apoplastic washing fluids and leaves of *Vicia faba*. Metabolic response to light in guard cell (GC) preparations, apoplastic washing fluids (AWF) and leaves of the *V. faba* varieties, Fuego and Scoop, under control and 100 mM NaCl conditions. Means of the fold-change$_{log2}$of relative metabolite contents are indicated by a colour code. Asterisks indicate the level of significance (*$p \leq .05$; **$p \leq .01$; ***$p \leq .001$; GC: $n = 9–10$; AWF: $n = 10$; leaves: $n = 5$; MST, mass spectral tag; the shown metabolites are restricted to detections in GCs and AWFs; full data set provided in Table S1) [Colour figure can be viewed at wileyonlinelibrary.com]

associated glycine and serine in leaves (Figure 6). This pattern was partly seen in GC preparations, as serine increased together with polyhydroxic and glyceric acid in response to light. However, increases in glutamic acid, GABA and serine pools of GC preparations were seen under control rather than under NaCl conditions. Throughout the various leaf fractions, sucrose was the only sugar exhibiting a similar pattern. Arabinose pools remained mostly unchanged within leaf and AWF fractions. In control GC preparations, arabinose pools slightly decreased in response to light. In the respective NaCl fractions, this trend was weaker.

4 | DISCUSSION

4.1 | Similar physiological response to long-term NaCl in both *Vicia faba* varieties

Plant growth and nutrient uptake seems to be disturbed under high salinity such as when K^+ is diminished and Na^+ and Cl^- is increased (Flowers, Munns, & Colmer, 2015; Kotula, Garcia, Zörb, Colmer, & Flowers, 2020; Zörb, Geilfus, & Dietz, 2019). This well-known pattern has also been found here for both *V. faba* varieties (Figures 1a and

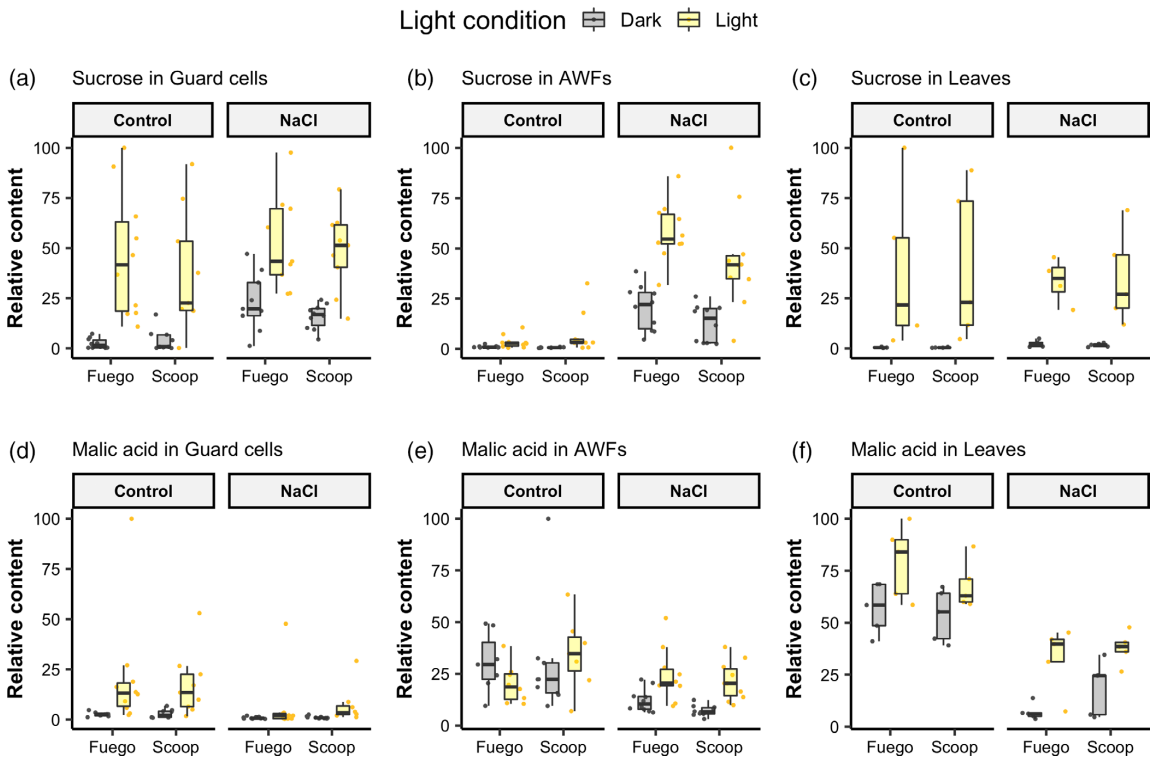

FIGURE 7 Sucrose and malate in various leaf fractions of *Vicia faba* in dark and light under salt and control conditions. Detail of sucrose (a–c) and malic acid (d–f) in guard cell preparations, apoplastic washing fluids (AWFs) and leaves, respectively, of the *V. faba* varieties, Fuego and Scoop, under control and 100 mM NaCl conditions at dark and light condition. Maximum scaled (%) relative metabolite contents presented as box plots featuring the maxima, 75 quartiles, medians, 25 quartiles and minima [Colour figure can be viewed at wileyonlinelibrary.com]

3a). In our experiment, K^+ was little changed in plant leaves of both varieties (Figure 3a) indicating that the NaCl stress was below the level of causing a K^+ deficiency (Zörb et al., 2019). In terms of the ion distribution in leaves of various ages, the younger leaves are clearly protected by the high salt ion load, which agrees with previous studies (Franzisky et al., 2019; Richter et al., 2019). The physiological stress response of the extent of gas exchange was similar in both varieties showing a stress-related delay in the stomatal opening (Figure 1c) and the reduction of transpiration more than half (Figure 1b) due to stomatal closure (Figure 2a). Both physiological reactions diminish plant productivity and water use efficiency in terms of unproductive water loss or the limitation of CO_2 diffusion into leaves (Lawson & Vialet-Chabrand, 2019). The assimilation of CO_2 decreased continuously over the stress period (Figure 1b) suggesting a salt stress-induced metabolic perturbation of photosynthesis beyond the limitation of CO_2 diffusion because the gas exchange in terms of transpiration was similarly reduced throughout the NaCl stress period. This illustrates that photosynthesis was negatively affected under long-term NaCl, but not at a severe level. Thus, the plants could produce sufficient assimilates and react with appropriate metabolic regulation to mitigate direct stress effects.

4.2 | Stomatal regulation resists increasing leaf Na^+ and Cl^- concentrations

The enrichment of acropetally transported Na^+ and Cl^- in leaves and apoplast was found in both *V. faba* varieties (Figure 3a, b) and is known to interfere with enzyme functioning and other metabolism at higher concentrations (Flowers et al., 2015; Geilfus, 2018; Munns et al., 2016). Increasing salt ion concentrations within the apoplast resulting inter alia from weak ion exclusion capabilities (Munns, Passioura, Colmer, & Byrt, 2020), in particular that of Na^+, have previously been reported for salt-sensitive dicots such as *V. faba* (Shahzad, Zörb, Geilfus, & Mühling, 2013; Speer & Kaiser, 1991). Because inorganic ions are imported from the apoplastic reservoirs during stomatal opening (Felle, Hanstein, Steinmeyer, & Hedrich, 2000; Roelfsema & Hedrich, 2002), apoplastic salt ion accumulation might interfere with GC ion transport (Hedrich & Shabala, 2018). In addition to the apparent reductions in K^+ concentrations in GC preparations compared with controls, reductions that are primarily a consequence of the NaCl-induced suppression of stomatal opening (Kollist et al., 2014; Munemasa et al., 2015; Roelfsema, Hedrich, & Geiger, 2012; Zhu, 2002), Na^+ concentrations were increased in GC preparations

(Figure 3c). Unlike the values obtained from surrounding mesophyll and apoplast (Figure 3a,b), Cl^- did not increase on NaCl treatment in the GC preparations of the two varieties (Figure 3c). The differential accumulation pattern of Na^+ and Cl^- implies that GCs rely on their Cl^- transport mechanisms (Jezek & Blatt, 2017) to avoid the accumulation of Cl^-, whereas the intake of Na^+ seems to be less well controlled. Although the stomatal pores of both varieties were closed 4 hrs after the end of the photoperiod same as the controls (Figure 2a), the stomatal response to darkness and low air humidity was markedly delayed in the variety Fuego (Figure 2b) suggesting a dysfunctional stomatal closing response as a result of Na^+ intake into GCs (Robinson, Véry, Sanders, & Mansfield, 1997; Thiel & Blatt, 1991) observed in Fuego but not in Scoop. Such a delayed closing response increases the probability of unproductive water loss (Lawson & Vialet-Chabrand, 2019; McAusland et al., 2016) and continued acropetal transport of deleterious salt ions to the shoot (Hedrich & Shabala, 2018). However, the general reduction of the stomatal pore widths (Figures 1b and Figure 2a), and thus, less intake of inorganic ions into GCs, might be advantageous to prevent accumulation of deleterious salt ions when apoplastic Na^+ and Cl^- concentrations increase because of continuous exposure to salinity.

4.3 | Diverging signatures of leaf and guard cell metabolic acclimatisation to NaCl

Long-term exposure to NaCl results in the accumulation of salt ions in plant tissues (Figure 3), challenging ion homeostasis (Munns et al., 2016), nutrient availability (Zörb et al., 2019) and primary metabolism (Sanchez et al., 2008). The last-mentioned is markedly affected in *V. faba* (Richter et al., 2019) and other legumes such as Lotus (Sanchez et al., 2008; Sanchez et al., 2011). Accordingly, the leaf metabolic profiles reflected changes in response to the long-term exposure to NaCl and the light condition, that is, when the stomata were open or closed (Figure 4). Changes of the levels of compatible solutes such as proline and stress-responsive metabolites such as sugars, free amino acids and the reduction of TCA cycle intermediates (Figures 4 and 5a) were in agreement with known patterns of metabolic responses to osmotic and high NaCl stress (Fàbregas & Fernie, 2019; Richter et al., 2019; Sanchez et al., 2008).

As far as GC metabolism is concerned, we have shown that the amount of changed metabolites under salt conditions is lower than in whole leaves indicating that GCs, in general, are not as sensitive to saline conditions as leaves (Figure 5). This is in accordance to the findings above and therefore suggests that the stomata of *V. faba* can still function, that is, control their aperture and the transpiration rate, albeit at a slower rate (Figures 1b,c and 2), to reduce water loss and the amount of salt delivered to the shoot (Hedrich & Shabala, 2018; Robinson et al., 1997), even when the mesophyll is affected by high salinity. Conserved leaf metabolic responses to high NaCl exposure, for example, increases of stress-responsive metabolites such as *myo*-inositol and free amino acids (Sanchez et al., 2008; Sanchez et al., 2011), were not present in GC preparations (Figure 5a). In *V. faba*, the metabolic response of the mesophyll, with respect to TCA cycle intermediates such as fumaric and malic acid, and the stress-responsive amino acid proline, is more affected by salinity with Cl^- (KCl, NaCl) than by exposition to Na^+ without Cl^- ($NaSO_4$) (Richter et al., 2019). Therefore, the absence of a conserved NaCl-stress signature in guard cell metabolism might be associated with the prevention of Cl^- accumulation (Figure 3c). In terms of increased photorespiratory pathway and reduced TCA cycle activity, GC and leaf metabolism were similarly affected, as associated metabolites were changed in response to NaCl exposure (Figures 4 and 5a) reflecting known signatures of leaf metabolic response to stress in many salt-sensitive glycophytes (Richter et al., 2019; Sanchez et al., 2008; Sanchez et al., 2011). In GC metabolism, however, the TCA cycle plays a pivotal role for osmolyte synthesis and energy production, which is required for energizing the proton pumps that drive the import of inorganic ions into GCs (Daloso et al., 2017; Robaina-Estévez, Daloso, Zhang, Fernie, & Nikoloski, 2017; Santelia & Lawson, 2016). In addition to Cl^-, organic anions such as malic acid counterbalance the positive charge resulting from K^+ that is accumulated during stomatal opening (Chen et al., 2012; Fernie & Martinoia, 2009; Hills, Chen, Amtmann, Blatt, & Lew, 2012; Horrer et al., 2016; Santelia & Lawson, 2016). In association with the decreased malic acid and increased GABA pools of the GC preparations (Mekonnen, Flügge, & Ludewig, 2016), the stomatal apertures of both the *V. faba* varieties were reduced in the light (Figure 2a) illustrating the tight correlation of GC metabolism and stomatal aperture (Daloso et al., 2017; Santelia & Lawson, 2016). In view of the impact of the stress hormone abscisic acid on GC sugar transport and the TCA cycle activity suggested by previous studies (Asai, Nakajima, Kondo, & Kamada, 1999; Jin et al., 2013; Yoshida et al., 2019; Zhu & Assmann, 2017) the observed changes of GC sucrose and malic acid pools might be part of the metabolic response to abscisic acid. Thus, GC metabolism under long-term NaCl seems to be primarily affected by stress-related abscisic acid signalling (Lee & Luan, 2012; Umezawa et al., 2010; Weiler, Schnabl, & Hornberg, 1982) rather than by direct NaCl stress effects as observed in the Na^+ and Cl^- accumulating mesophyll-dominated whole leaf fractions (Figures 3a and 5a). Hence, the differential metabolic response of GC metabolism to long-term salinity indicates that the ability for transient turgor adjustments of GCs remains preserved under conditions of increasing salt ion loads in the leaves and the apoplast.

4.4 | Sucrose replete pattern in guard cells indicates metabolic feedforward function during long-term salinity

We observed increased sucrose pools in AWFs and GC preparations both at darkness and in the light under conditions of NaCl stress (Figure 7a–c), when stomata remained mostly closed (Figures 1b,c and 2a). Sucrose pools of controls were lower at darkness and then increased over the photoperiod in all fractions (Figure 7a–c). In *V. faba*, sucrose represents the primary photosynthate and transport form for sugars, which are translocated to the phloem with an

apoplastic step. This leads to the transpiration-stream-driven enrichment of sucrose in the apoplast during the photoperiod (Ewert, Outlaw Jr, Zhang, Aghoram, & Riddle, 2000; Outlaw & De Vlieghere-He, 2001). Concomitant with sucrose accumulation in the apoplast during the late diel period, the stomatal aperture declines, although environmental conditions remain unchanged. In addition to a potential osmotic effect of apoplastic sucrose, Kelly et al. (2013) proposed a metabolic feedforward functioning of sucrose coordinating stomatal conductivity and photosynthesis by the stimulation of stomatal closure via a sugar-sensing hexokinase, which in turn stimulates the abscisic acid-signalling pathway in GCs resulting in stomatal closing. Such metabolic regulation has been hypothesized to be relevant under conditions of limited sink capacity and therefore saturated phloem loading in the late diel period (Lawson, Simkin, Kelly, & Granot, 2014; Lima et al., 2018) but might also apply to the physiological condition of *V. faba* under long-term NaCl exposure favouring leaf sugar accumulation of, for example, sucrose (Kempa, Krasensky, Dal Santo, Kopka, & Jonak, 2008; Krasensky & Jonak, 2012; Sanchez et al., 2008). We therefore hypothesize that the sucrose feedforward mechanism acts not only as a positive regulator of GC abscisic-signalling in the late diel period leading to stomatal closure (Kelly et al., 2013; Lugassi et al., 2015), but also under conditions of long-term NaCl, when sucrose accumulates in the apoplast and GCs as a consequence of stress-related carbon partitioning.

In conclusion, this study shows that NaCl exposure increased Na^+ in GCs and triggered responses that indicated a reduced TCA cycle and increased photorespiration activity, both of which are attributable to stress-related hormone signalling. Metabolic stress markers and compatible solutes accumulated in leaf tissue but not in GC preparations. Diverging metabolic regulation of GCs might be a prerequisite for maintaining GC functionality under long-term NaCl, that is, facilitation of a constant adjustment of GC turgor that affects stomatal aperture and water loss. In contrast to controls, the sucrose levels of the apoplast and GC preparations from NaCl-treated plants were high irrespective of the photoperiod indicating that a metabolic sucrose-mediated feedforward mechanism is involved in coordinating stomatal closure under conditions of long-term NaCl.

ACKNOWLEDGMENTS

We thank Gyöngyi Bárdos and Christiane Beierle for their assistance during the GC preparation, Dr. Monika Wimmer and Dr. Nikolaus Merkt for discussions and remarks, and Dr. Sabine Stürz for supporting the gas exchange measurements. We are grateful to the Deutsche Forschungsgemeinschaft (ZO/08; grant number 320167376) for funding this project. Open Access funding enabled and organized by ProjektDEAL.

CONFLICT OF INTEREST

The authors declare no conflict of interest.

ORCID

Bastian Leander Franzisky https://orcid.org/0000-0003-2590-2118
Christoph-Martin Geilfus https://orcid.org/0000-0002-9820-8111
Maria Luisa Romo-Pérez https://orcid.org/0000-0001-7554-0501
Christian Zörb https://orcid.org/0000-0003-0000-5138

REFERENCES

Antunes, W. C., de Menezes Daloso, D., Pinheiro, D. P., Williams, T. C. R., & Loureiro, M. E. (2017). Guard cell-specific down-regulation of the sucrose transporter SUT1 leads to improved water use efficiency and reveals the interplay between carbohydrate metabolism and K^+ accumulation in the regulation of stomatal opening. *Environmental and Experimental Botany*, *135*, 73–85.

Araújo, W. L., Nunes-Nesi, A., Osorio, S., Usadel, B., Fuentes, D., Nagy, R., … Tohge, T. (2011). Antisense inhibition of the iron-Sulphur subunit of succinate dehydrogenase enhances photosynthesis and growth in tomato via an organic acid–mediated effect on stomatal aperture. *The Plant Cell*, *23*(2), 600–627.

Asai, N., Nakajima, N., Kondo, N., & Kamada, H. (1999). The effect of osmotic stress on the solutes in guard cells of *Vicia faba* L. *Plant and Cell Physiology*, *40*(8), 843–849.

Bates, D., Maechler, M., Bolker, B., & Walker, S. (2015). Fitting linear mixed-effects models using {lme4}. *Journal of Statistical Software*, *67*, 1–48.

Bauer, H., Ache, P., Lautner, S., Fromm, J., Hartung, W., Al-Rasheid, K. A. S., … Lachmann, N. (2013). The stomatal response to reduced relative humidity requires guard cell-autonomous ABA synthesis. *Current Biology*, *23*(1), 53–57.

Chen, H., & Boutros, P. C. (2011). VennDiagram: A package for the generation of highly-customizable Venn and Euler diagrams in R. *BMC Bioinformatics*, *12*(1), 35.

Chen, Z.-H., Hills, A., Bätz, U., Amtmann, A., Lew, V. L., & Blatt, M. R. (2012). Systems dynamic modeling of the stomatal guard cell predicts emergent behaviors in transport, signaling, and volume control. *Plant Physiology*, *159*(3), 1235–1251.

Cornish, K., & Zeevaart, J. A. (1986). Abscisic acid accumulation by in situ and isolated guard cells of *Pisum sativum* L. and *Vicia faba* L. in relation to water stress. *Plant Physiology*, *81*(4), 1017–1021.

Daloso, D. M., Anjos, L., & Fernie, A. R. (2016). Roles of sucrose in guard cell regulation. *New Phytologist*, *211*(3), 809–818.

Daloso, D. M., Antunes, W. C., Pinheiro, D. P., Waquim, J. P., Araújo, W. L., Loureiro, M. E., … Williams, T. C. R. (2015). Tobacco guard cells fix CO_2 by both rubisco and PEPcase while sucrose acts as a substrate during light-induced stomatal opening. *Plant, Cell & Environment*, *38*(11), 2353–2371.

Daloso, D. M., Medeiros, D. B., Dos Anjos, L., Yoshida, T., Araújo, W. L., & Fernie, A. R. (2017). Metabolism within the specialized guard cells of plants. *New Phytologist*, *216*(4), 1018–1033.

Dethloff, F., Erban, A., Orf, I., Alpers, J., Fehrle, I., Beine-Golovchuk, O., … Kopka, J. (2014). Profiling methods to identify cold-regulated primary metabolites using gas chromatography coupled to mass spectrometry. *Plant Cold Acclimation*, Methods in Molecular Biology (Methods and Protocols), *1166*, 171–197. New York, NY: Humana Press.

Erban, A., Martinez-Seidel, F., Rajarathinam, Y., Dethloff, F., Orf, I., Fehrle, I., … Kopka, J. (2020). Multiplexed profiling and data processing methods to identify temperature-regulated primary metabolites using gas chromatography coupled to mass spectrometry. In *Plant cold acclimation*, *2156*, 203–239. New York, NY: Humana Press.

Ewert, M. S., Outlaw, W. H., Jr., Zhang, S., Aghoram, K., & Riddle, K. A. (2000). Accumulation of an apoplastic solute in the guard-cell wall is sufficient to exert a significant effect on transpiration in *Vicia faba* leaflets. *Plant, Cell & Environment*, *23*(2), 195–203.

Fàbregas, N., & Fernie, A. R. (2019). The metabolic response to drought. *Journal of Experimental Botany*, *70*(4), 1077–1085.

Felle, H. H., Hanstein, S., Steinmeyer, R., & Hedrich, R. (2000). Dynamics of ionic activities in the apoplast of the sub-stomatal cavity of intact *Vicia faba* leaves during stomatal closure evoked by ABA and darkness. *The Plant Journal*, *24*(3), 297–304.

Fernie, A. R., & Martinoia, E. (2009). Malate. Jack of all trades or master of a few? *Phytochemistry*, *70*(7), 828–832.

Floerl, S., Druebert, C., Majcherczyk, A., Karlovsky, P., Kües, U., & Polle, A. (2008). Defence reactions in the apoplastic proteome of oilseed rape (*Brassica napus var. napus*) attenuate *Verticillium longisporum* growth but not disease symptoms. *BMC Plant Biology*, *8*(1), 129.

Flowers, T. J., Munns, R., & Colmer, T. D. (2015). Sodium chloride toxicity and the cellular basis of salt tolerance in halophytes. *Annals of Botany*, *115*(3), 419–431.

Flütsch, S., Wang, Y., Takemiya, A., Vialet-Chabrand, S. R., Klejchova, M., Nigro, A., … Santelia, D. (2020). Guard cell starch degradation yields glucose for rapid stomatal opening in Arabidopsis. *The Plant Cell*, *32*(7), 2325–2344.

Franzisky, B. L., Geilfus, C.-M., Kränzlein, M., Zhang, X., & Zörb, C. (2019). Shoot chloride translocation as a determinant for NaCl tolerance in *Vicia faba* L. *Journal of Plant Physiology*, *236*, 23–33.

Geilfus, C.-M. (2018). Chloride: From nutrient to toxicant. *Plant and Cell Physiology*, *59*(5), 877–886.

Geilfus, C.-M., Lan, J., & Carpentier, S. (2018). Dawn regulates guard cell proteins in *Arabidopsis thaliana* that function in ATP production from fatty acid beta-oxidation. *Plant Molecular Biology*, *98*(6), 525–543.

Geilfus, C.-M., Mithofer, A., Ludwig-Muller, J., Zörb, C., & Mühling, K.-H. (2015). Chloride-inducible transient apoplastic alkalinizations induce stomata closure by controlling abscisic acid distribution between leaf apoplast and guard cells in salt-stressed *Vicia faba*. *New Phytologist*, *208*(3), 803–816.

Geilfus, C.-M., Niehaus, K., Godde, V., Hasler, M., Zörb, C., Gorzolka, K., … Muhling, K. H. (2015). Fast responses of metabolites in *Vicia faba* L. to moderate NaCl stress. *Plant Physiology and Biochemistry*, *92*, 19–29.

Granot, D., & Kelly, G. (2019). Evolution of guard-cell theories: The story of sugars. *Trends in Plant Science.*, *24*, 507–518.

Hedrich, R., & Shabala, S. (2018). Stomata in a saline world. *Current Opinion in Plant Biology*, *46*, 87–95.

Herrmann, H. A., Schwartz, J.-M., & Johnson, G. N. (2019). Metabolic acclimation—A key to enhancing photosynthesis in changing environments? *Journal of Experimental Botany*, *70*(12), 3043–3056.

Hills, A., Chen, Z.-H., Amtmann, A., Blatt, M. R., & Lew, V. L. (2012). OnGuard, a computational platform for quantitative kinetic modeling of guard cell physiology. *Plant Physiology*, *159*(3), 1026–1042.

Horrer, D., Flütsch, S., Pazmino, D., Matthews, J. S. A., Thalmann, M., Nigro, A., … Santelia, D. (2016). Blue light induces a distinct starch degradation pathway in guard cells for stomatal opening. *Current Biology*, *26*(3), 362–370.

Hummel, I., Pantin, F., Sulpice, R., Piques, M., Rolland, G., Dauzat, M., … Muller, B. (2010). Arabidopsis plants acclimate to water deficit at low cost through changes of carbon usage: An integrated perspective using growth, metabolite, enzyme, and gene expression analysis. *Plant Physiology*, *154*(1), 357–372.

Jezek, M., & Blatt, M. R. (2017). The membrane transport system of the guard cell and its integration for stomatal dynamics. *Plant Physiology*, *174*(2), 487–519.

Jin, X., Wang, R.-S., Zhu, M., Jeon, B. W., Albert, R., Chen, S., & Assmann, S. M. (2013). Abscisic acid-responsive guard cell metabolomes of Arabidopsis wild-type and gpa1 G-protein mutants. *The Plant Cell*, *25*(12), 4789–4811.

Kelly, G., Moshelion, M., David-Schwartz, R., Halperin, O., Wallach, R., Attia, Z., … Granot, D. (2013). Hexokinase mediates stomatal closure. *The Plant Journal*, *75*(6), 977–988.

Kempa, S., Krasensky, J., Dal Santo, S., Kopka, J., & Jonak, C. (2008). A central role of abscisic acid in stress-regulated carbohydrate metabolism. *PLoS One*, *3*(12), e3935.

Kolde, R. (2019). pheatmap: Pretty Heatmaps. R package version 1.0.12. https://CRAN.R-project.org/package=pheatmap.

Kollist, H., Nuhkat, M., & Roelfsema, M. R. G. (2014). Closing gaps: Linking elements that control stomatal movement. *New Phytologist*, *203*(1), 44–62.

Kopka, J., Provart, N. J., & Müller-Röber, B. (1997). Potato guard cells respond to drying soil by a complex change in the expression of genes related to carbon metabolism and turgor regulation. *The Plant Journal*, *11*(4), 871–882.

Kopka, J., Schauer, N., Krueger, S., Birkemeyer, C., Usadel, B., Bergmüller, E., … Steinhauser, D. (2005). GMD@CSB.DB: The Golm metabolome database. *Bioinformatics*, *21*(8), 1635–1638.

Kotula, L., Garcia, P., Zörb, C., Colmer, T. D., & Flowers, T. J. (2020). Improving crop salt tolerance using transgenic approaches: An update and physiological analysis. *Plant, Cell & Environment*, *43*, 2932–2956.

Krasensky, J., & Jonak, C. (2012). Drought, salt, and temperature stress-induced metabolic rearrangements and regulatory networks. *Journal of Experimental Botany*, *63*(4), 1593–1608.

Lawson, T., & Blatt, M. R. (2014). Stomatal size, speed, and responsiveness impact on photosynthesis and water use efficiency. *Plant Physiology*, *164*(4), 1556–1570.

Lawson, T., & Matthews, J. (2020). Guard cell metabolism and stomatal function. *Annual Review of Plant Biology*, *71*(1), 273–302.

Lawson, T., Simkin, A. J., Kelly, G., & Granot, D. (2014). Mesophyll photosynthesis and guard cell metabolism impacts on stomatal behaviour. *New Phytologist*, *203*(4), 1064–1081.

Lawson, T., & Vialet-Chabrand, S. (2019). Speedy stomata, photosynthesis and plant water use efficiency. *New Phytologist*, *221*(1), 93–98.

Lee, S. C., & Luan, S. (2012). ABA signal transduction at the crossroad of biotic and abiotic stress responses. *Plant, Cell & Environment*, *35*(1), 53–60.

Lima, V. F., Medeiros, D. B., Dos Anjos, L., Gago, J., Fernie, A. R., & Daloso, D. M. (2018). Toward multifaceted roles of sucrose in the regulation of stomatal movement. *Plant Signaling & Behavior*, *13*(8), e1494468.

Lohaus, G., Pennewiss, K., Sattelmacher, B., Hussmann, M., & Mühling, K.-H. (2001). Is the infiltration-centrifugation technique appropriate for the isolation of apoplastic fluid? A critical evaluation with different plant species. *Physiologia Plantarum*, *111*(4), 457–465.

Luedemann, A., Strassburg, K., Erban, A., & Kopka, J. (2008). TagFinder for the quantitative analysis of gas chromatography—Mass spectrometry (GC-MS)-based metabolite profiling experiments. *Bioinformatics*, *24*(5), 732–737.

Lugassi, N., Kelly, G., Fidel, L., Yaniv, Y., Attia, Z., Levi, A., … Carmi, N. (2015). Expression of Arabidopsis hexokinase in citrus guard cells controls stomatal aperture and reduces transpiration. *Frontiers in Plant Science*, *6*, 1114–1114.

McAusland, L., Vialet-Chabrand, S., Davey, P., Baker, N. R., Brendel, O., & Lawson, T. (2016). Effects of kinetics of light-induced stomatal responses on photosynthesis and water-use efficiency. *New Phytologist*, *211*(4), 1209–1220.

McLachlan, D. H., Lan, J., Geilfus, C.-M., Dodd, A. N., Larson, T., Baker, A., … Graham, I. (2016). The breakdown of stored triacylglycerols is required during light-induced stomatal opening. *Current Biology*, *26*(5), 707–712.

Medeiros, D. B., Perez Souza, L., Antunes, W. C., Araújo, W. L., Daloso, D. M., & Fernie, A. R. (2018). Sucrose breakdown within guard cells provides substrates for glycolysis and glutamine biosynthesis during light-induced stomatal opening. *The Plant Journal*, *94*(4), 583–594.

Mekonnen, D. W., Flügge, U.-I., & Ludewig, F. (2016). Gamma-aminobutyric acid depletion affects stomata closure and drought tolerance of *Arabidopsis thaliana*. *Plant Science*, *245*, 25–34.

Mott, K. A., Sibbernsen, E. D., & Shope, J. C. (2008). The role of the mesophyll in stomatal responses to light and CO2. *Plant, Cell & Environment*, *31*(9), 1299–1306.

Munemasa, S., Hauser, F., Park, J., Waadt, R., Brandt, B., & Schroeder, J. I. (2015). Mechanisms of abscisic acid-mediated control of stomatal aperture. *Current Opinion in Plant Biology*, *28*, 154–162.

Munns, R., James, R. A., Gilliham, M., Flowers, T. J., & Colmer, T. D. (2016). Tissue tolerance: An essential but elusive trait for salt-tolerant crops. *Functional Plant Biology*, *43*(12), 1103–1113.

Munns, R., Passioura, J. B., Colmer, T. D., & Byrt, C. S. (2020). Osmotic adjustment and energy limitations to plant growth in saline soil. *New Phytologist*, *225*(3), 1091–1096.

Munns, R., Wallace, P. A., Teakle, N. L., & Colmer, T. D. (2010). Measuring soluble ion concentrations (Na^+, K^+, Cl^-) in salt-treated plants. *Plant stress tolerance*, Methods in Molecular Biology (Methods and Protocols), *639*, 371–382. New York, NY: Humana Press.

Obata, T., & Fernie, A. R. (2012). The use of metabolomics to dissect plant responses to abiotic stresses. *Cellular and Molecular Life Sciences*, *69* (19), 3225–3243.

Outlaw, W. H., & De Vlieghere-He, X. (2001). Transpiration rate. An important factor controlling the sucrose content of the guard cell Apoplast of broad bean. *Plant Physiology*, *126*(4), 1716–1724.

R Core Team (2020). *R: A language and environment for statistical computing. R Foundation for Statistical Computing, Vienna, Austria*. Retrieved from https://www.r-project.org/ https://www.R-project.org/.

Raschke, K. (1979). Movements of stomata. *Encyclopedia of Plant Physiology*, *7*, 383–441.

Richter, J. A., Behr, J. H., Erban, A., Kopka, J., & Zörb, C. (2019). Ion-dependent metabolic responses of *Vicia faba* L. to salt stress. *Plant, Cell & Environment*, *42*(1), 295–309.

Robaina-Estévez, S., Daloso, D. M., Zhang, Y., Fernie, A. R., & Nikoloski, Z. (2017). Resolving the central metabolism of Arabidopsis guard cells. *Scientific Reports*, *7*(1), 1–13.

Robinson, M. F., Véry, A.-A., Sanders, D., & Mansfield, T. A. (1997). How can stomata contribute to salt tolerance? *Annals of Botany*, *80*(4), 387–393.

Roelfsema, M. R. G., & Hedrich, R. (2002). Studying guard cells in the intact plant: Modulation of stomatal movement by apoplastic factors. *New Phytologist*, *153*(3), 425–431.

Roelfsema, M. R. G., Hedrich, R., & Geiger, D. (2012). Anion channels: Master switches of stress responses. *Trends in Plant Science*, *17*(4), 221–229.

Sanchez, D. H., Pieckenstain, F. L., Escaray, F., Erban, A., Kraemer, U., Udvardi, M. K., & Kopka, J. (2011). Comparative ionomics and metabolomics in extremophile and glycophytic lotus species under salt stress challenge the metabolic pre-adaptation hypothesis. *Plant, Cell & Environment*, *34*(4), 605–617.

Sanchez, D. H., Siahpoosh, M. R., Roessner, U., Udvardi, M. K., & Kopka, J. (2008). Plant metabolomics reveals conserved and divergent metabolic responses to salinity. *Physiologia Plantarum*, *132*(2), 209–219.

Santelia, D., & Lawson, T. (2016). Rethinking guard cell metabolism. *Plant Physiology*, *172*(3), 1371–1392.

Santelia, D., & Lunn, J. E. (2017). Transitory starch metabolism in guard cells: Unique features for a unique function. *Plant Physiology*, *174*(2), 539–549.

Schwachtje, J., Whitcomb, S. J., Firmino, A. A. P., Zuther, E., Hincha, D. K., & Kopka, J. (2019). Induced, imprinted, and primed responses to changing environments: Does metabolism store and process information? *Frontiers in Plant Science*, *10*, 106.

Shahzad, M., Zörb, C., Geilfus, C.-M., & Mühling, K.-H. (2013). Apoplastic Na^+ in *Vicia faba* leaves rises after short-term salt stress and is remedied by silicon. *Journal of Agronomy and Crop Science*, *199*(3), 161–170.

Speer, M., & Kaiser, W. M. (1991). Ion relations of symplastic and apoplastic space in leaves from *Spinacia oleracea* L. and *Pisum sativum* L. under salinity. *Plant Physiology*, *97*(3), 990–997.

Stevens, R., & Martin, E. (1977). Ion-adsorbent substomatal structures in *Tradescantia pallidus*. *Nature*, *268*(5618), 364–365.

Stitt, M., Lunn, J., & Usadel, B. (2010). Arabidopsis and primary photosynthetic metabolism–More than the icing on the cake. *The Plant Journal*, *61*(6), 1067–1091.

Stitt, M., & Zeeman, S. C. (2012). Starch turnover: Pathways, regulation and role in growth. *Current Opinion in Plant Biology*, *15*(3), 282–292.

Szecowka, M., Heise, R., Tohge, T., Nunes-Nesi, A., Vosloh, D., Huege, J., … Arrivault, S. (2013). Metabolic fluxes in an illuminated *Arabidopsis* rosette. *The Plant Cell*, *25*(2), 694–714.

Tcherkez, G., Boex-Fontvieille, E., Mahé, A., & Hodges, M. (2012). Respiratory carbon fluxes in leaves. *Current Opinion in Plant Biology*, *15*(3), 308–314.

Thiel, G., & Blatt, M. R. (1991). The mechanism of ion permeation through K^+ channels of stomatal guard cells: Voltage-dependent block by Na^+. *Journal of Plant Physiology*, *138*(3), 326–334.

Thompson, D. S. (2005). How do cell walls regulate plant growth? *Journal of Experimental Botany*, *56*(419), 2275–2285.

Umezawa, T., Nakashima, K., Miyakawa, T., Kuromori, T., Tanokura, M., Shinozaki, K., & Yamaguchi-Shinozaki, K. (2010). Molecular basis of the core regulatory network in ABA responses: Sensing, signaling and transport. *Plant and Cell Physiology*, *51*(11), 1821–1839.

Weiler, E. W., Schnabl, H., & Hornberg, C. (1982). Stress-related levels of abscisic acid in guard cell protoplasts of *Vicia faba* L. *Planta*, *154*(1), 24–28.

Wickham, H. (2016). *ggplot2: Elegant Graphics for Data Analysis*. Springer-Verlag, New York. https://ggplot2.tidyverse.org

Yoshida, T., Anjos, L. d., Medeiros, D. B., Araújo, W. L., Fernie, A. R., & Daloso, D. M. (2019). Insights into ABA-mediated regulation of guard cell primary metabolism revealed by systems biology approaches. *Progress in Biophysics and Molecular Biology*, *146*, 37–49.

Zhu, J.-K. (2002). Salt and drought stress signal transduction in plants. *Annual Review of Plant Biology*, *53*(1), 247–273.

Zhu, M., & Assmann, S. M. (2017). Metabolic signatures in response to abscisic acid (ABA) treatment in *Brassica napus* guard cells revealed by metabolomics. *Scientific Reports*, *7*(1), 12875.

Zörb, C., Geilfus, C.-M., & Dietz, K.-J. (2019). Salinity and crop yield. *Plant Biology*, *21*, 31–38.

SUPPORTING INFORMATION

Additional supporting information may be found online in the Supporting Information section at the end of this article.

How to cite this article: Franzisky BL, Geilfus C-M, Romo-Pérez ML, et al. Acclimatisation of guard cell metabolism to long-term salinity. *Plant Cell Environ*. 2020;1–15. https://doi.org/10.1111/pce.13964

Supplementary material

Supplementary material 3.1: Relative malate dehydrogenase (MDH) activity of apoplastic washing fluids (AWF) extracted from leaves of the *V. faba* varieties, Fuego and Scoop, under control and 100 mM NaCl conditions. MDH was used to check the purity of AWF, which might be contaminated by symplastic solutes because of stress-related increases of membrane leakage. The activity is expressed as relative to that of whole leaves. Means ± SE; different letters indicate significant differences of comparisons between varieties and treatments; ($p \leq .05$; $n = 5$).

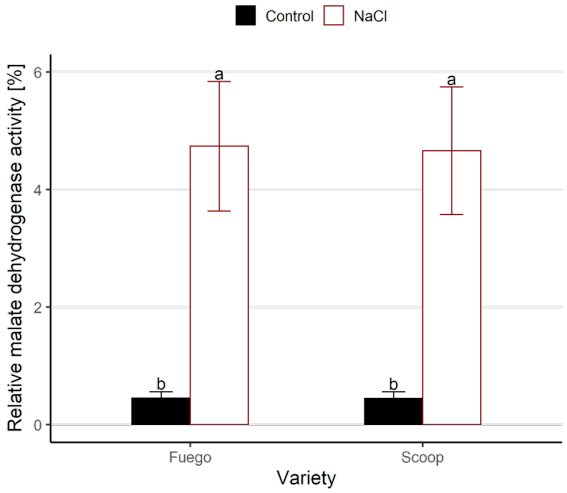

Supplementary material 3.2: Illustration of the conditions of the harvest in terms of light and time. After 20 days of NaCl treatment, plant materials were harvested. Material of the light condition was collected starting from after 2.5 hr lights on, whereas material of the dark condition was collected in an unlit laboratory (~1 µmol photons m^2/s) from plants that had been kept in the darkness until harvest.

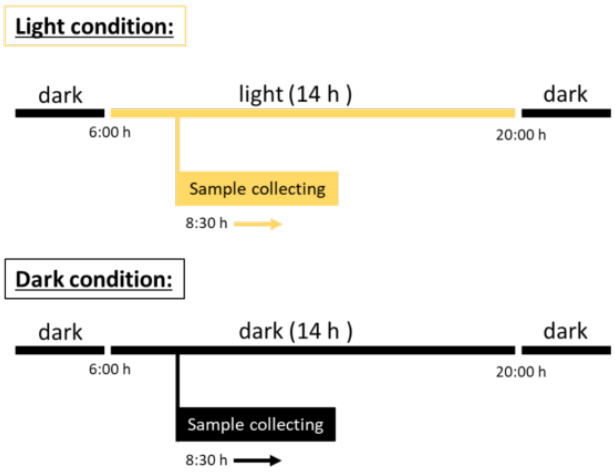

Supplementary material 3.3: Metabolome and stomatal kinetic data set. Relative contents of primary metabolites in whole leave material, apoplastic washing fluids (AWF) and guard cell (GC) preparations of the *V. faba* varieties, Fuego and Scoop, under control and 100 mM NaCl, and dark and light conditions. Stomatal kinetics of transitions from dark-to-light and from light-to-dark under control and 100 mM NaCl conditions.

Data set available online (13 January 2021):
https://onlinelibrary.wiley.com/action/downloadSupplement?doi=10.1111%2Fpce.13964&file=pce13964-sup-0003-TableS1.xlsx

Chapter 5

General discussion

5. General discussion

A better understanding of the physiological traits that contribute to salt tolerance of crops is of great importance to meet the future demands of human nutrition. Therefore, in this work, the contribution of the tolerance mechanisms 'ion exclusion' and 'tissue tolerance' to plant performance has been evaluated in diverse varieties of the two crop species *V. faba* and *Z. mays*. As an aspect of 'tissue tolerance', the impact of the accumulation of excess salt ions in leaves and the apoplast on stomatal physiology was characterized in *V. faba* exposed to long-term salinity in order to improve our knowledge of guard cell physiology and the stomatal control of transpiration and leaf CO_2 assimilation under saline conditions.

5.1 Tolerant *Vicia faba* varieties sequester Na^+ and exclude Cl^- from shoots

To assess the toxic effects of high Na^+ and Cl^- in salt-sensitive *V. faba*, 13 diverse varieties were grown hydroponically and stressed with 100 mM NaCl until necrotic leaf spots appeared (Chapter 2, Fig. 2). Sensitive and tolerant varieties differed by approximately a factor of two in the stress period until salt-induced lesions appeared (Chapter 2, Fig. 2 A), indicating a broad plasticity of tolerance to NaCl salinity in *V. faba*. To prevent such salt-induced lesions, the plant either has to exclude excess ions into the soil or cope with the physiological inconveniences resulting from increasing tissue concentrations of Na^+ and Cl^-, a characteristic referred to as 'tissue tolerance' (Munns et al., 2016). Because high cytosolic Na^+ concentrations disturb K^+ homeostasis and, thus, enzyme functioning and stomatal regulation (Deinlein et al., 2014; Flowers et al., 2015), Na^+ is often considered as the primary toxic ion under salinity. Therefore, the maintenance of low tissue Na^+ concentrations is an important trait of salt tolerance in many crop species (Roy et al., 2014; Zörb et al., 2019). However, leaf Na^+ concentrations increase with the length of NaCl exposure leading to the highest Na^+/K^+ ratios in those varieties developing salt-induced lesions the latest (Chapter 2, Fig. 8 E, F). This finding indicates that

that tolerant varieties are effectively able to sequester Na^+ in order to maintain K^+ homeostasis (Munns et al., 2016) and moreover, that the ability of Na^+ retention from shoots is not decisive for NaCl tolerance in *V. faba*.

In agreement with a few reports of legumes being primarily sensitive to Cl^- (Li et al., 2017; Teakle & Tyerman, 2010), adverse effects on photosynthesis and plant growth in *V. faba* were initially attributed to high Cl^- rather than high Na^+ (Slabu et al., 2009; Tavakkoli et al., 2010). Irrespective of the variable NaCl stress dose, leaf Cl^- concentrations were similar throughout the varieties at the time point when necrotic spots appeared (Chapter 2, Fig. 6, 7), suggesting that varieties with higher tolerance profit from lower Cl^- translocation to the shoots (Chapter 2, Fig. 8 C, D) and, further, that the Cl^- concentration in developing leaves is a critical factor for ion toxicity in *V. faba* growing under NaCl salinity (Geilfus, 2018; Tavakkoli et al., 2010). Toxic effects of high Cl^- are expected to result from unbalanced chloroplastidial Cl^- homeostasis, because the salinity-induced accumulation of Cl^- in the chloroplasts (Slabu et al., 2009) is associated with the inhibition of CO_2-fixing enzymes, disturbed chloroplast dark relaxation, damage of PSII reaction centres and excessive accumulation of reactive oxygen species in chloroplasts (Geilfus, 2018). In this context, the tolerant varieties are able to improve the protection of their chloroplasts from excess Cl^- intake and, thus, prevent excessive reactive oxygen species production (Bose et al., 2017), chlorophyll degradation (Chapter 2, Supplemental table 1) and the related reductions in energy and redox equivalent pools.

5.2 *Zea mays* excludes Cl^- from shoot and restricts leaf Cl^- accumulation to leaf sheaths

To identify physiological dysfunctions of *Z. mays* in response to excess Cl^- in soil, 8 diverse genotypes were grown in soil and stressed with mild and high $CaCl_2$ treatments (63.2 and 757.1 mg Cl^- kg^{-1} soil DM) for 10 d (Chapter 3, section 2.1). None of the genotypes except for P8589 developed Cl^- toxicity symptoms, such as leaf chlorosis or necrosis, indicating that

the high Cl^- application represented a mild stress for *Z. mays*. The $CaCl_2$ treatment-related increases of Cl^- concentrations in aerial plant parts (Chapter 3, Fig. 5 A, B & C) were smaller than those in roots (Chapter 3, Fig. 5 D) suggesting that *Z. mays* is a Cl^--excluder restraining most of the Cl^- from acropetal transport.

The exclusion of excess salt ions is an important attribute of salt tolerance in many crop plants (Munns & Gilliham, 2015; Roy et al., 2014), as has been particular well documented for Na^+ in *Z. mays* (Farooq et al., 2015; Fortmeier & Schubert, 1995; Tester & Davenport, 2003). Accordly, the lowest Cl^- exclusion capability among the genotypes was found for P8589, that had developed chlorotic leaf edges (Chapter 3, Fig. 5 F). Moreover, the Cl^- concentrations of the various leaf fractions illustrated a differential spatial leaf Cl^- accumulation pattern, because Cl^- primarily accumulated in leaf sheaths instead of, for example, in the photosynthetically active leaf blades. This strategy was effective in preventing the harmful effects of high chloride concentrations on chloroplasts (Geilfus, 2018), because the chlorophyll content and photosynthesis remained unaffected by the Cl^- treatments (Chapter 3, Fig. 9).

5.3 Guard cell metabolism is less sensitive to salt stress compared with whole leaf tissue in *Vicia faba*

Stomatal movements are enabled by changes in guard cell turgor facilitated via the transient accumulation of inorganic and organic ions imported from the apoplast or biosynthesized within guard cells. Because inorganic ions are imported from the apoplastic reservoirs during stomatal opening (Felle et al., 2000; Roelfsema & Hedrich, 2002), the salt-stress-related Na^+ and Cl^- accumulation in the apoplast might interfere with guard cell ion transport and physiology (Hedrich & Shabala, 2018; Roelfsema & Hedrich, 2005).

In response to long-term salinity (20 days; 100 mM NaCl), Na^+ and Cl^- concentrations increased in leaves and the apoplast (Chapter 4, Fig. 3 A, B) illustrating the weak ion exclusion

capability of the salt-sensitive *V. faba* (Franzisky et al., 2019; Geilfus et al., 2015; Slabu et al., 2009). In guard cell preparations, however, only Na^+ increased, whereas Cl^- levels remained similar to those of the controls without NaCl treatment (Chapter 4, Fig. 3 C). The differential accumulation pattern implies that guard cells rely on their Cl^- transport mechanisms (Jezek & Blatt, 2017) to avoid excessive Cl^- accumulation under conditions of increased salt ion concentrations in leaf tissue, whereas the intake of Na^+ seems to be less controlled. Although the stomatal pores of both varieties were closed at night (Chapter 4; Fig. 2 A) the closing response to darkness and low air humidity was markedly delayed in the variety Fuego (Chapter 4; Fig. 2 B) suggesting a dysfunctional stomatal closing response as a result of Na^+ intake into GCs (Jarvis & Mansfield, 1980; MacRobbie, 1983; Robinson et al., 1997; Thiel & Blatt, 1991). However, a general reduction of aperture during NaCl stress (Chapter 4, Fig. 1; Fig. 2) and, thus, less detrimental intake of Na^+ into GCs (Thiel & Blatt, 1991) might be a strategy to protect from Na^+ toxicity in guard cells (Hedrich & Shabala, 2018).

In comparison with leaf metabolic acclimatisation to long-term NaCl, guard cell preparations showed a lower amount of increases of stress-responsive metabolites and compatible solutes (Chapter 4, Fig. 5), indicating that guard cells are less sensitive to salinity than mesophyll dominated leaf tissue. The differential regulation of guard cell metabolism is in accordance with the finding that stomata can still function, *i.e*. they can still control the aperture and water loss (Chapter 4, Fig. 1 B, C; Fig. 2 A), even when the mesophyll is affected by increased salt loads under salinity (Chapter 4, Fig. 3; Fig. 4). The regulation of stomatal aperture depends on fast changes in guard cell turgor (Jezek et al., 2017). Thus, the avoidance of a permanent, salt-stress-related accumulation of compatible solutes within guard cells might be a prerequisite to maintain the ability to regulate stomatal aperture during salt stress.

Moreover, we observed the shift from a light-dependent sucrose accumulation in guard cells and apoplast under control conditions towards a light-independent replete pattern under long-term NaCl (Chapter 4, Fig. 7 A). In *V. faba*, mesophyll-derived sucrose functions as a

metabolic feedback in coordinating stomatal aperture with photosynthesis. Increasing sucrose levels in guard cells are sensed by hexokinases, which in turn, stimulate the abscisic-acid-signalling pathway in guard cells resulting in stomatal closing in the late diel period when photosynthesis is saturated (Granot & Kelly, 2019; Kelly et al., 2013). This metabolic sucrose-mediated regulation might also induce stomatal closure during long-term salinity, which favours the accumulation of sugars, *e.g.* sucrose, in leaves (Kempa et al., 2008; Krasensky & Jonak, 2012; Sanchez et al., 2008). Hence, the sucrose-mediated feedforward mechanism might act as positive regulator of guard cell abscisic-acid-signalling in the late diel period (Granot & Kelly, 2019), but also under conditions of long-term salinity, when sucrose accumulates in the apoplast and guard cells (Chapter 4, Fig. 7 A) as a consequence of stress-related alterations in carbon transport and metabolism (Asai et al., 1999; Jin et al., 2013; Yoshida et al., 2019; Zhu & Assmann, 2017).

References

Asai, N., Nakajima, N., Kondo, N., & Kamada, H. (1999). The Effect of Osmotic Stress on the Solutes in Guard Cells of *Vicia faba* L. *Plant and Cell Physiology, 40*(8), 843-849.

Bose, J., Munns, R., Shabala, S., Gilliham, M., Pogson, B., & Tyerman, S. D. (2017). Chloroplast function and ion regulation in plants growing on saline soils: lessons from halophytes. *Journal of Experimental Botany, 68*(12), 3129-3143.

Deinlein, U., Stephan, A. B., Horie, T., Luo, W., Xu, G., & Schroeder, J. I. (2014). Plant salt-tolerance mechanisms. *Trends in Plant Science, 19*(6), 371-379.

Farooq, M., Hussain, M., Wakeel, A., & Siddique, K. H. M. (2015). Salt stress in maize: effects, resistance mechanisms, and management. A review. *Agronomy for Sustainable Development, 35*(2), 461-481.

Felle, H. H., Hanstein, S., Steinmeyer, R., & Hedrich, R. (2000). Dynamics of ionic activities in the apoplast of the sub-stomatal cavity of intact *Vicia faba* leaves during stomatal closure evoked by ABA and darkness. *The Plant Journal, 24*(3), 297-304.

Flowers, T. J., Munns, R., & Colmer, T. D. (2015). Sodium chloride toxicity and the cellular basis of salt tolerance in halophytes. *Annals of Botany, 115*(3), 419-431.

Fortmeier, R., & Schubert, S. (1995). Salt tolerance of maize (*Zea mays* L.): the role of sodium exclusion. *Plant, Cell & Environment, 18*(9), 1041-1047.

Franzisky, B. L., Geilfus, C.-M., Kränzlein, M., Zhang, X., & Zörb, C. (2019). Shoot chloride translocation as a determinant for NaCl tolerance in *Vicia faba* L. *Journal of Plant Physiology, 236*, 23-33.

Geilfus, C.-M. (2018). Chloride: from nutrient to toxicant. *Plant and Cell Physiology, 59*(5), 877-886.

Geilfus, C.-M., Mithofer, A., Ludwig-Muller, J., Zörb, C., & Mühling, K.-H. (2015). Chloride-inducible transient apoplastic alkalinizations induce stomata closure by controlling abscisic acid distribution between leaf apoplast and guard cells in salt-stressed *Vicia faba*. *New Phytologist, 208*(3), 803-816.

Granot, D., & Kelly, G. (2019). Evolution of guard-cell theories: the story of sugars. *Trends in Plant Science, 24*(6), 507-518.

Hedrich, R., & Shabala, S. (2018). Stomata in a saline world. *Current Opinion in Plant Biology, 46*, 87-95.

Jarvis, R. G., & Mansfield, T. A. (1980). Reduced stomatal responses to light, carbon dioxide and abscisic acid in the presence of sodium ions. *Plant, Cell and Environment, 3*(4), 279-283.

Jezek, M., & Blatt, M. R. (2017). The Membrane Transport System of the Guard Cell and Its Integration for Stomatal Dynamics. *Plant Physiology, 174*(2), 487-519.

Jin, X., Wang, R.-S., Zhu, M., Jeon, B. W., Albert, R., Chen, S., & Assmann, S. M. (2013). Abscisic acid-responsive guard cell metabolomes of Arabidopsis wild-type and gpa1 G-protein mutants. *The Plant Cell, 25*(12), 4789-4811.

Kelly, G., Moshelion, M., David-Schwartz, R., Halperin, O., Wallach, R., Attia, Z., Belausov, E., & Granot, D. (2013). Hexokinase mediates stomatal closure. *The Plant Journal, 75*(6), 977-988.

Kempa, S., Krasensky, J., Dal Santo, S., Kopka, J., & Jonak, C. (2008). A central role of abscisic acid in stress-regulated carbohydrate metabolism. *PloS one, 3*(12), e3935-e3935.

Krasensky, J., & Jonak, C. (2012). Drought, salt, and temperature stress-induced metabolic rearrangements and regulatory networks. *Journal of Experimental Botany, 63*(4), 1593-1608.

Lawson, T., Simkin, A. J., Kelly, G., & Granot, D. (2014). Mesophyll photosynthesis and guard cell metabolism impacts on stomatal behaviour. *New Phytologist, 203*(4), 1064-1081.

Li, B., Tester, M., & Gilliham, M. (2017). Chloride on the Move. *Trends in Plant Science, 22*(3), 236-248.

Lima, V. F., Medeiros, D. B., Dos Anjos, L., Gago, J., Fernie, A. R., & Daloso, D. M. (2018). Toward multifaceted roles of sucrose in the regulation of stomatal movement. *Plant signaling & behavior, 13*(8), e1494468-e1494468.

MacRobbie, E. A. C. (1983). Effects of light/dark on cation fluxes in guard cells of *Commelina communis* L. *Journal of Experimental Botany, 34*(12), 1695-1710.

Marschner, H. (2011). *Marschner's mineral nutrition of higher plants, 3rd edn*: Academic Press, Waltham.

Munns, R., & Gilliham, M. (2015). Salinity tolerance of crops – what is the cost? *New Phytologist, 208*(3), 668-673.

Munns, R., James, R. A., Gilliham, M., Flowers, T. J., & Colmer, T. D. (2016). Tissue tolerance: an essential but elusive trait for salt-tolerant crops. *Functional Plant Biology, 43*(12), 1103-1113.

Robinson, M. F., Véry, A.-A., Sanders, D., & Mansfield, T. A. (1997). How Can Stomata Contribute to Salt Tolerance? *Annals of Botany, 80*(4), 387-393.

Roelfsema, M. R. G., & Hedrich, R. (2002). Studying guard cells in the intact plant: modulation of stomatal movement by apoplastic factors. *New Phytologist, 153*(3), 425-431.

Roelfsema, M. R. G., & Hedrich, R. (2005). In the light of stomatal opening: new insights into 'the Watergate'. *New Phytologist, 167*(3), 665-691.

Roy, S. J., Negrão, S., & Tester, M. (2014). Salt resistant crop plants. *Current Opinion in Biotechnology, 26*, 115-124.

Sanchez, D. H., Siahpoosh, M. R., Roessner, U., Udvardi, M. K., & Kopka, J. (2008). Plant metabolomics reveals conserved and divergent metabolic responses to salinity. *Physiologia Plantarum, 132*(2), 209-219.

Slabu, C., Zörb, C., Steffens, D., & Schubert, S. (2009). Is salt stress of faba bean (*Vicia faba*) caused by Na^+ or Cl^- toxicity? *Journal of Plant Nutrition and Soil Science, 172*(5), 644-651.

Tavakkoli, E., Rengasamy, P., & McDonald, G. K. (2010). High concentrations of Na^+ and Cl^- ions in soil solution have simultaneous detrimental effects on growth of faba bean under salinity stress. *Journal of Experimental Botany, 61*(15), 4449-4459.

Teakle, N. L., & Tyerman, S. D. (2010). Mechanisms of Cl^- transport contributing to salt tolerance. *Plant, Cell & Environment, 33*(4), 566-589.

Tester, M., & Davenport, R. (2003). Na^+ tolerance and Na^+ transport in higher plants. *Annals of Botany, 91*(5), 503-527.

Thiel, G., & Blatt, M. R. (1991). The mechanism of ion permeation through K^+ channels of stomatal guard cells: voltage-dependent block by Na^+. *Journal of Plant Physiology, 138*(3), 326-334.

Yoshida, T., Anjos, L. d., Medeiros, D. B., Araújo, W. L., Fernie, A. R., & Daloso, D. M. (2019). Insights into ABA-mediated regulation of guard cell primary metabolism revealed by systems biology approaches. *Progress in Biophysics and Molecular Biology, 146*, 37-49.

Zhu, M., & Assmann, S. M. (2017). Metabolic Signatures in Response to Abscisic Acid (ABA) Treatment in Brassica napus Guard Cells Revealed by Metabolomics. *Scientific Reports, 7*(1), 12875-12875.

Zörb, C., Geilfus, C.-M., & Dietz, K.-J. (2019). Salinity and crop yield. *Plant Biology, 21*, 31-38.

Chapter 6

Summary

Summary

Soil salinity is a major challenge for agriculture, because most crop plants are sensitive to high salt concentrations in soil, an environment that results in reduced growth and yield. One major constraint imposed by salinity is the disruption of ion homeostasis attributable to the uptake competition of salts and nutrients and the accumulation of deleterious ions, which are toxic to plants at high concentrations. For a better understanding of ion-homeostasis-associated traits contributing to salt tolerance in salt-sensitive crops, such as *Vicia faba* and *Zea mays*, the capabilities of ion exclusion and tissue tolerance were assessed in diverse genotype selections under saline conditions. In addition, the impact of increased salt ion concentrations in leaves and in the apoplast on stomatal physiology and guard cell integrity was characterized in *V. faba* exposed to long-term salinity in order to improve our knowledge of stomatal physiology and functioning under conditions of NaCl stress.

The treatment of diverse *V. faba* varieties with 100 mM NaCl demonstrated that ion-homeostasis-associated tolerance mechanisms are differentially managed for Na^+ and Cl^-. The longer-withstanding varieties were tolerant to the accumulation of Na^+ suggesting that tolerance to Na^+ predominantly occurred at the level of tissue tolerance after Na^+ had entered the leaves. Conversely, tissue tolerance for Cl^- was weak throughout all varieties suggesting that the tolerance to Cl^- was facilitated instead by the restriction of the intrusion of Cl^- into the plant's shoots; this process might be crucial for the ability of *V. faba* to withstand NaCl salinity. The treatment of diverse *Z. mays* hybrids with mild and high doses of Cl^- added to the soil revealed that most genotypes restricted Cl^- root-to-shoot translocation. This suggests that *Z. mays* effectively prevents Cl^- from entering the xylem and, thus, the acropetal transport of Cl^-, thereby hindering harmful Cl^- accumulations building up in the photosynthetically active leaf blades.

A detailed analysis of guard cell physiology under long-term NaCl demonstrated that guard cell primary metabolism differentially responds to altered ion composition resulting from

salt stress in comparison with whole leaf tissue in *V. faba*; such a differential response might be a prerequisite for the maintenance of guard cell functionality under conditions of stress, *i.e.* the adjustment of guard cell turgor that affects stomatal aperture and water loss. Moreover, the shift from a photoperiod-dependent accumulation of sucrose in guard cells and the apoplast to a photoperiod-independent under salinity suggests that a metabolic sucrose-mediated feedforward mechanism is involved in coordinating stomatal closure under conditions of long-term NaCl and might be beneficial for reducing water loss under conditions of stress-related carbon partitioning.

In summary, this work shows that ion-homeostasis-associated tolerance traits vary between crop species and that the differential metabolic acclimatisation of guard cells to disturbed ion homeostasis might represent an important aspect of tissue tolerance enabling the maintenance of stomatal regulation during long-term salinity.

Chapter 7

Zusammenfassung

Zusammenfassung

Die Anreicherung von Salz in Ackerböden stellt eine große Herausforderung für die Landwirtschaft dar, da die wichtigsten Kulturpflanzen salzsensitiv sind und es folglich zu Ernteausfällen kommen kann. Eine Folge der Bodensalinität ist die Störung der Ionenhomöostase der Pflanze, die aus der Konkurrenz zwischen Salzionen und Nährstoffen um die Aufnahme sowie der Akkumulation von schädlichen Salzionen resultiert. Um das Wissen über Toleranzmechanismen von salzsensitiven Kulturpflanzen wie der Ackerbohne (*Vicia faba* L.) und Mais (*Zea mays* L.) zu erweitern, wurden die physiologischen Eigenschaften die Aufnahme von Salzionen in die Pflanze zu vermindern (Ionenexklusion) und hohe Salzkonzentrationen in pflanzlichem Gewebe zu tolerieren (Gewebetoleranz) in unterschiedlichen Genotypen beider Spezies untersucht. Des Weiteren wurde der Einfluss von erhöhten Salzkonzentrationen in Blättern und dem Apoplast auf die stomatäre Physiologie und Schließzellintegrität in *V. faba* unter Salzstress charakterisiert.

Die Behandlung einer Auswahl von 13 Ackerbohnensorten mit der Zugabe von 100 mM NaCl zur hydroponischen Nährlösung bis nekrotische Flecken auf den Blättern auftraten zeigte, dass Ionenhomöostase assoziierten Toleranzmechanismen der Ackerbohne bezüglich der Salzionen Na^+ und Cl^- unterschiedlich gehandhabt werden. Die widerstandsfähigeren Sorten waren gegenüber der Akkumulation von Na^+ tolerant, was darauf hindeutet, dass die Toleranz gegenüber Na^+ vorwiegend in Form von Gewebetoleranz nach der Aufnahme in die Pflanze auftritt. Die Gewebetoleranz für Cl^- war bei allen Sorten schwach ausgeprägt, was impliziert, dass die Toleranz gegenüber Cl^- durch die Limitierung des Cl^- Transports in den Pflanzenspross erreicht wird. In Übereinstimmung mit der postulierten Cl^--Empfindlichkeit von Leguminosen, stellt die Translokation von Cl^- zum Pflanzenspross in *V. faba* einen Schlüsselprozess für die Toleranz gegenüber salzhaltigen Böden dar.

Die Behandlung einer Auswahl von 8 Mais-Hybriden mit niedriger und hoher Zugabe von Chlorid zum Boden (63.2 und 757.1 mg Cl^- kg^{-1} Boden TM; gegeben als $CaCl_2$) zeigte,

dass die physiologische Reaktion auf Cl^- im Vergleich zu equimolarer Zugabe von z.B. Na^+ schwächer ausfiel. Außerdem zeigten die Profile der Cl^--Verteilung in den Maispflanzen, dass die meisten Hybriden die Cl^--Translokation aus der Wurzel in den Pflanzenspross limitierten. Dies deutet darauf hin, dass Mais den Cl^--Transport in das Xylem effektiv beschränkt und somit den akropetalen Cl^--Transport verringert, was einer der Photosynthese schädlichen Akkumulation von Cl^- in Blattspreiten vorbeugt.

Die Untersuchung der Schließzellphysiologie von *V. faba* unter Salzstress zeigte, dass der Primärstoffwechsel von Schließzellen im Vergleich zum Gesamtblatt unterschiedlich auf eine gestörte Ionenhomöostase reagiert. Dies könnte eine wichtige Voraussetzung für die Aufrechterhaltung der Schließzellfunktionalität unter Salzstress sein, welche eine konstante Anpassung des Schließzellturgors und damit der stomatäre Apertur ermöglicht. Darüber hinaus wurde unter Salzstress die Veränderung einer von der Fotoperiode abhängigen Saccharose-Akkumulation in Schließzellen und dem Apoplast zu einer permanenten, von der Fotoperiode unabhängigen Saccharose-Akkumulation beobachtet. Dies weist auf einen metabolischen, Saccharose-vermittelten ‚feedforward'-Mechanismus hin, welcher an der Koordinierung des stomatären Schlusses unter Salzstress beteiligt ist und somit zur Reduktion des Wasserverlustes beiträgt.

Diese Arbeit zeigt, dass Ionen-Homöostase assoziierte Toleranzmerkmale zwischen der Ackerbohne und Mais variieren und dass die vom Mesophyll abweichende metabolische Akklimatisation von Schließzellen an eine durch Salzionen gestörte Ionenhomöostase einen wichtigen Aspekt der Gewebetoleranz darstellen könnte, welcher die Aufrechterhaltung der stomatären Regulation während andauerndem Salzstress begünstigt.

Total list of all publications:

Peer-reviewed articles integrated in this dissertation:

Franzisky, B. L., Geilfus, C.-M., Romo-Pérez, M. L., Fehrle, I., Erban, A., Kopka, J., & Zörb, C. (2020). Acclimatisation of guard cell metabolism to long-term salinity. *Plant, Cell &Environment,* 1-15.

Franzisky, B. L., Geilfus, C.-M., Kränzlein, M., Zhang, X., & Zörb, C. (2019). Shoot chloride translocation as a determinant for NaCl tolerance in *Vicia faba* L. *Journal of Plant Physiology, 236*, 23-33.

Zhang, X., Zörb, C., Kränzlein, M., Franzisky, B. L., Kaiser, H., & Geilfus, C.-M. (2019). The early stress response of maize (Zea mays L.) to chloride salinity. *Journal of Agronomy and Crop Science, 205*(6), 586-597.

Other articles:

Zhang, X., Franzisky, B. L., Eigner, L., Geilfus, C.-M., & Zörb, C. Antagonism of chloride and nitrate inhibits nitrate reductase activity in chloride-stressed maize. *Plant Growth Regulation,* accepted (2020).

Kränzlein, M., Geilfus, C.-M., Franzisky, B. L., Zhang, X., Kaiser, H., Wimmer, M. A., & Zörb, C. Physiological responses of contrasting maize (*Zea mays* L.) hybrids to repeated drought. *Journal of Plant Growth Regulation,* accepted (2021).

Romo-Pérez, M. L., Weinert, C. H., Franzisky, B. L., Kulling, S. E., Zörb, C. Sodium accumulation has minimal effect on onion bulb metabolome. *Plant science,* in revision.

Conference contributions:

"Screening the *Vicia Faba* L. Diversity for NaCl-Tolerance":

Bastian L. Franzisky, Christoph-Martin Geilfus, Christian Zörb

- **Publication date:** 2017/4
  Conference: Regio Plant Science Meeting, Tübingen, Germany

- **Publication date:** 2017/5
  Conference: Annual Conference of the German Society of Plant Nutrition, Giessen, Germany

Bastian L. Franzisky, Christoph-Martin Geilfus, Monika Wimmer, Christian Zörb

- **Publication date:** 2018/9
  Conference: Annual Conference of the German Society of Plant Nutrition, Osnabrück, Germany

“Salinity induced ionic stress in guard cells”:

Bastian L. Franzisky, Christoph-Martin Geilfus, Christian Zörb

- **Publication date:** 2019/3
  Conference: Regio Plant Science Meeting, Hohenheim, Germany

Bastian L. Franzisky, Christoph-Martin Geilfus, Alexander Erban, Joachim Kopka, Christian Zörb

- **Publication date**: 2019/3
  Conference: Annual Conference of the German Society of Plant Nutrition, Berlin, Germany

- **Publication date:** 2019/9
  Conference: International Plant Science Conference of the German Botanical Society, Rostock, Germany

- **Publication date:** 2019/10
  Conference: Plant Science Symposium: Towards Abiotic Stress Tolerance, Freising, Germany

Danksagung

Mein Dank gilt meinem Doktorvater Prof. Dr. Christian Zörb, der mir die Durchführung dieser Arbeit ermöglicht hat. Für die Unterstützung bei der Konzeption der Projekte, der Erstellung wissenschaftlicher Beiträge und der vorliegenden Arbeit möchte ich danken. Darüber hinaus bin ich für das stete Motivieren, die Ansprechbarkeit, die Diskussionsbereitschaft, die Ermunterung zur Effizienz sowie die wissenschaftliche Förderung sehr dankbar.

Mein Dank gilt Prof. Dr. Christoph-Martin Geilfus, für die tatkräftige Unterstützung meiner wissenschaftlichen Arbeit. Danke für die freundliche, kompetente Betreuung, inspirierende Diskussionen und die Hilfestellungen sowie Geduld während des Verfassens gemeinsamer wissenschaftlicher Beiträge.

Dr. Monika Wimmer und Dr. Nikolaus Merkt danke ich für stetig offene Ohren, das Teilen von Expertise, die Unterstützung bei der Planung und Durchführung von Experimenten, welche für mein Forschen und die Lehre äußerst hilfreich waren.

Dr. Joachim Kopka und Alexander Erban danke ich für die erfolgreiche Kooperation in diesem Projekt und den freundlichen Empfang sowie den inspirierenden Aufenthalt in Golm.

Ich danke meinen Mitdoktoranden Maria Romo Pérez, Lena Werner, Carina Lang, Azin Rekowski, Mellissa Kleb, Jan Behr, Markus Dier, Xudong Zhang, Markus Kränzlein sowie den Kollegeninnen Gyöngyi Bárdos und Christiane Beierle für die angenehme, unterhaltsame und positive Atmosphäre in unserer Arbeitsgruppe, die Hilfsbereitschaft, die tatkräftige Unterstützung und lebendige Diskussionen zu diversen Themenkomplexen.

Mein herzlicher Dank gilt meiner Familie, Tosca, Sophia, Cornelia, Kurosch, Anna-Maria, Edith, Gunter, Else, Erich, Gisela, Willi und besonders Anna Alexandra für das Fördern meines Interesses an den Naturwissenschaften, für unablässige Motivation, für die Beratung und das zur Seite stehen in schwierigen Lebenslagen. Euer Interesse an meiner Forschung hat mich stets erfreut.

Curriculum vitae

Profile:

Name:	Bastian Leander Franzisky
Birthday:	31 December 1988
Birthplace:	Meckesheim, Germany

Education:

Dec. 2020 to Nov. 2016:	Academic researcher, Dr. sc. agr. Candidate University of Hohenheim, Stuttgart, Germany Crop Science / Quality of plant products
May 2016 to Sept. 2013:	M. Sc.– Biological Sciences University of Konstanz, Germany
Sept. 2013 to Oct. 2010:	B. Sc. – Biological Sciences University of Konstanz, Germany
Jun. 2008 to Jul. 1996:	Abitur Nordseegymnasium, St. Peter-Ording, Germany

Hohenheim, Bastian Franzisky

Annex 3

Declaration in lieu of an oath on independent work

according to Sec. 18(3) sentence 5 of the University of Hohenheim's Doctoral Regulations for the Faculties of Agricultural Sciences, Natural Sciences, and Business, Economics and Social Sciences

1. The dissertation submitted on the topic

Aspects of stomatal physiology during salt-stress-related disturbances of ion homeostasis

……...

is work done independently by me.

2. I only used the sources and aids listed and did not make use of any impermissible assistance from third parties. In particular, I marked all content taken word-for-word or paraphrased from other works.

3. I did not use the assistance of a commercial doctoral placement or advising agency.

4. I am aware of the importance of the declaration in lieu of oath and the criminal consequences of false or incomplete declarations in lieu of oath.

I confirm that the declaration above is correct. I declare in lieu of oath that I have declared only the truth to the best of my knowledge and have not omitted anything.

Stuttgart, 18.01.2021 _____ 

Place, Date Signature